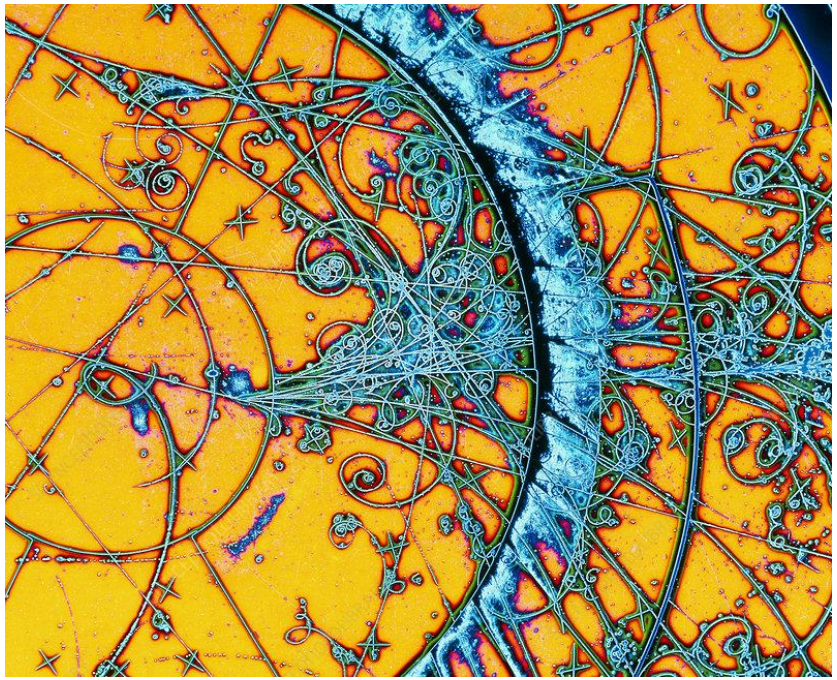

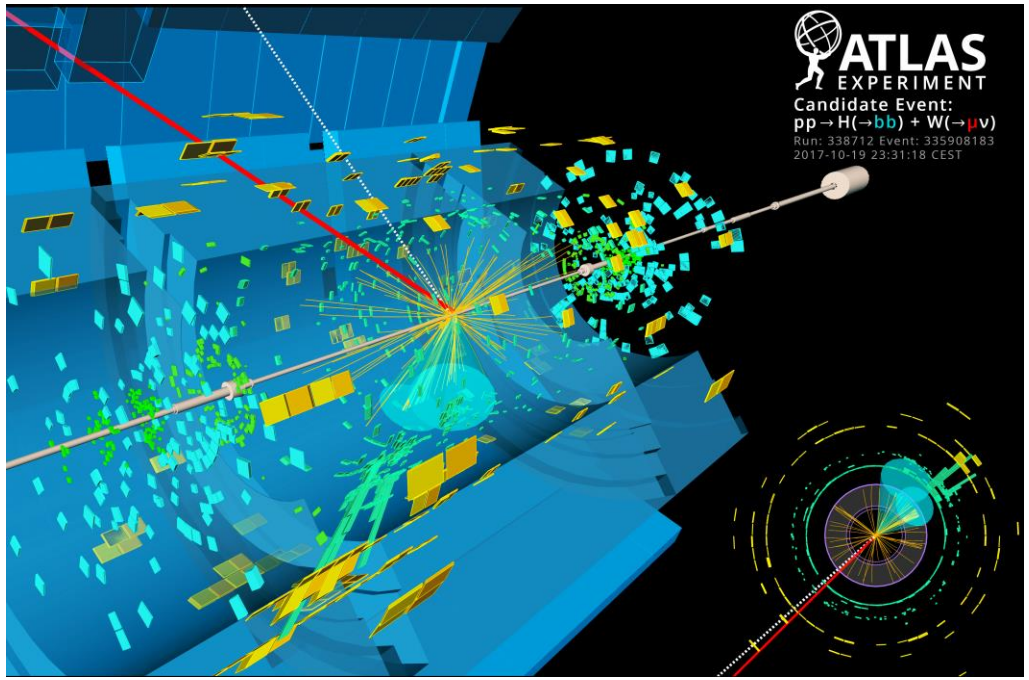
ATLAS
EXPERIMENT
Candidate Event:
pp→H(→bb) + W(→μν)
Run: 338712 Event: 335908183
2017-10-19 23:31:18 CEST

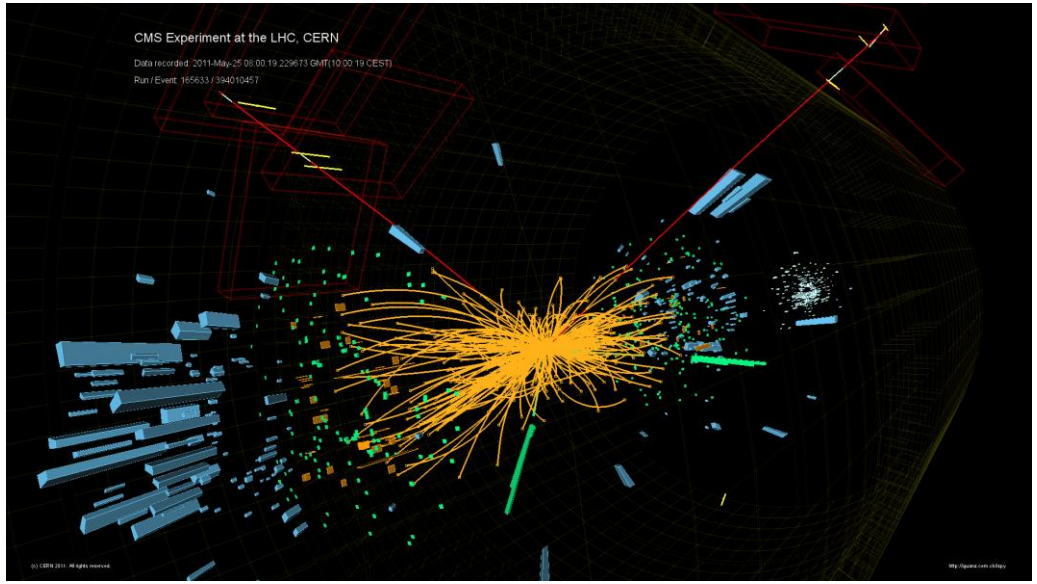
CMS Experiment at the LHC, CERN

Signals, Noise and Signal processing in Particle Detectors 1/5

Academic Training Lectures

Werner Riegler, CERN, werner.riegler@cern.ch

Oct. 14-18 2024, Council Chamber

Signals in particle detectors, 2019

Main Auditorium, Mon. 2 Dec.

Lecture 1:

- Electrostatics
- Principles
- Reciprocity
- Induced currents
- Induced voltages
- Ramo-Shockley theorem
- Mean value theorem
- Capacitance matrix
- Equivalent circuits

Council Chamber, Tue. 3 Dec.

Lecture 2:

Signals in

- Ionization chambers
- Liquid argon calorimeters
- Diamond detectors
- Silicon detectors
- GEMs (Gas Electron Multiplier)
- Micromegas (Micromesh gas detector)
- APDs (Avalanche Photo Diodes)
- LGADs (Low Gain Avalanche Diodes)
- SiPMs (Silicon Photo Multipliers)
- Strip detectors
- Pixel detectors
- Wire Chambers
- Liquid Argon TPCs

TH conference room (4/3-006), Wed. 4 Dec.

Lecture 3:

- Media with conductivity
- Quasi-static approximations
- Signal theorem extensions
- Time dependent weighting fields
- Resistive plate chambers (RPCs)
- Un-depleted silicon sensors
- Monolithic pixel sensors

Filtration Plant (222/R-001), Thu. 5.Dec.

Lecture 4:

- Signal propagation
- Transmission lines
- Termination
- Linear signal processing
- Noise
- Optimum filters

Main Auditorium, Fri. 6 Dec.

Lecture 5:

- Possible overflow, wrap-up and Q&A session

Why another lecture series on signals ?

- The 2019 lecture series was quite popular with many follow up questions.
- The entire topic of signal processing, noise and optimum filters was not covered
- In the meantime, we made quite some progress on:
  - Generalized Signal Theorems
  - Simulation of detectors with resistive elements
  - Statistics and dynamics of electron-hole avalanches

This lecture series will cover these topics.

Please ask questions – I can also adapt the lecture according to requests for specific topics.

Signals, Noise and Signal processing in Particle Detectors

Mon. 14 Oct.

Lecture 1:

- Recap
- Simulation of resistive elements
- Theorem extensions
- Radio signals for particle detection

Tue. 15 Oct.

Lecture 2:

- Electron avalanches
- Electron-Hole avalanches
- APDs (Avalanche Photo Diodes)
- LGADs (Low Gain Avalanche Diodes)
- SiPMs (Silicon Photo Multipliers)

Wed. 16 Oct.

Lecture 3:

- Linear Signal processing
- Noise

Thu. 17 Oct.

Lecture 4:

- Optimum Filters
- Sampling Theorem
- Applications

Fri. 18 Oct.

Lecture 5:

- Overflow, wrap-up and Q&A session

Recap

Induced charges on metal electrodes

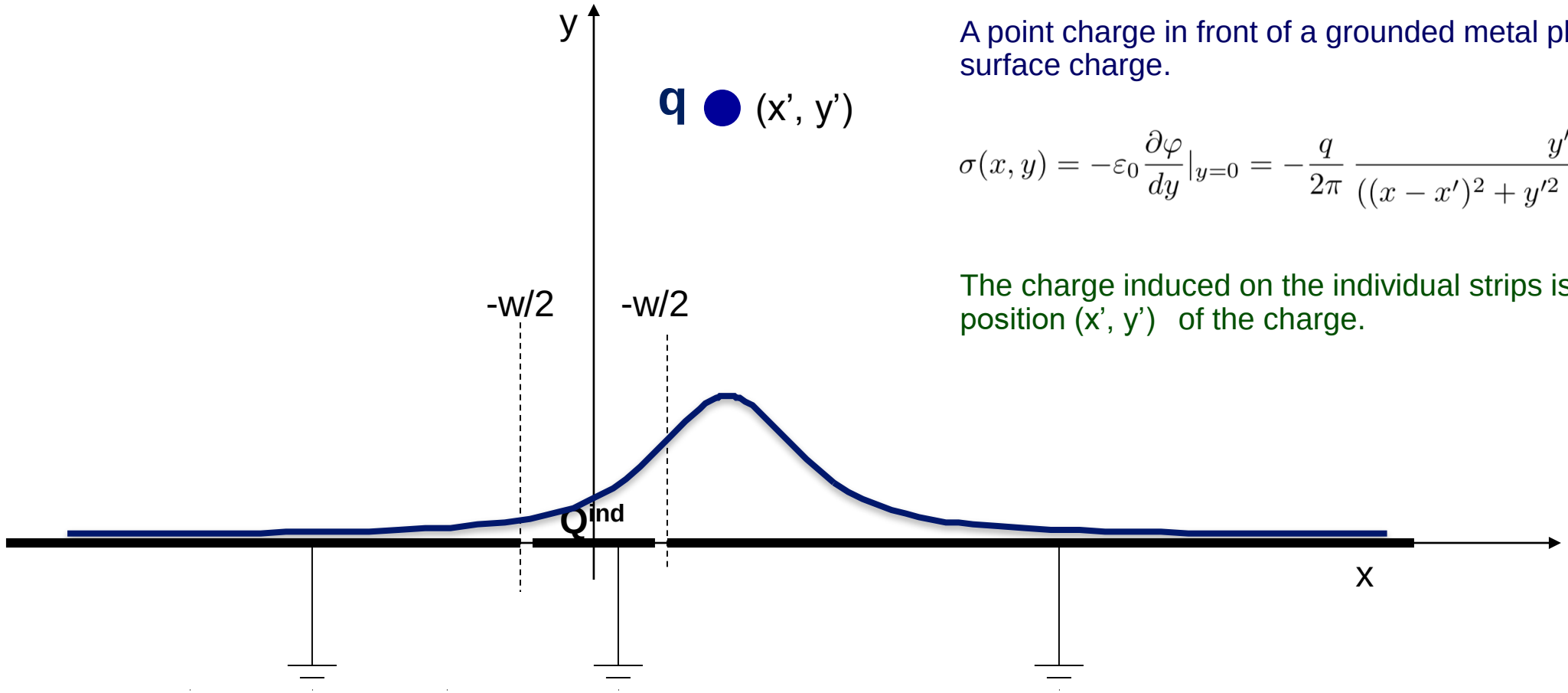

A point charge in front of a grounded metal plane indices a surface charge.

$$\sigma(x,y) = -\varepsilon_0 \frac{\partial \varphi}{dy}|_{y=0} = -\frac{q}{2\pi} \frac{y'}{((x-x')^2 + y'^2 + (z-z')^2)^{3/2}}$$

The charge induced on the individual strips is depends on the position (x', y') of the charge.

$$Q^{ind}(x',y') = \int_{-\infty}^{\infty} \int_{-w/2}^{w/2} \sigma(x,y) dx dy = -\frac{q}{\pi} \left(\arctan \frac{w-2x'}{2y'} - \arctan \frac{w+2x'}{2y'} \right)$$

Induced currents on metal electrodes

If the charge is moving with a velocity v towards the strip we have

$$Q^{ind}(y') = -\frac{2q}{\pi}\arctan\frac{w}{2y'}$$

$$y'(t) = -vt$$

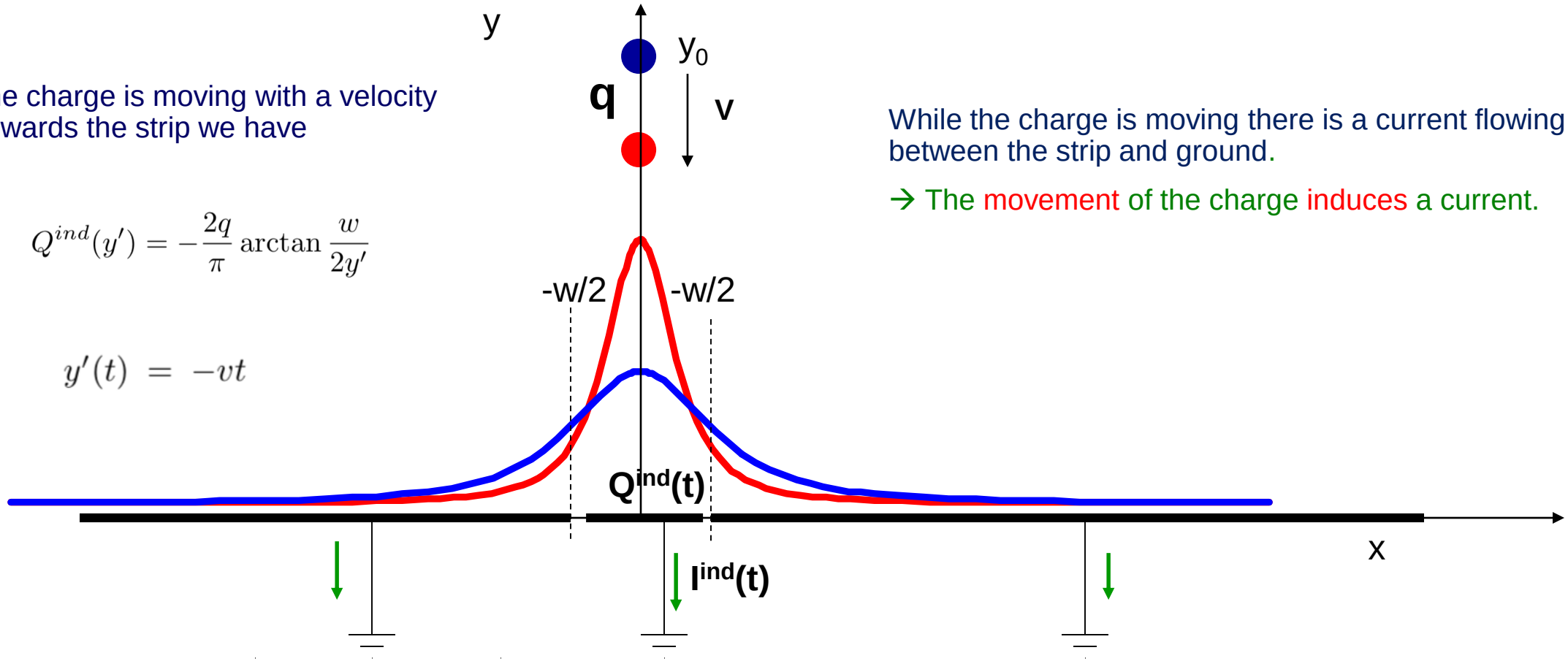

While the charge is moving there is a current flowing between the strip and ground.

→ The movement of the charge induces a current.

$$Q^{ind}(t) = q\frac{2}{\pi}\arctan\frac{w}{2vt} \qquad t < 0$$

$$I^{ind}(t) = -\frac{dQ^{ind}(t)}{dt} = q\frac{4w}{\pi\left(w^2 + 4v^2t^2\right)}v \qquad t < 0$$

Reciprocity theorem

Two arbitrary charge distributions $\rho(\mathbf{x})$ and $\overline{\rho}(\mathbf{x})$

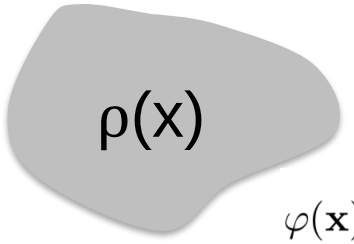

$$\varphi(\mathbf{x}) = \int \frac{\rho(\mathbf{x}')}{|\mathbf{x}-\mathbf{x}'|} d^3x'$$

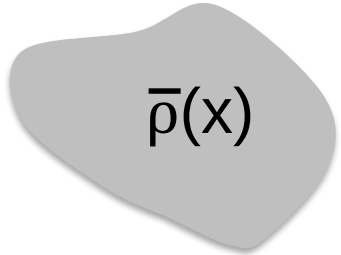

$$\overline{\varphi}(\mathbf{x}) = \int \frac{\overline{\rho}(\mathbf{x}')}{|\mathbf{x}-\mathbf{x}'|} d^3x'$$

$$W = \int \overline{\rho}(\mathbf{x})\varphi(\mathbf{x}) d^3x = \int\int \frac{\overline{\rho}(\mathbf{x})\rho(\mathbf{x}')}{|\mathbf{x}-\mathbf{x}'|} d^3x d^3x' = \int \rho(\mathbf{x}')\overline{\varphi}(\mathbf{x}') d^3x'$$

$$\int \overline{\rho}(\mathbf{x})\varphi(\mathbf{x}) d^3x = \int \rho(\mathbf{x})\overline{\varphi}(\mathbf{x}) d^3x$$

Sounds like a trivial statement, but has very practical consequences.

Theorem, induced current

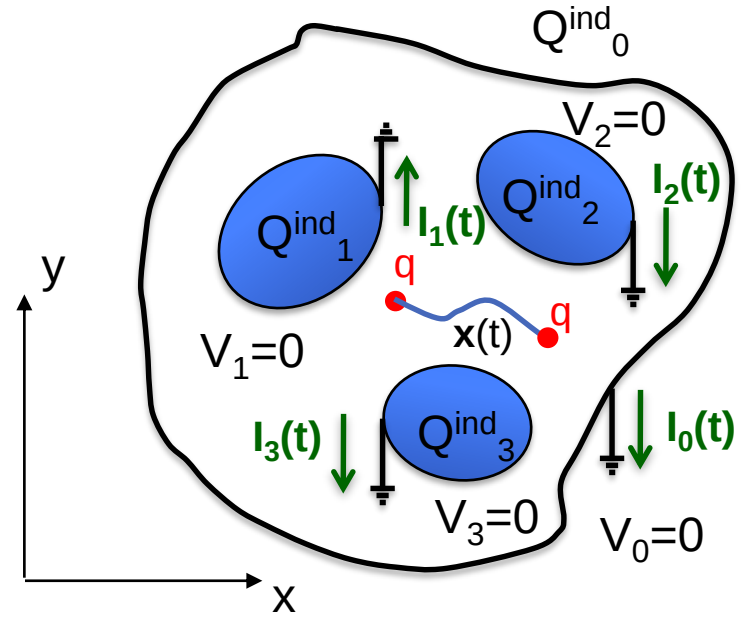

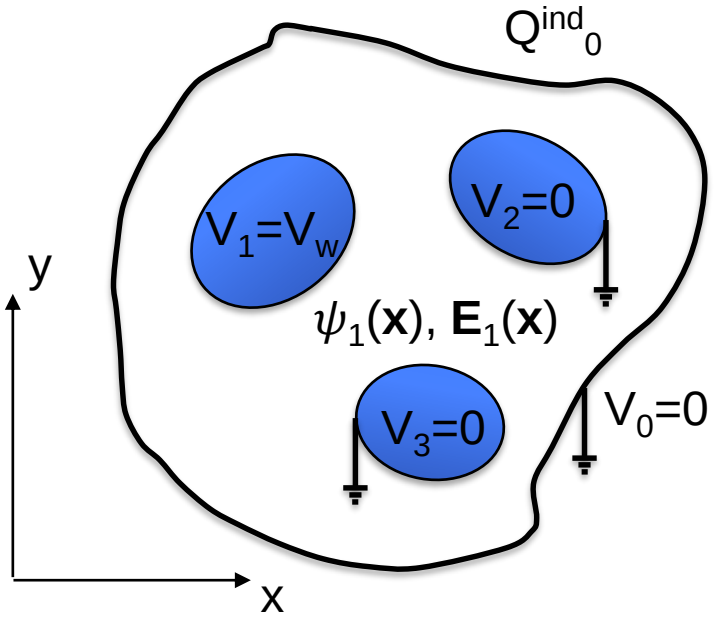

The current induced on a grounded conducting electrode by a point charge q moving along a trajectory **x(t)** can be calculated the following way:

$$I_n^{ind}(t) = -\frac{Q_n^{ind}(\mathbf{x}(t))}{dt} = \frac{q}{V_w}\nabla\psi_n(\mathbf{x}(t))\dot{\mathbf{x}}(t) = -\frac{q}{V_w}\mathbf{E}_n(\mathbf{x}(t))\dot{\mathbf{x}}(t)$$

This weighting field $\mathbf{E}_n(\mathbf{x})$ is given by

$$\mathbf{E}_n(\mathbf{x}) = -\nabla\psi_n(\mathbf{x})$$

where $\mathbf{E}_n(\mathbf{x})$ is the electric field in case we remove the charge, put electrode n to potential V_w an we ground all other electrodes.

→ Ramo-Shockley theorem

Ramo Shockley theorem (reciprocity theorem)

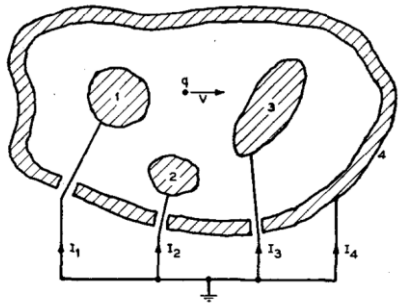

FIG. 1. Schematic representation of conductors and currents.

Currents to Conductors Induced by a Moving Point Charge

W. SHOCKLEY
Bell Telephone Laboratories, Inc., New York, N. Y.
(Received May 14, 1938)

General expressions are derived for the currents which flow in the external circuit connecting a system of conductors when a point charge is moving among the conductors. The results are applied to obtain explicit expressions for several cases of practical interest.

Currents Induced by Electron Motion*

SIMON RAMO†, ASSOCIATE MEMBER, I.R.E.

Summary—*A method is given for computing the instantaneous current induced in neighboring conductors by a given specified motion of electrons. The method is based on the repeated use of a simple equation giving the current due to a single electron's movement and is believed to be simpler than methods previously described.*

METHOD OF COMPUTATION

The method is based on the following equation, whose derivation is given later:

Signals in particle detectors, 2019

Main Auditorium, Mon. 2 Dec.

Lecture 1:

- Electrostatics
- Principles
- Reciprocity
- Induced currents
- Induced voltages
- Ramo-Shockley theorem
- Mean value theorem
- Capacitance matrix
- Equivalent circuits

Council Chamber, Tue. 3 Dec.

Lecture 2:

Signals in

- Ionization chambers
- Liquid argon calorimeters
- Diamond detectors
- Silicon detectors
- GEMs (Gas Electron Multiplier)
- Micromegas (Micromesh gas detector)
- APDs (Avalanche Photo Diodes)
- LGADs (Low Gain Avalanche Diodes)
- SiPMs (Silicon Photo Multipliers)
- Strip detectors
- Pixel detectors
- Wire Chambers
- Liquid Argon TPCs

TH conference room (4/3-006), Wed. 4 Dec.

Lecture 3:

- Media with conductivity
- Quasi-static approximations
- Signal theorem extensions
- Time dependent weighting fields
- Resistive plate chambers (RPCs)
- Un-depleted silicon sensors
- Monolithic pixel sensors

Filtration Plant (222/R-001), Thu. 5.Dec.

Lecture 4:

- Signal propagation
- Transmission lines
- Termination
- Linear signal processing
- Noise
- Optimum filters

Main Auditorium, Fri. 6 Dec.

Lecture 5:

- Possible overflow, wrap-up and Q&A session

Quasi-static approximation of Maxwell's equations

Assuming a conductivity sigma of the material we have a current according to

$$\mathbf{j}(\mathbf{x},t) = \sigma(\mathbf{x})\mathbf{E}(\mathbf{x},t)$$

Maxwell's equations for this situation

$$\begin{aligned}
\nabla\mathbf{D}(\mathbf{x},t) &= \rho(\mathbf{x},t) \qquad \mathbf{D}(\mathbf{x},t) = \varepsilon(\mathbf{x})\mathbf{E}(\mathbf{x},t) \\
\nabla\mathbf{B}(\mathbf{x},t) &= 0 \qquad\quad \mathbf{B}(\mathbf{x},t) = \mu(\mathbf{x})\mathbf{H}(\mathbf{x},t) \\
\nabla\times\mathbf{E}(\mathbf{x},t) &= -\frac{\partial\mathbf{B}(\mathbf{x},t)}{\partial t} \\
\nabla\times\mathbf{H}(\mathbf{x},t) &= \frac{\partial\mathbf{D}(\mathbf{x},t)}{\partial t} + \mathbf{j}_e(\mathbf{x},t) + \sigma(\mathbf{x})\mathbf{E}(\mathbf{x},t)
\end{aligned}$$

The current $j_e(x, t)$ is an 'externally impressed' current, which is related to the 'externally impressed' charge density ρ_e by

$$\nabla\mathbf{j}_e(\mathbf{x},t) = -\frac{\partial\rho_e(\mathbf{x},t)}{\partial t}$$

If we assume that this impressed current is only changing slowly we can neglect Faraday's law and approximate

$$\nabla\times\mathbf{E}(\mathbf{x},t) \approx 0 \qquad\qquad \mathbf{E}(\mathbf{x},t) = -\nabla\varphi(\mathbf{x},t)$$

and we can then write the electric field as the gradient of a potential, an by taking the divergence of the last equation …

$$\nabla(\nabla\times\mathbf{H}(\mathbf{x},t)) = \frac{\partial\nabla\mathbf{D}(\mathbf{x},t)}{\partial t} + \nabla\mathbf{j}_e(\mathbf{x},t) + \nabla[\sigma(\mathbf{x})\mathbf{E}(\mathbf{x},t)] = 0$$

$$\nabla\left[\varepsilon(\mathbf{x})\nabla\frac{\partial\varphi(\mathbf{x},t)}{\partial t} + \sigma(\mathbf{x})\nabla\varphi(\mathbf{x},t)\right] = -\frac{\partial\rho_e(\mathbf{x},t)}{\partial t}$$

Quasi-static approximation of Maxwell's equations

Performing the Fourier Transform of the quasi-static equation

we find

$$\nabla\left[\varepsilon(\mathbf{x})\nabla\frac{\partial\varphi(\mathbf{x},t)}{\partial t}+\sigma(\mathbf{x})\nabla\varphi(\mathbf{x},t)\right]=-\frac{\partial\rho_e(\mathbf{x},t)}{\partial t}$$

$$\nabla\left[\varepsilon(x)\nabla i\omega\varphi(\mathbf{x},\omega)+\sigma(\mathbf{x})\nabla\varphi(\mathbf{x},\omega)\right]=-i\omega\rho_e(\mathbf{x},\omega)$$

$$\nabla\left[\left(\varepsilon(x)+\sigma(\mathbf{x})/i\omega\right)\nabla\varphi(\mathbf{x},\omega)\right]=-\rho_e(\mathbf{x},\omega)$$

[1] H.A. Haus, J.R. Melcher, Electromagentic Fields and Energy, Prentice-Hall, Englewood Cliffs, NJ, 1989.

ELSEVIER

Nuclear Instruments and Methods in Physics Research A 478 (2002) 444–447

NUCLEAR INSTRUMENTS & METHODS IN PHYSICS RESEARCH Section A

www.elsevier.com/locate/nima

The quasi-static electromagnetic approximation for weakly conducting media ☆

Th. Heubrandtner, B. Schnizer*

Institut für Theoretische Physik, Technische Universität Graz, Petersgrasse 16, 8010 Graz, Austria

So we can write this equation as

$$\nabla\left[\varepsilon_{\text{eff}}(\mathbf{x})\nabla\varphi(\mathbf{x},\omega)\right]=-\rho_e(\mathbf{x},\omega)\qquad\varepsilon_{\text{eff}}(\mathbf{x})=\varepsilon(x)+\sigma(\mathbf{x})/i\omega\qquad\rho(\mathbf{x},\omega)=-\nabla\left[\varepsilon(\mathbf{x})\nabla\varphi(\mathbf{x},\omega)\right]\qquad\rho_e(\mathbf{x},\omega)=-\nabla\left[\varepsilon_{\text{eff}}(\mathbf{x})\nabla\varphi(\mathbf{x},\omega)\right]$$

This is the Poisson equation with an effective permittivity !

→ We can therefore find the time dependent solutions for a medium with a given conductivity by solving the electrostatic Poisson equation in the Fourier domain !

→ Knowing the electrostatic solution for a given permittivity ε(x) we just have to replace ε(x) by ε(x)+σ(x)/iω and perform the inverse Fourier transform !

Extension of the Ramo Shockley theorem

Available online at www.sciencedirect.com
SCIENCE DIRECT®
Nuclear Instruments and Methods in Physics Research A 535 (2004) 287–293
NUCLEAR INSTRUMENTS & METHODS IN PHYSICS RESEARCH Section A
www.elsevier.com/locate/nima

Extended theorems for signal induction in particle detectors VCI 2004

W. Riegler*

CERN, PH Division, Rt. De Meyrin, Geneva 23CH-1211, Switzerland

Available online 13 August 2004

Abstract

Most particle detectors are based on the principle that charged particles leave a trail of ionization in the detector and that the movement of these charges in an electric field induces signals on the detector electrodes. Assuming detector elements that are insulating and electrodes with infinite conductivity one can calculate the signals with an electrostatic approximation using the so-called 'Ramo theorem'. This is the standard way for the calculation of signals e.g. in wire chambers and silicon detectors. In case the detectors contain resistive elements, which is, e.g. the case in resistive plate chambers or underdepleted silicon detectors, the time dependence of the signals is not only given by the movement of the charges but also by the time-dependent reaction of the detector materials. Using the quasistatic approximation of Maxwell's equations we present an extended formalism that allows the calculation of induced signals for detectors with general materials by time dependent weighting fields. As examples, we will discuss the signals in resistive plate chambers and underdepleted silicon detectors.

Theorem, induced current

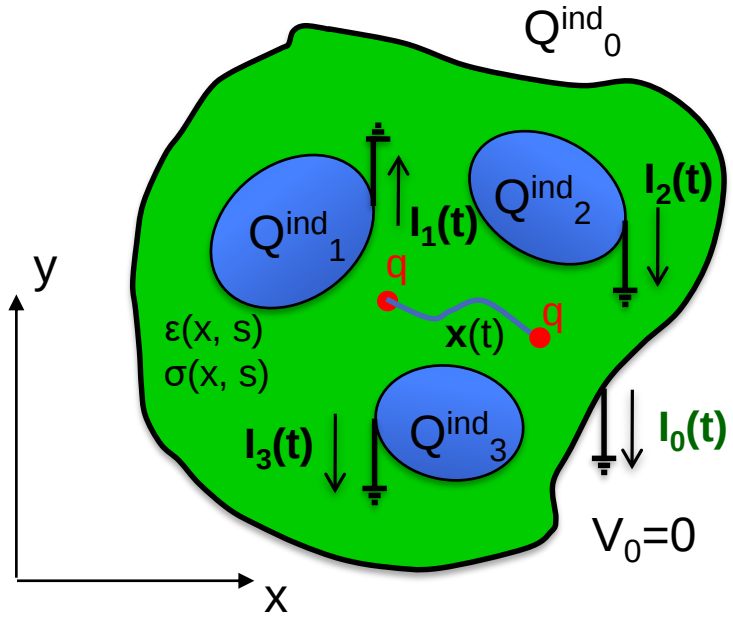

Applying the delta voltage pulse to the electrode in question we find the potential $\psi_n(x, t)$ and the field $E_n(x, t)$ from which the induced current can be calculated the following way:

$$I_n^{ext}(s) = -sQ_n^{ext}(s) = \frac{s}{V_w}\int_V \psi_n(\mathbf{x}, s)\rho_e(\mathbf{x}, s)d^3x$$

$$\rho_e(\mathbf{x}, t) = q\delta(\mathbf{x} - \mathbf{x}_1(t))$$

$$I_n^{ext}(t) = -\frac{q}{V_w}\int_0^t \mathbf{E}_n(\mathbf{x}_1(t'), t - t')\dot{\mathbf{x}}_1(t')dt'$$

→ Ramo-Shockley theorem extension for conducting media

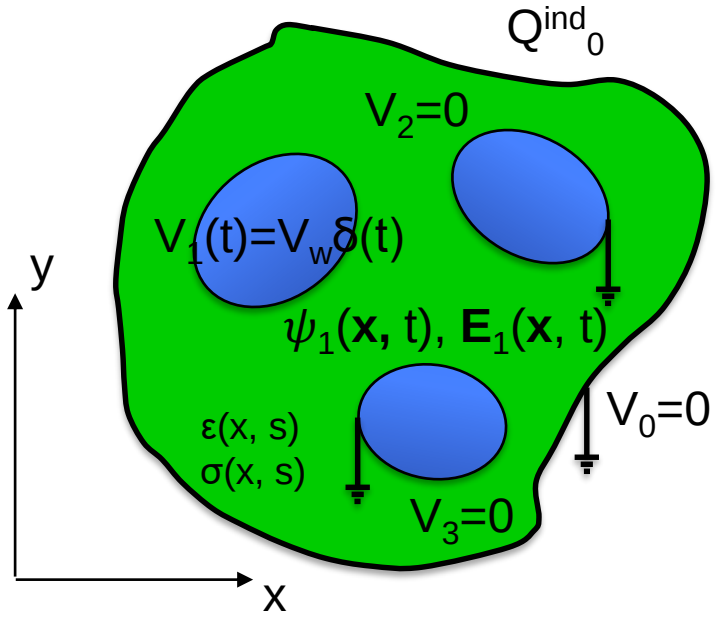

Note that E_n is not physical potential, since the delta function gives it a dimension of V/cm s.

In case the material is an insulator there is no time dependence of the weighting field and we recuperate Ramo's theorem.

$$\mathbf{E}_n(\mathbf{x}, t) = \mathbf{E}_{n0}(\mathbf{x})\delta(t - t') \qquad I_n^{ext}(t) = -\frac{q}{V_w}\mathbf{E}_{n0}(\mathbf{x}_1(t))\dot{\mathbf{x}}_1(t)dt$$

Theorem, induced voltage, dynamic

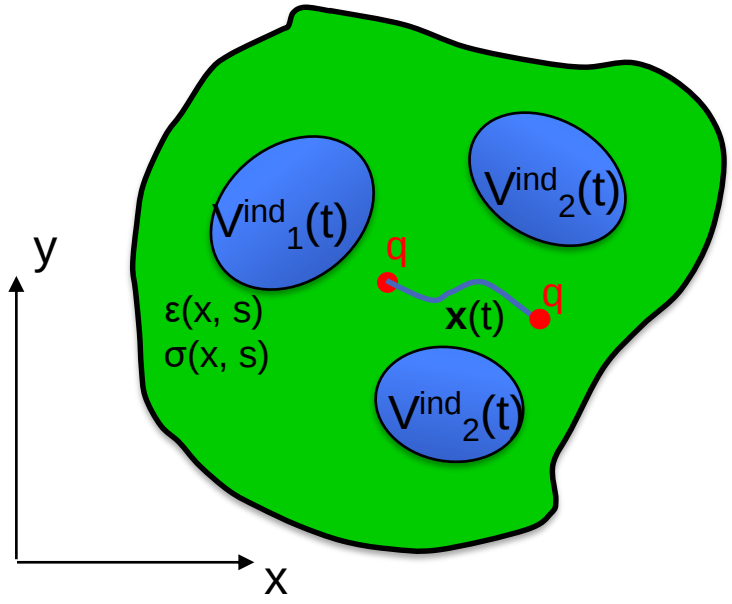

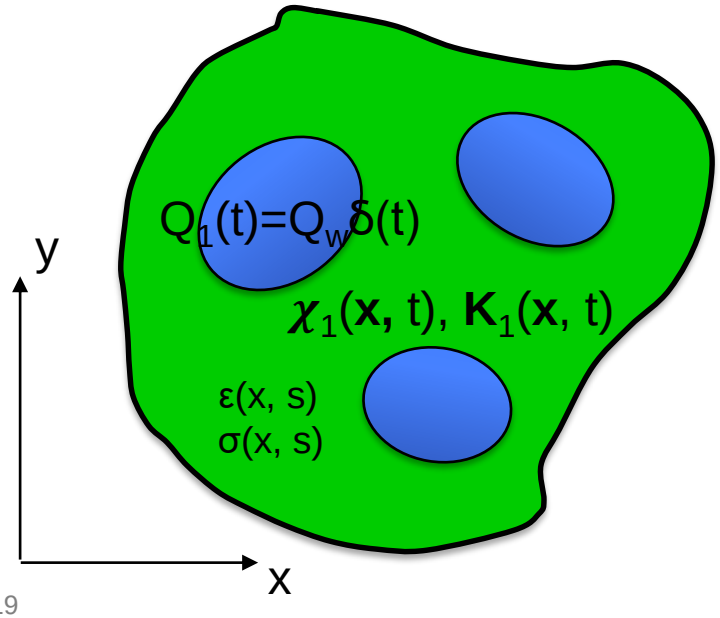

Applying the delta voltage pulse to the electrode in question we find the potential $\psi_n(x, t)$ and the field $E_n(x, t)$ from which the induced current can be calculated the following way:

$$V_n^{ind}(s) = \frac{s}{Q_w}\int_V \chi_n(\mathbf{x}, s)\rho_e(\mathbf{x}, t)d^3x$$

$$\rho_e(\mathbf{x}, t) = q\delta(\mathbf{x} - \mathbf{x}_1(t))$$

$$V_n^{ind}(s) = -\frac{q}{Q_w}\int_0^t \mathbf{K}(\mathbf{x}_1(t'), t - t')\dot{\mathbf{x}}_1(t')dt'$$

Since the admittance matrix relates currents and voltages on the electrodes in absence of charge, the admittance matrix relates the weighting fields $\mathbf{E_n}$ and $\mathbf{K_n}$ and therefore related the currents induced on grounded electrodes and the voltages induced on insulated electrodes.

$$I_n^{ind}(s) = \sum_{n=1}^{N} y_{nm}(s)V_m^{ind}(s)$$

This means in turn that we can first calculate the current induced on grounded electrodes and then place these currents as ideal current sources on the equivalent circuit of the medium.

Equivalent circuit, Impedance elements

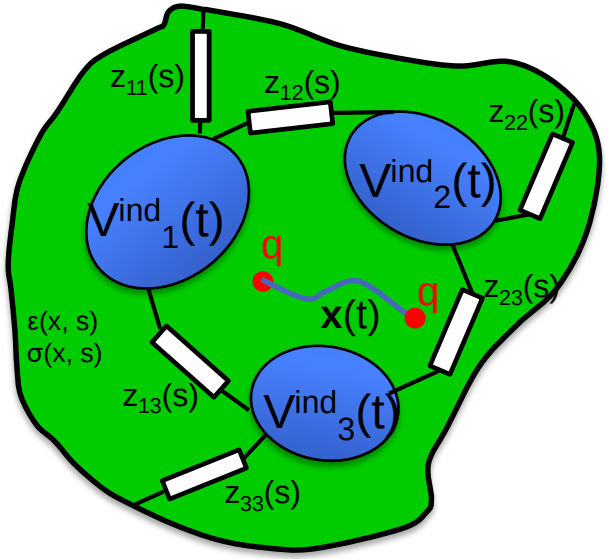

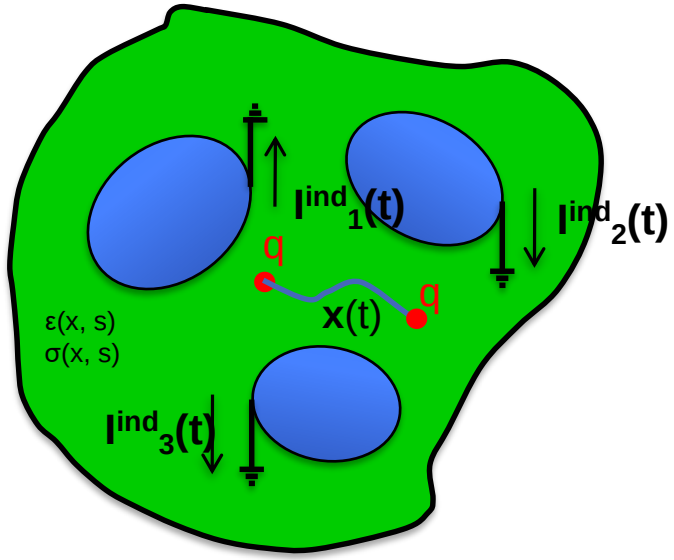

In case the electrodes are not insulated but connected with discrete linear impedance components we can consider them as part of the medium and we therefore just have to add these elements in the equivalent circuit.

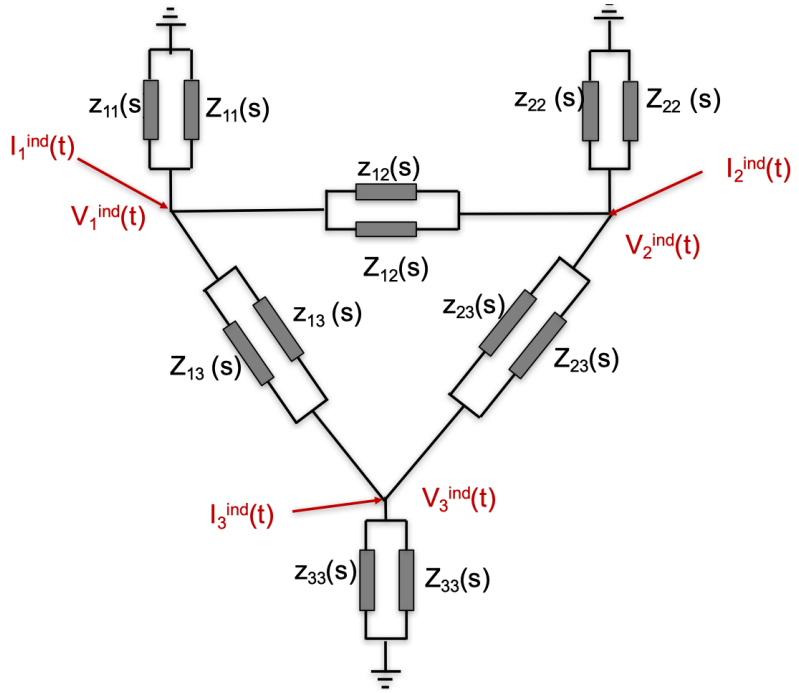

$$Z_{nm}(s) = -\frac{1}{y_{nm}(s)} \quad n \neq m \qquad Z_{nn}(s) = \frac{1}{\sum_{m=1}^{N} y_{nm}(s)} = -\frac{1}{y_{0n}} \quad n = m$$

$$y_{mn}(s) = \frac{s}{V_w} \oint_{\mathbf{A}_n} \varepsilon_{eff}(\mathbf{x}, s) \nabla \psi_m(\mathbf{x}, s) d\mathbf{A}$$

VRIJE UNIVERSITEIT BRUSSEL

Thesis submitted in fulfilment of the requirements for the award of the degree of Doctor of Sciences

RESISTIVE ELECTRODES AND PARTICLE DETECTORS

Modeling and Measurements of Novel Detector Structures

Djunes Janssens

February 2024

Promotor: Prof. Dr. J. D'Hondth
Co-promotors: Dr. H. Schindler

Sciences and Bio-Engineering Sciences
Physics department

Djunes Janssens

https://cds.cern.ch/record/2890572

Micromegas toy-model example

The time-dependent weighting potential $\psi_i(\mathbf{x}, t)$ is comprised of a static prompt and a dynamic delayed component:

Static weighting potential of a readout strip

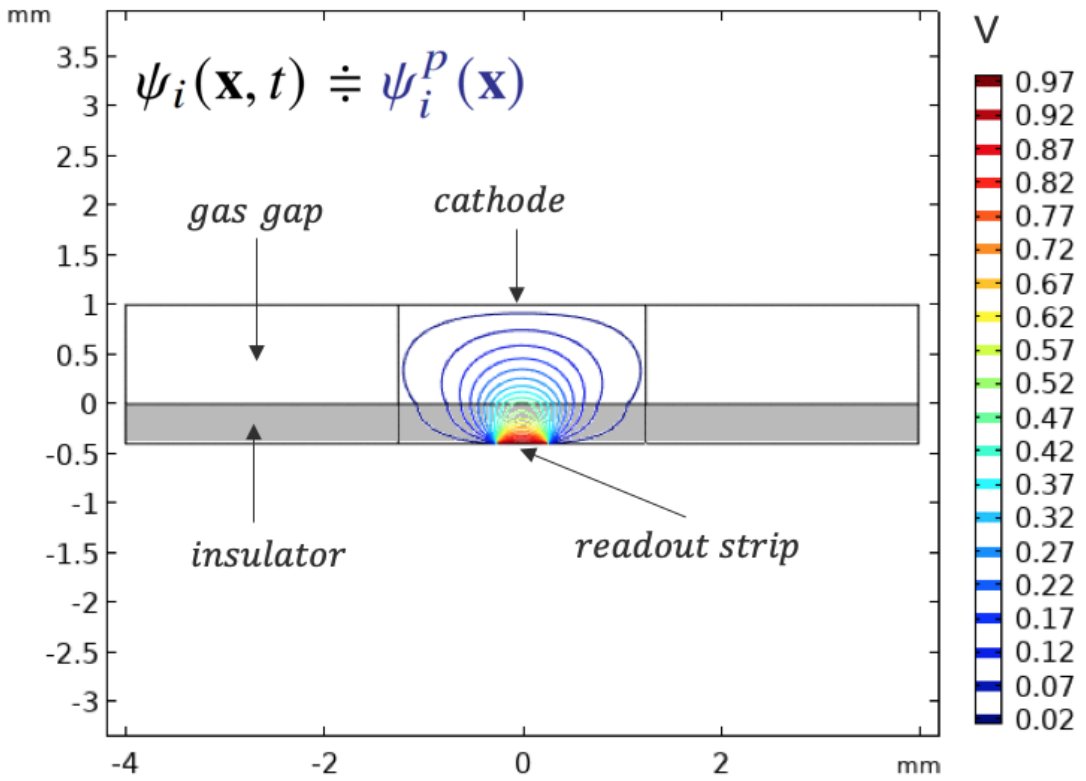

Dynamic weighting potential of a readout strip with resistive layer

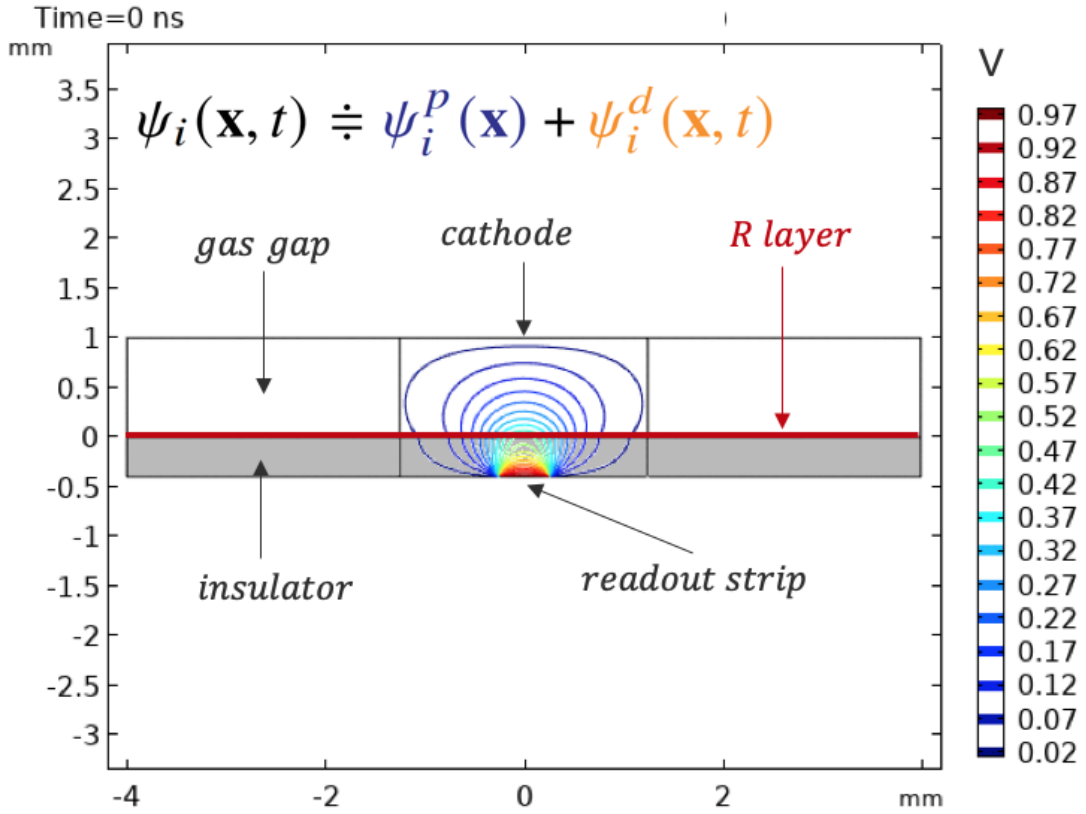

Micromegas toy-model example

The time-dependent weighting potential $\psi_i(\mathbf{x}, t)$ is comprised of a static prompt and a dynamic delayed component:

Static weighting potential of a readout strip

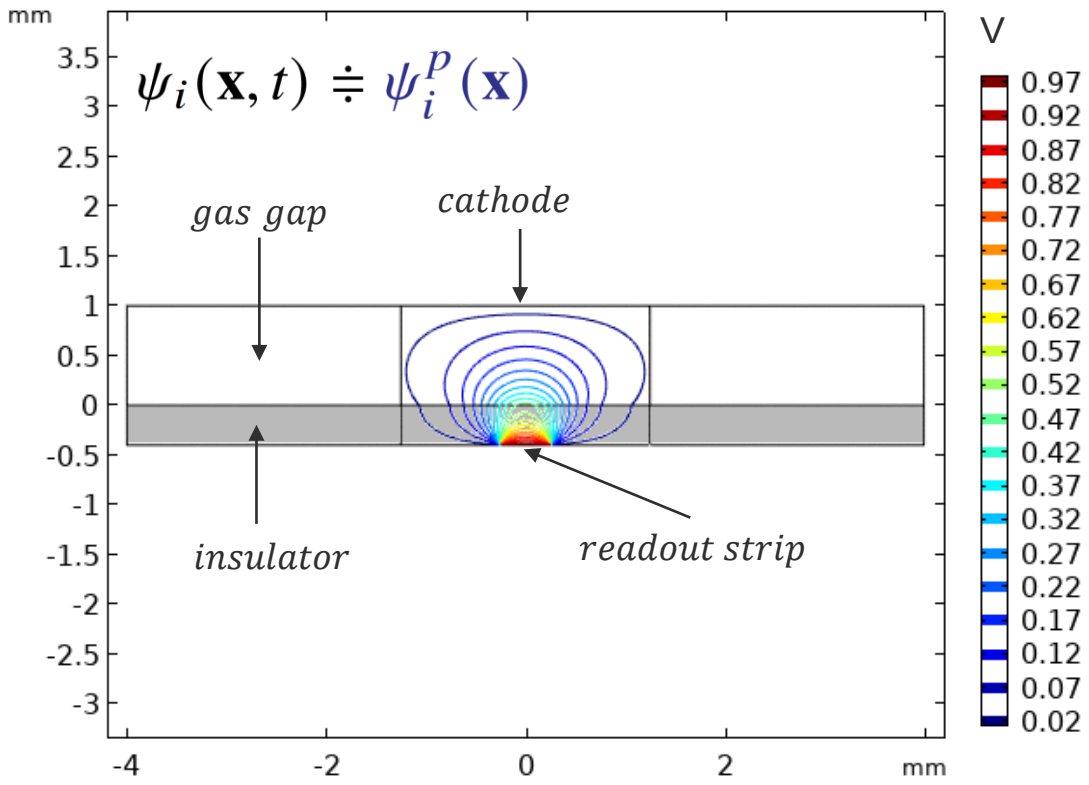

Dynamic weighting potential of a readout strip with resistive layer

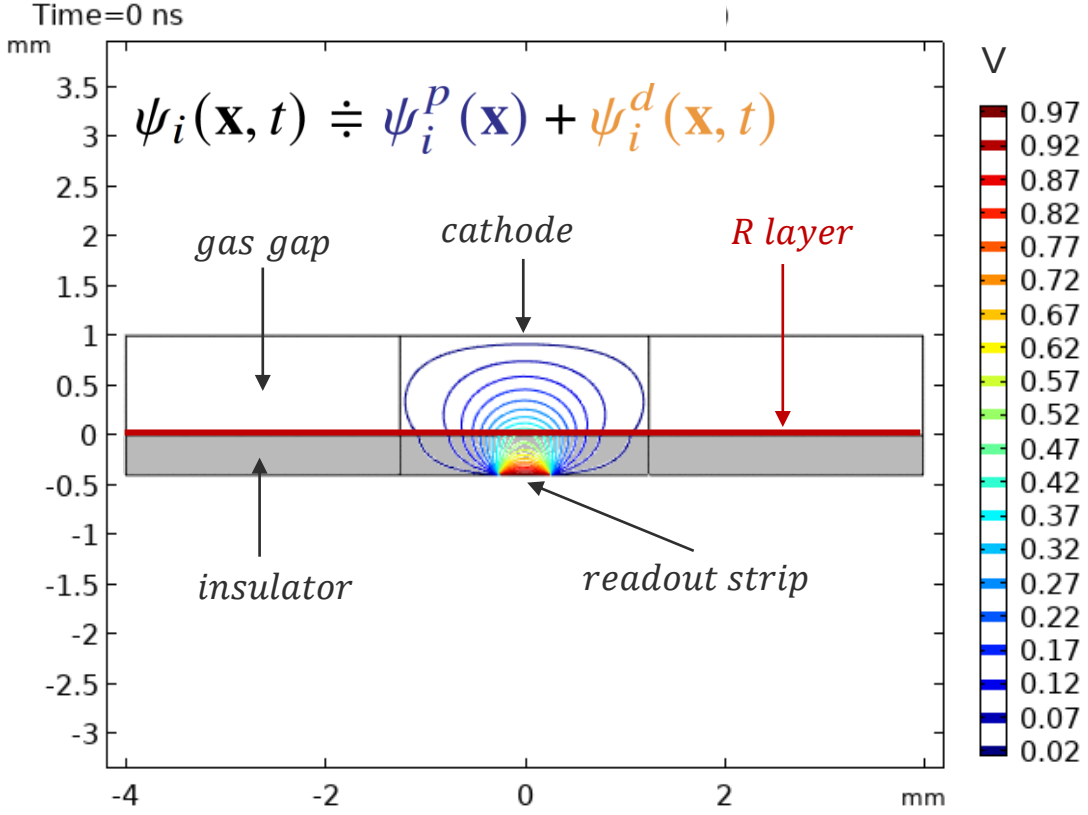

Resistive strip bulk Micromegas

While the previous slide the embedded readout electrodes were beneath a thin resistive layer, the ATLAS-type MM, used in the NSW upgrade, instead features perpendicular resistive strips over a dielectric foil.

Here we use a 2D strip readout to capture the delayed component coming from the resistive strips.

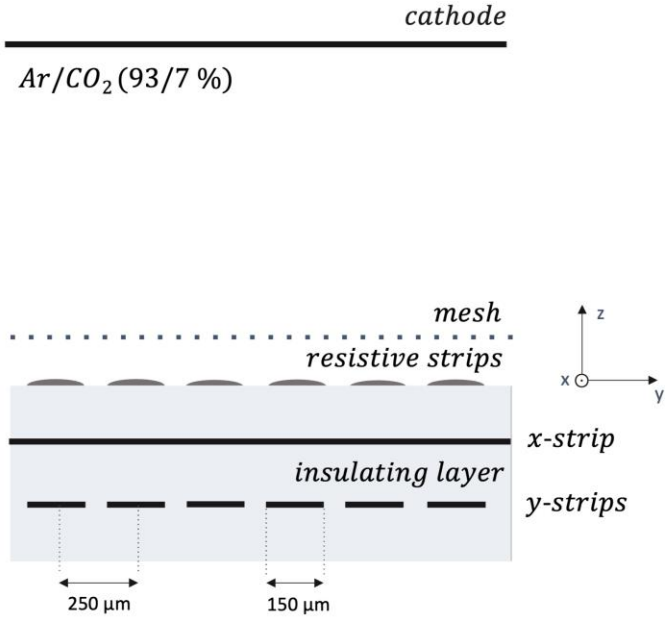

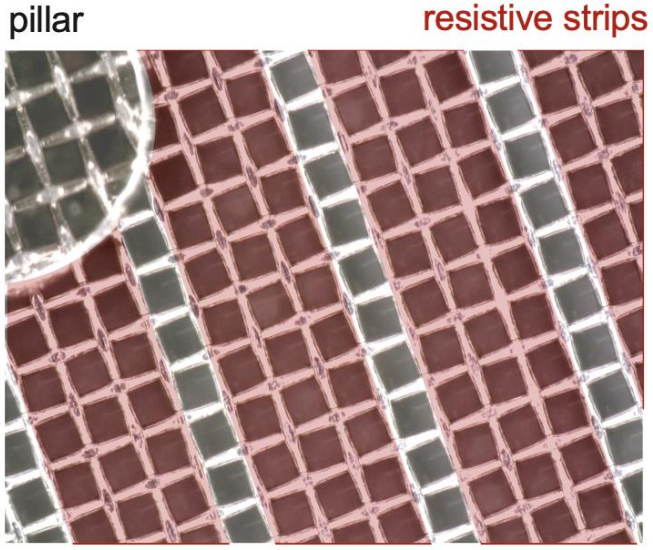

Calculated dynamic weighting potential

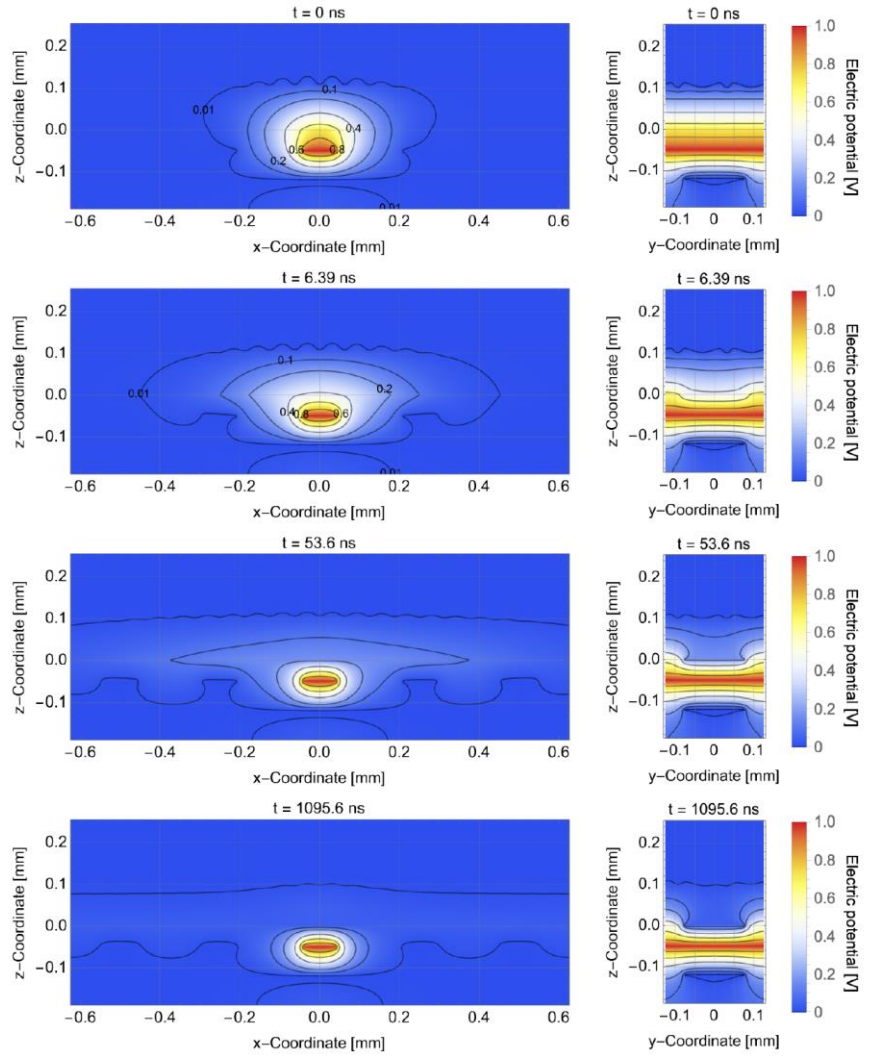

T. Alexopoulos, et al., Nucl. Instrum. Meth. A 640 (2011) 110.
M. Byszewski and J. Wotschack, JINST 7 C02060 (2011).

Resistive strip bulk Micromegas

After having calculated the signals induced on the strip electrodes, the electronics with which the detector is read out needs to be taken into account.

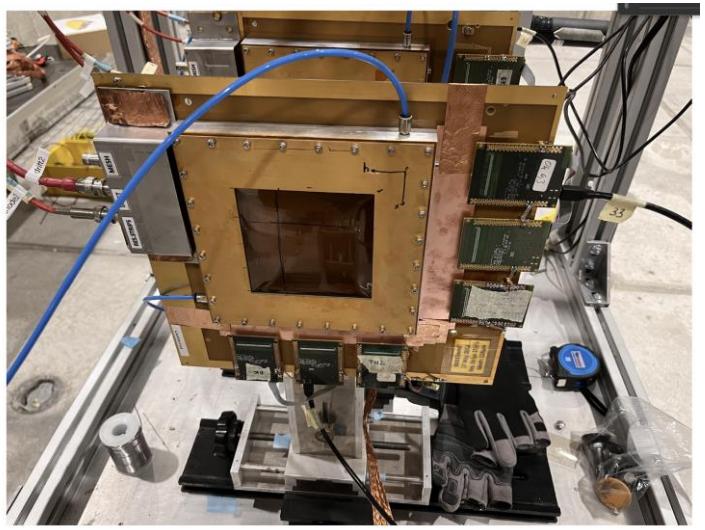

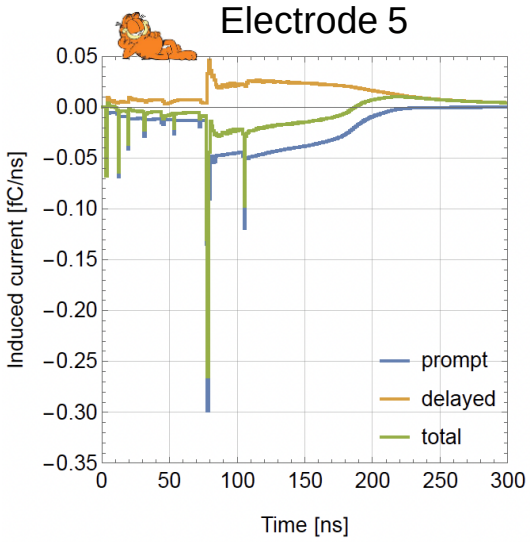

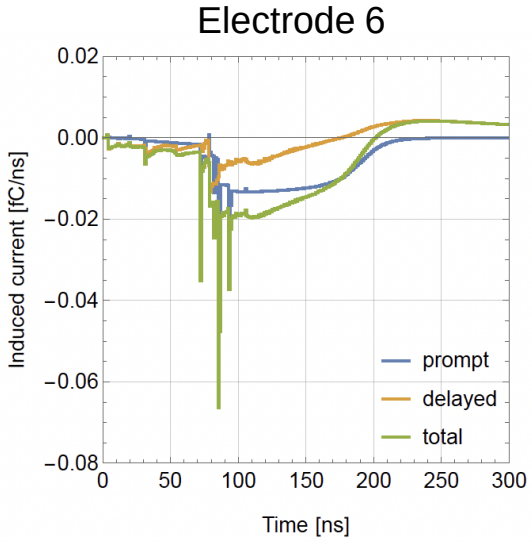

APV25

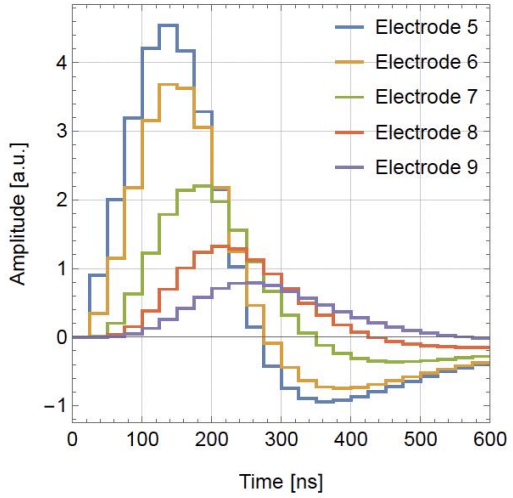

Resistive strip bulk Micromegas

For the comparison we look at the average induced current response of neighboring strips. This averaging is performed over muon events positioned between the leading and the next-to-leading strip.

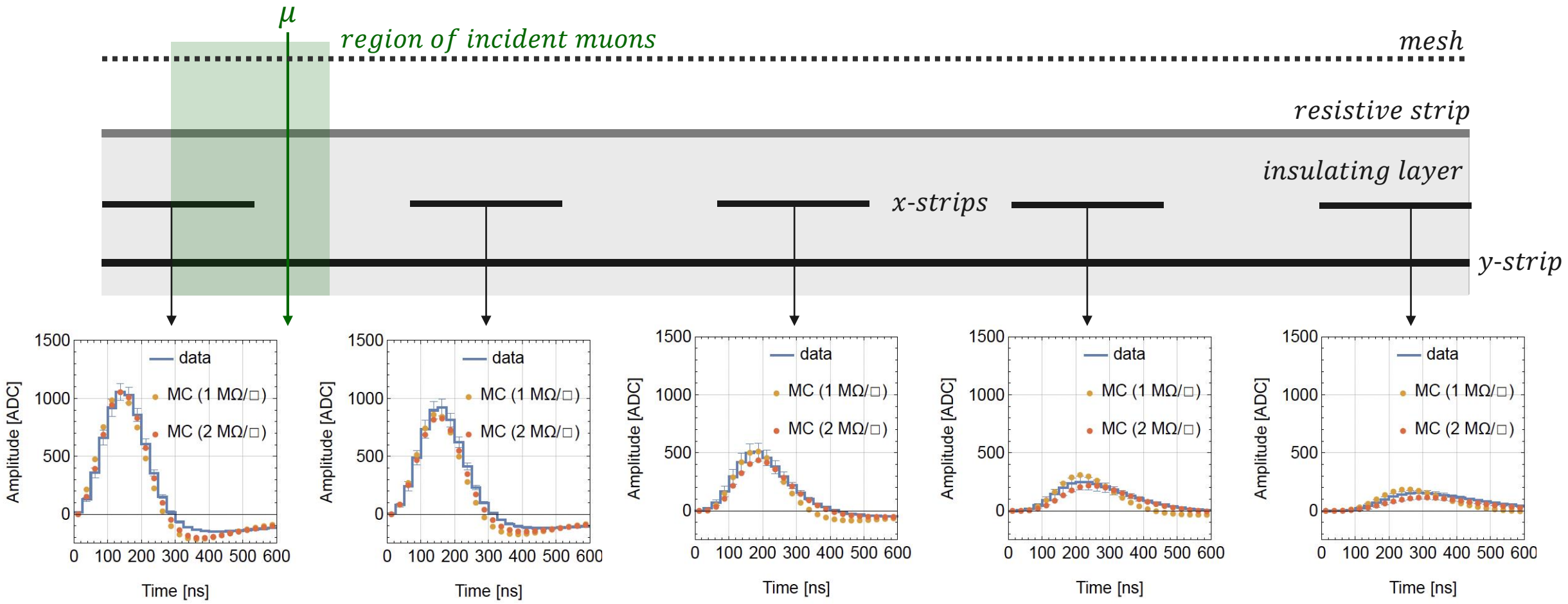

6-gap MRPC

The dynamic weighting potential was calculated using COMSOL and then imported into Garfield++ for the induced signal calculations. Given a graphite layers with O(100 kΩ/□), the signal induced by electrons remains unaffected.

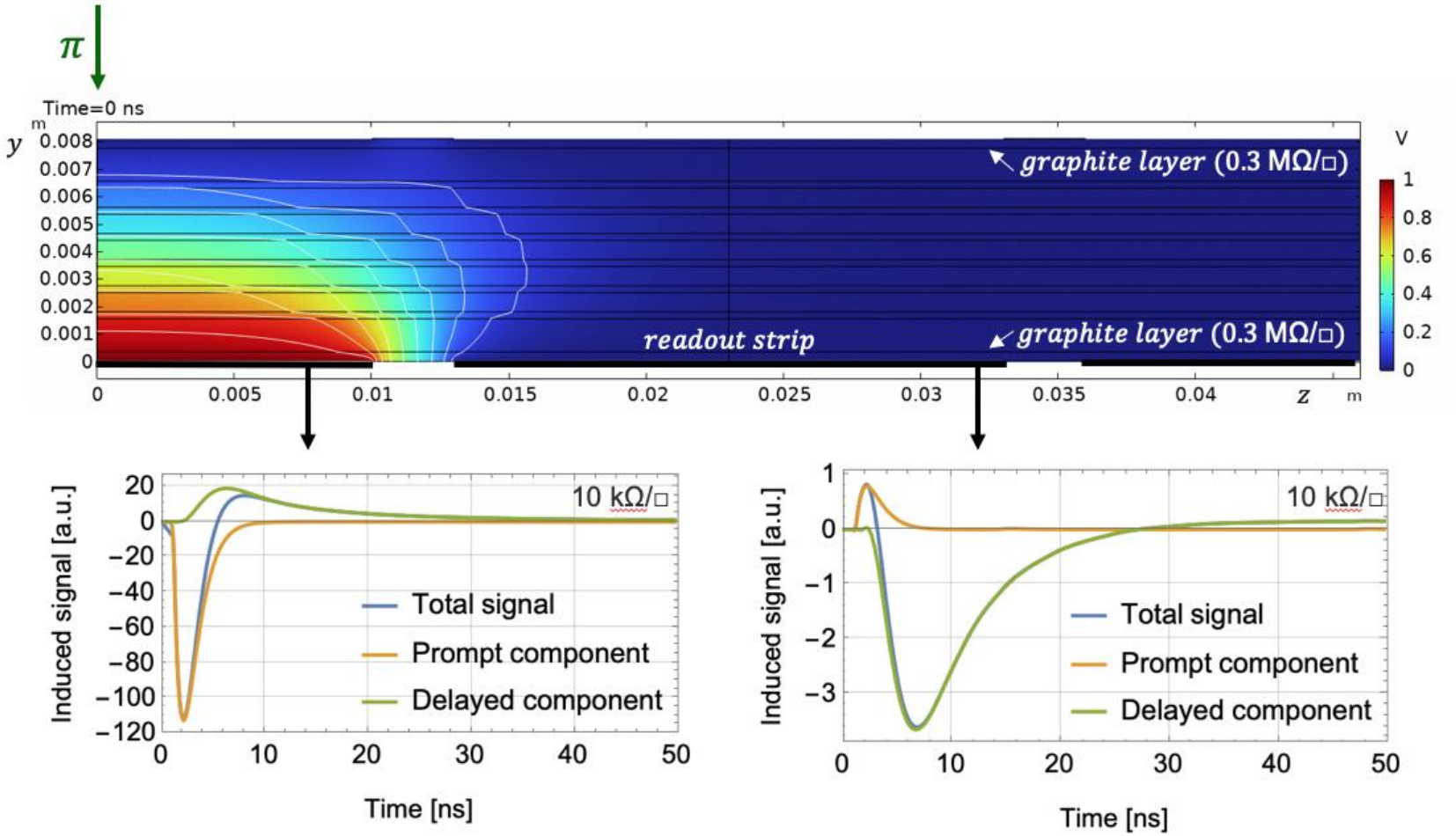

Consistent with G. Battistoni et al., NIM in Physics Research 202 (1982) 459.

6-gap MRPC

The dynamic weighting potential was calculated using COMSOL and then imported into Garfield++ for the induced signal calculations. Given a graphite layers with O(100 kΩ/□), the signal induced by electrons remains unaffected.

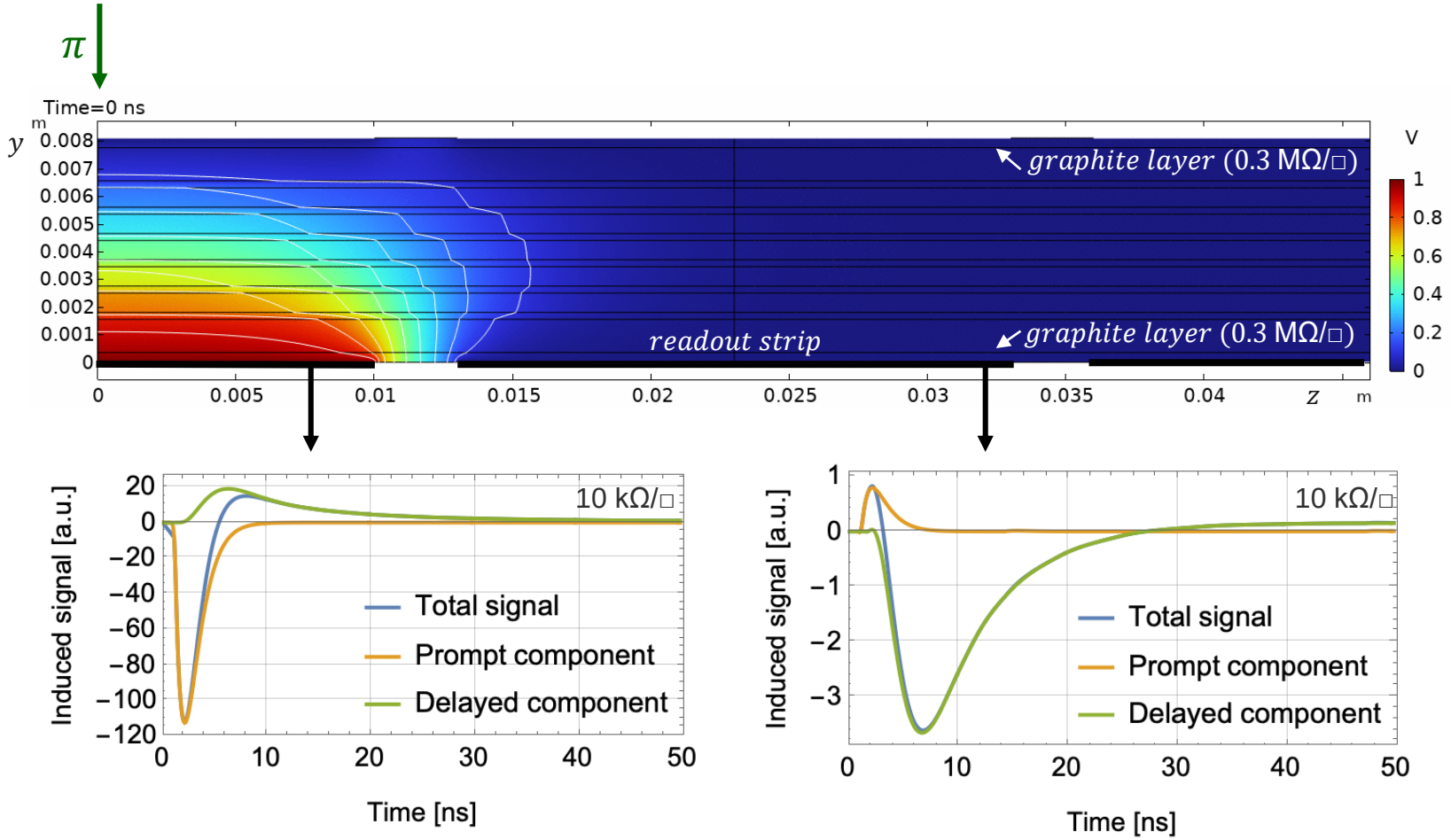

Consistent with G. Battistoni et al., NIM in Physics Research 202 (1982) 459.

Signal formation in a MicroCAT detector

The MicroCAT's two-dimensional interpolating readout structure allows for a reduced number of electronic readout channels without loss of spatial resolution.

This resistive readout concept has recently enjoyed renewed interest with the development of a DC-Coupled LGAD device: *arXiv:2204.07226 [physics.ins-det]*.

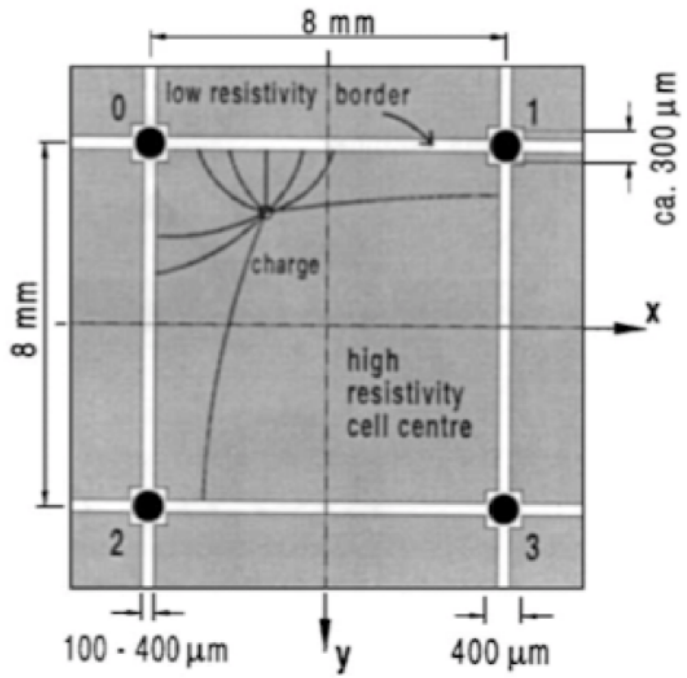

Weighting potential map for one readout node

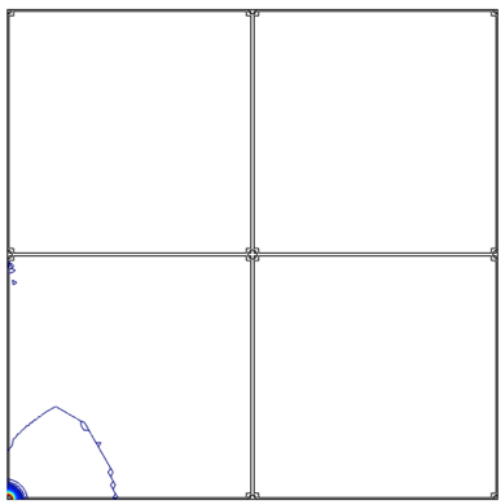

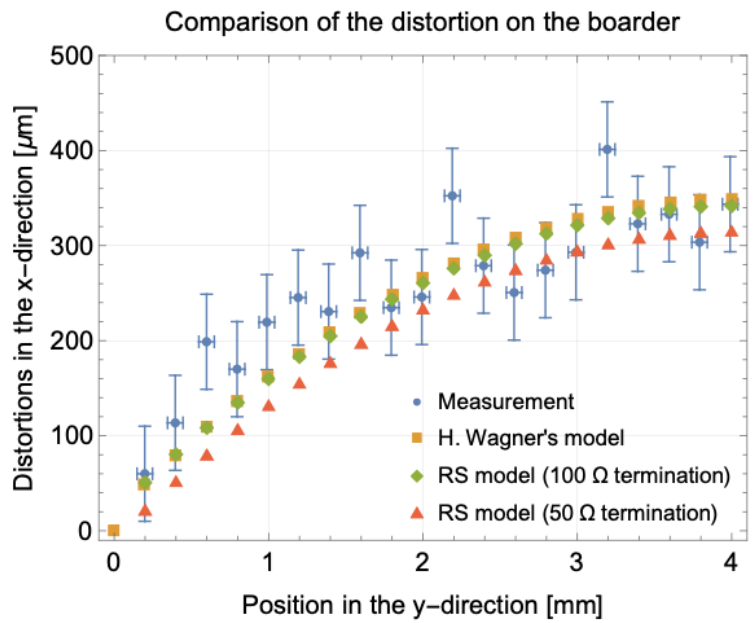

F. Bartol et al. J. Phys. III France, 6 (1996), p. 337
A. Sarvestani et al., Nucl. Instrum. Meth. A 410 (1998) 238–258
H. Wagner et al. Nucl. Instrum. Meth. A 482 (2002) 334–346

Signal formation in a MicroCAT detector

The MicroCAT's two-dimensional interpolating readout structure allows for a reduced number of electronic readout channels without loss of spatial resolution.

This resistive readout concept has recently enjoyed renewed interest with the development of a DC-Coupled LGAD device: *arXiv:2204.07226 [physics.ins-det]*.

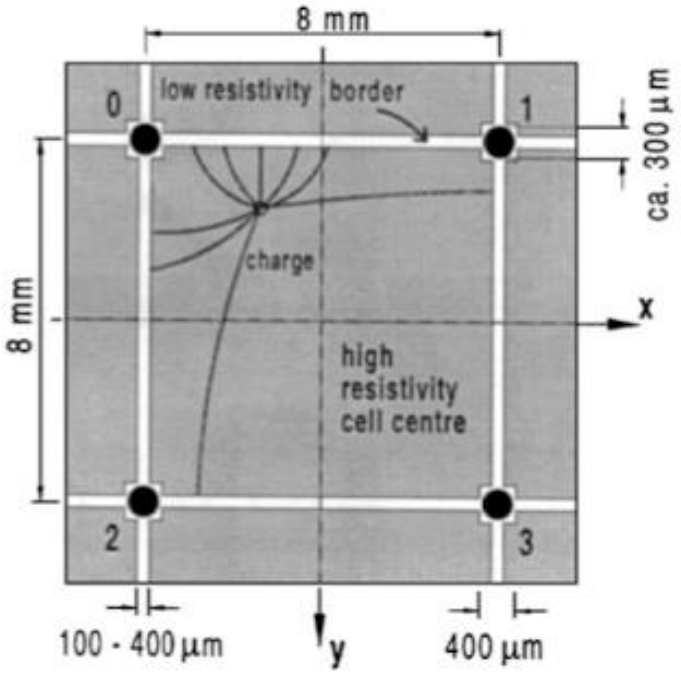

Weighting potential map for one readout node

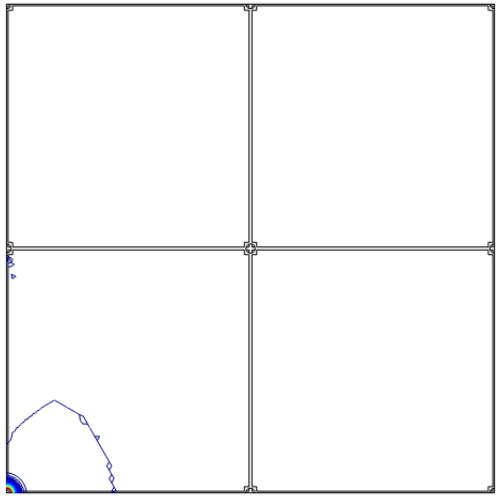

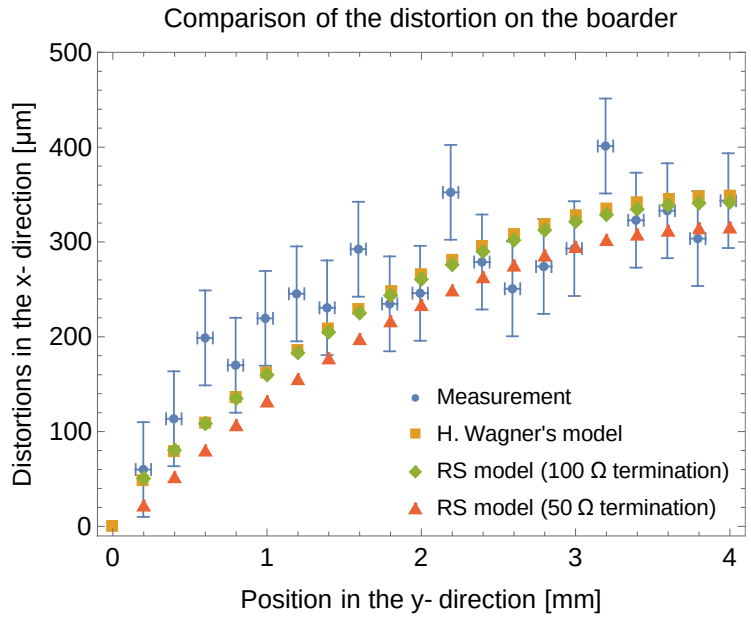

F. Bartol et al. J. Phys. III France, 6 (1996), p. 337
A. Sarvestani et al., Nucl. Instrum. Meth. A 410 (1998) 238–258
H. Wagner et al. Nucl. Instrum. Meth. A 482 (2002) 334–346

MicroCAT resistive position interpolation readout

During production, the resistivity can fluctuate on the surface of the resistive layer. This could make the timing response or reconstruction capability of your detector non-uniform over the active area.

High-Precision 4D Tracking with Large Pixels using Thin Resistive Silicon Detectors

R. Arcidiacono[a,b,*], G. Borghi[d], M. Boscardin[e], N.Cartiglia[a], M. Centis Vignali[e], M. Costa[c], G-F. Dalla Betta[f], M. Ferrero[a], F. Ficorella[e], G. Gioachin[c], L. Lanteri[c], M. Mandurrino[a], L. Menzio[a], R. Mulargia[a,c], L. Pancheri[f], G. Paternoster[e], A. Rojas[a], H-F W. Sadrozinski[g], A. Seiden[g], F. Siviero[a], V. Sola[a,c], M. Tornago[a,c]

[a] *INFN, Sezione di Torino, Italy*
[b] *Università del Piemonte Orientale, Italy*
[c] *Università di Torino, Torino, Italy*
[d] *Politecnico di Milano, Milano, Italy*
[e] *Fondazione Bruno Kessler, Trento, Italy*
[f] *Università degli Studi di Trento, Trento, Italy*
[g] *University of California at Santa Cruz, CA, US*

- σ_{sensor} this term groups all sensor imperfections contributing to an uneven signal sharing among pads. The most obvious one is a varying n^+ resistivity: a 2% difference in n^+ resistivity turns an equal signal mV - 50.5 mV split, yielding a shift of the position assignment of ~ 7 μm for the 450 μm geometry and 20 μm for the 1300 μm design. The uniformity of the n^+ resistive layer (and that of the gain implant) is a crucial parameter in RSD optimized for micron-level position resolution.

R. Arcidiacono et al., arXiv:2211.13809v1 [physics.ins-det]

Map of non-uniform resistivity in one readout cell

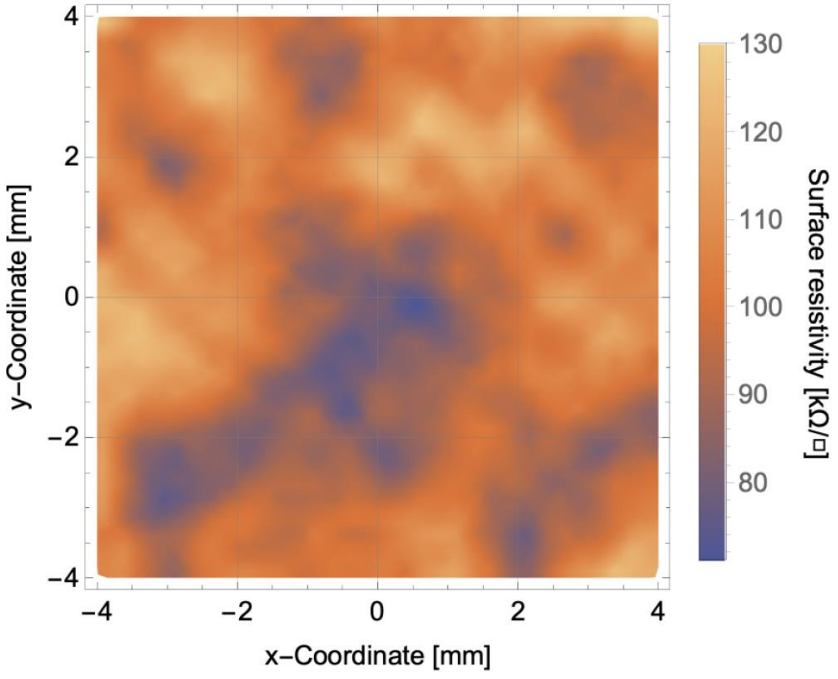

Correction map

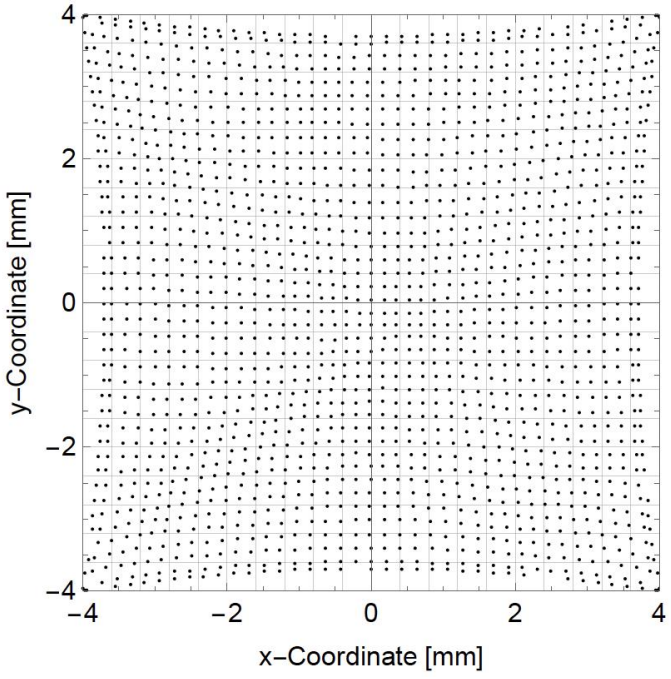

Resistive Silicon Detectors

An exemplar geometry that makes full use of the dynamics of the resistive layers is the Resistive Silicon Detectors (RSDs) by spreading the signal to surrounding "small" electrodes.

Here, an n^+ resistive layer of $\mathcal{O}(k\Omega/\square)$ is separated from the readout electrodes by a SiO_2 layer.

LGAD

RSD

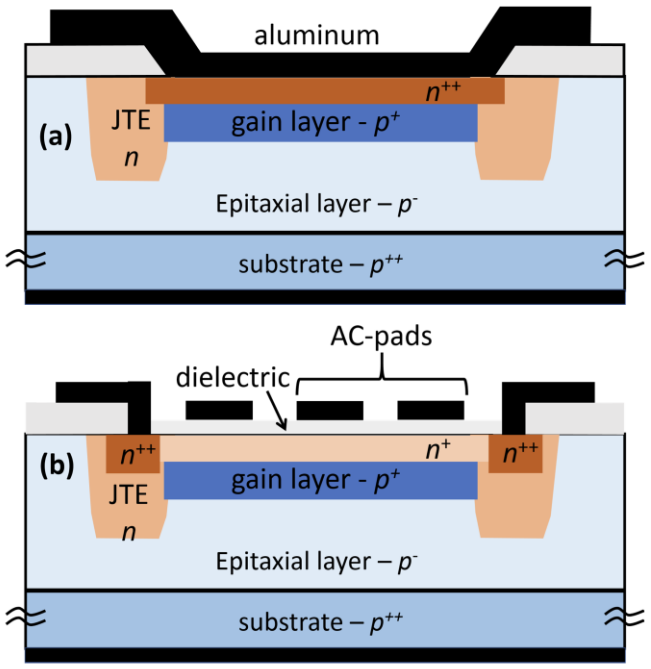

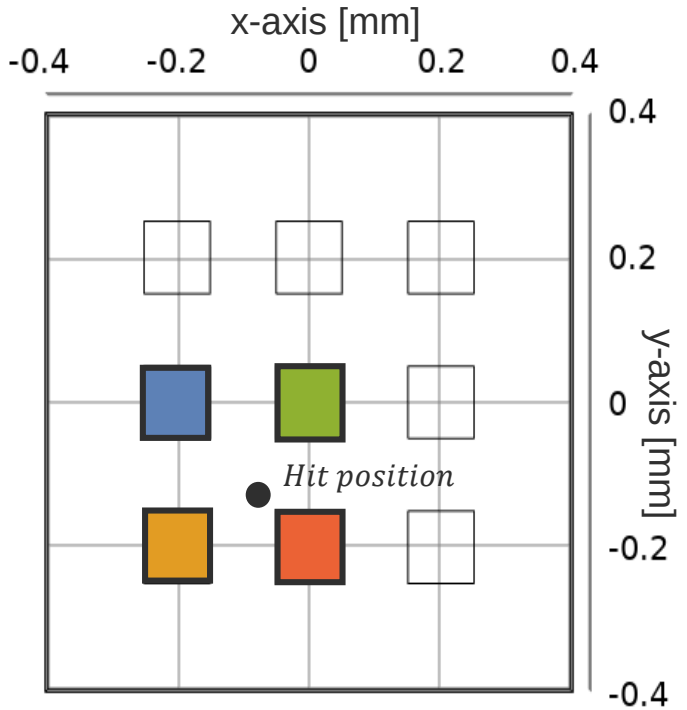

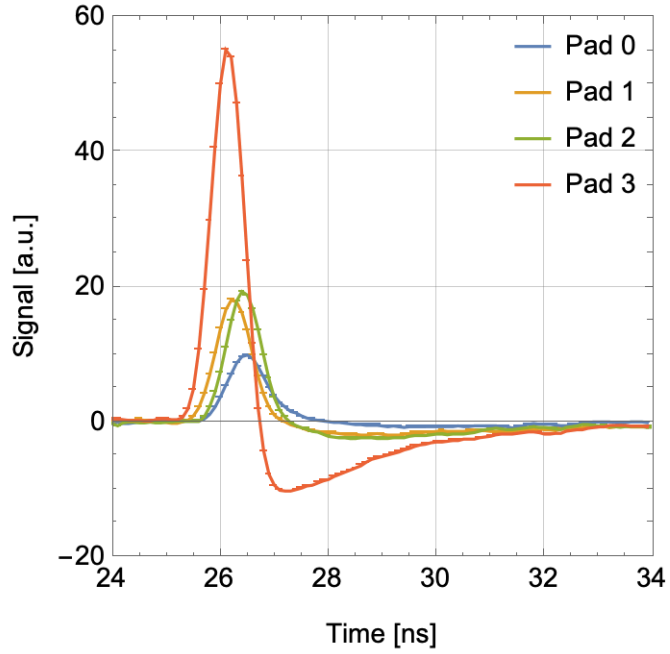

M. Tornago, R. Arcidiacono, N. Cartiglia et al., Nucl. Instrum. Meth. A **1003** (2021).

Resistive Silicon Detectors

We can plot the induced signal sourced by a moving hole traversing the 50 µm gap and arriving at time t= T.

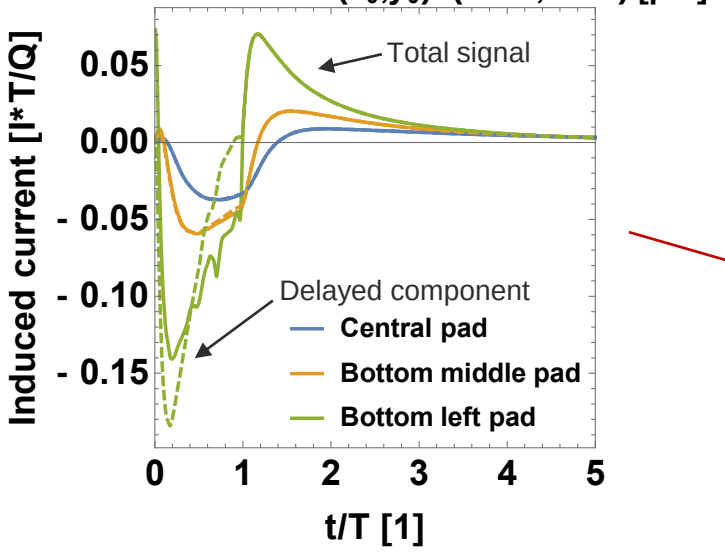

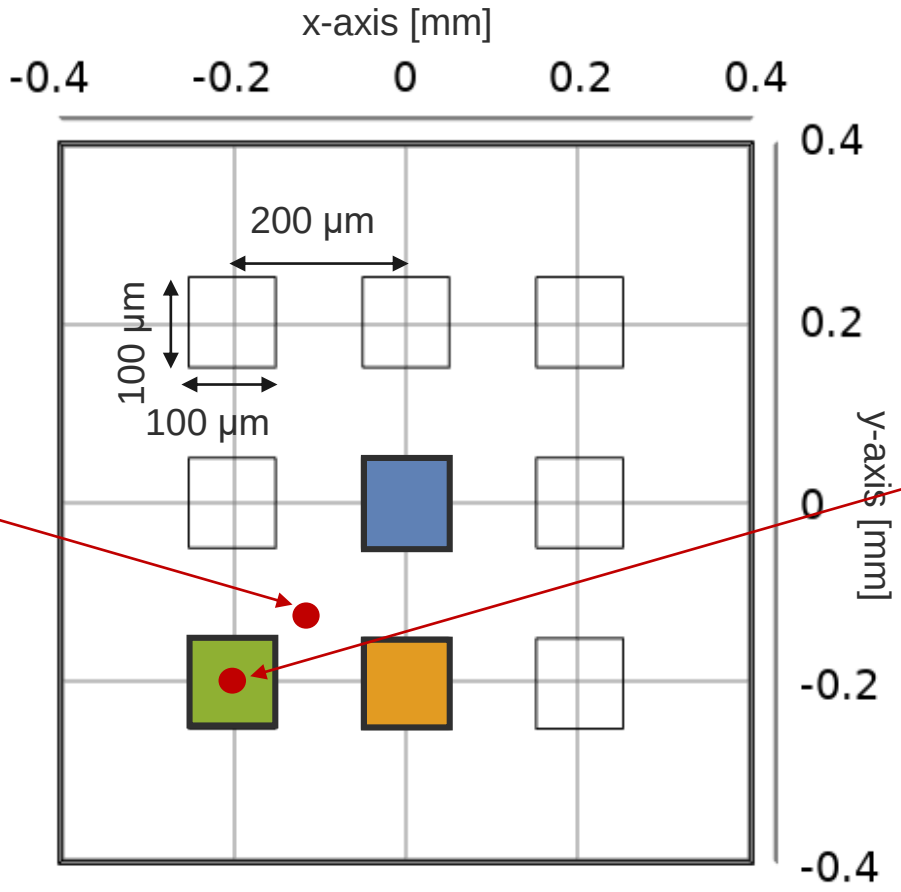

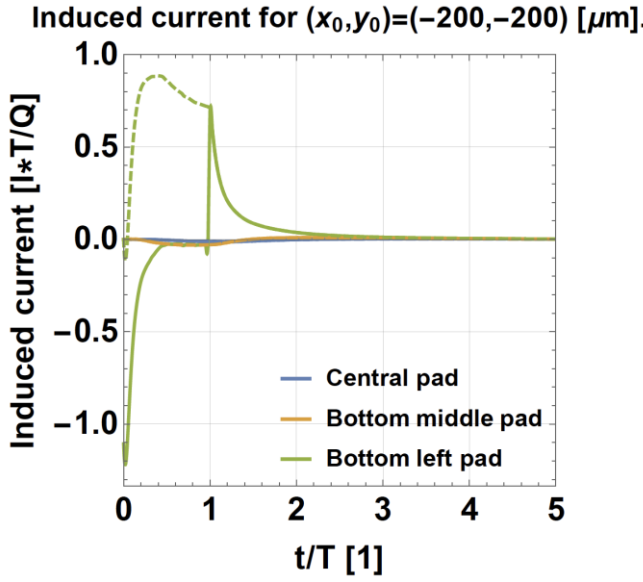

Resistive Silicon Detectors

It is suggested that to optimize for a uniform response, the electrodes should maximize pixel coverage to control signal spread while minimizing metal use to ensure a uniform response across the entire area. Different AC-coupled readout structures are suggested.

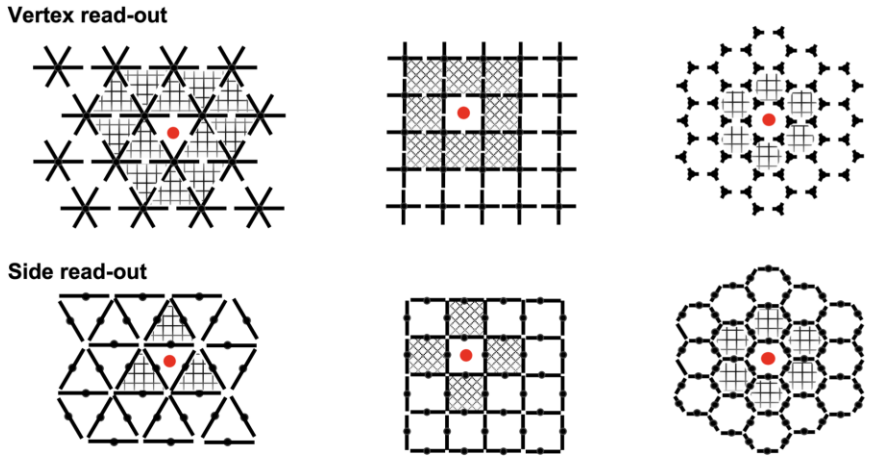

R. Arcidiacono et al., arXiv:2211.13809v1 [physics.ins-det]

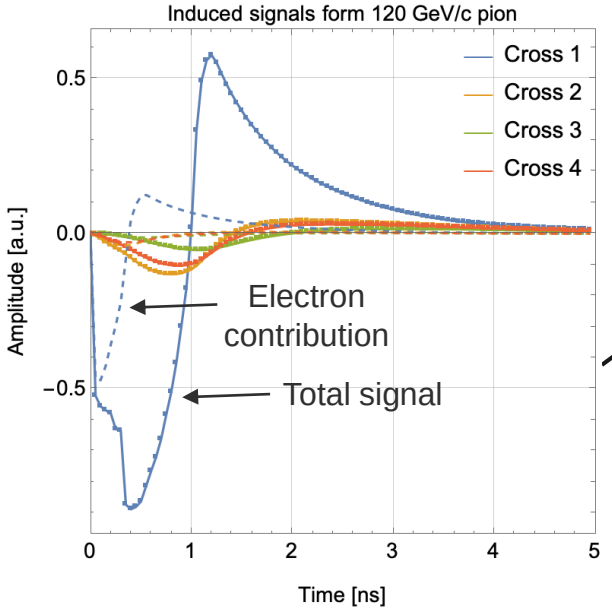

Dynamic weighting potential at the 1 kΩ/□ resistive layer

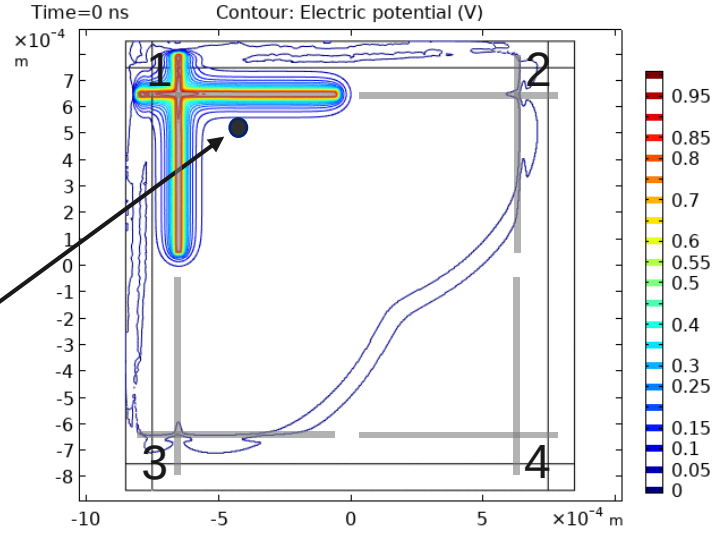

3D diamond sensor

3D Silicon Sensor

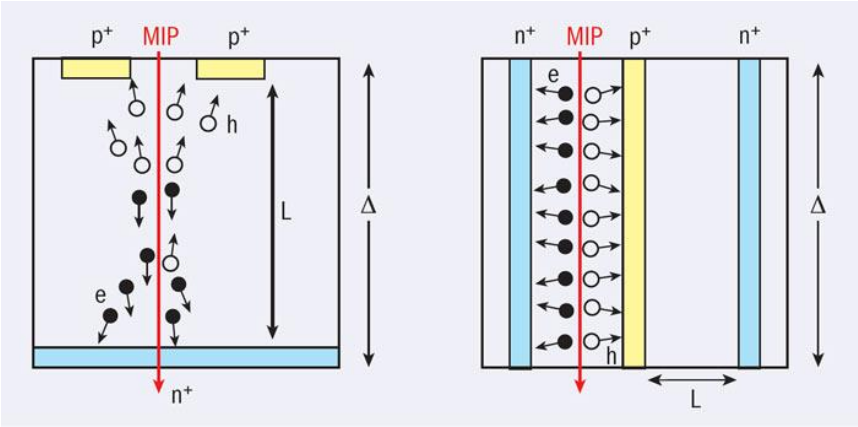

3D Diamond Sensor, electrodes are ‘burnt’ into the diamond with a laser. Columns have significant resistivity.

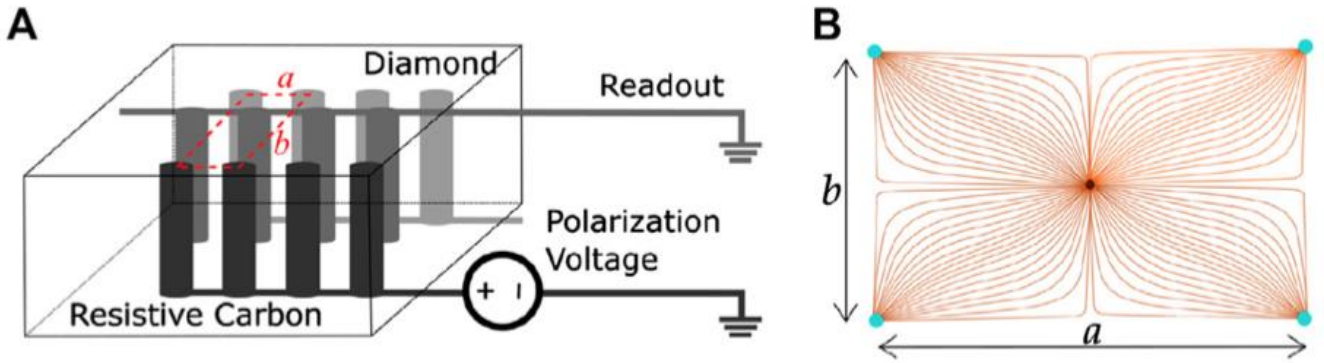

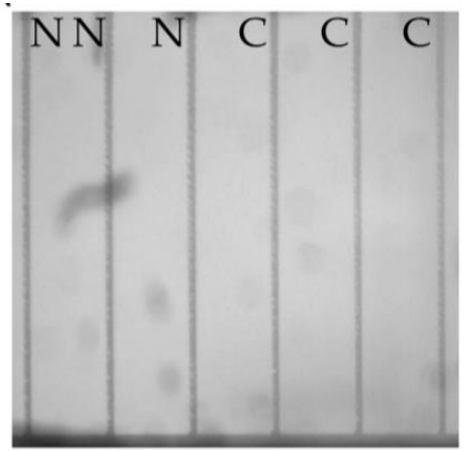

3D Diamond sensor

In contrast to its silicon counterpart, the 3D electrode structure is achieved by inducing a local phase transition in the diamond, resulting in graphitic pillar electrodes that have a finite conductivity.

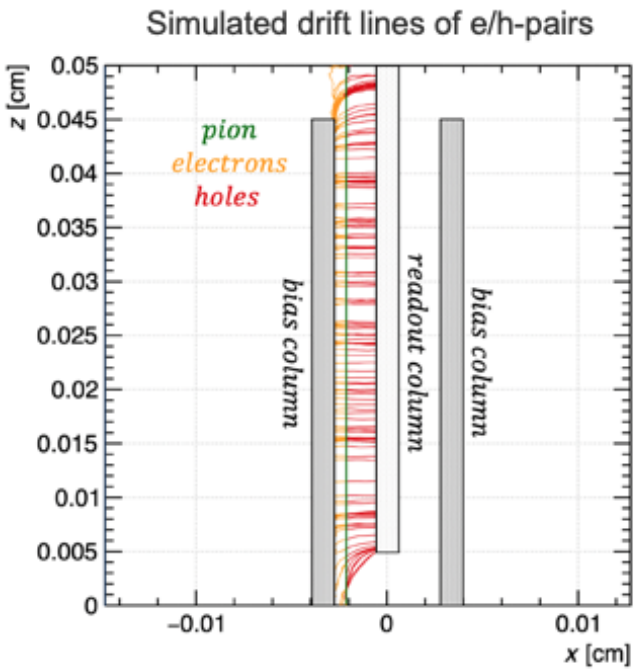

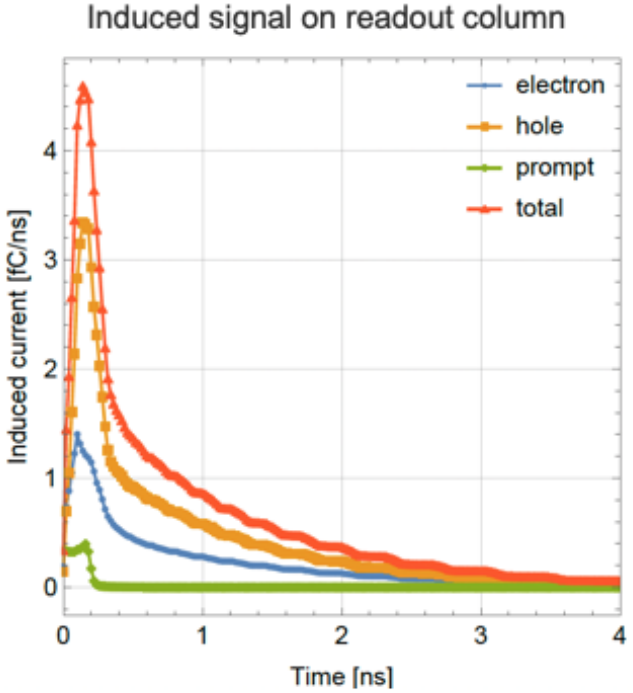

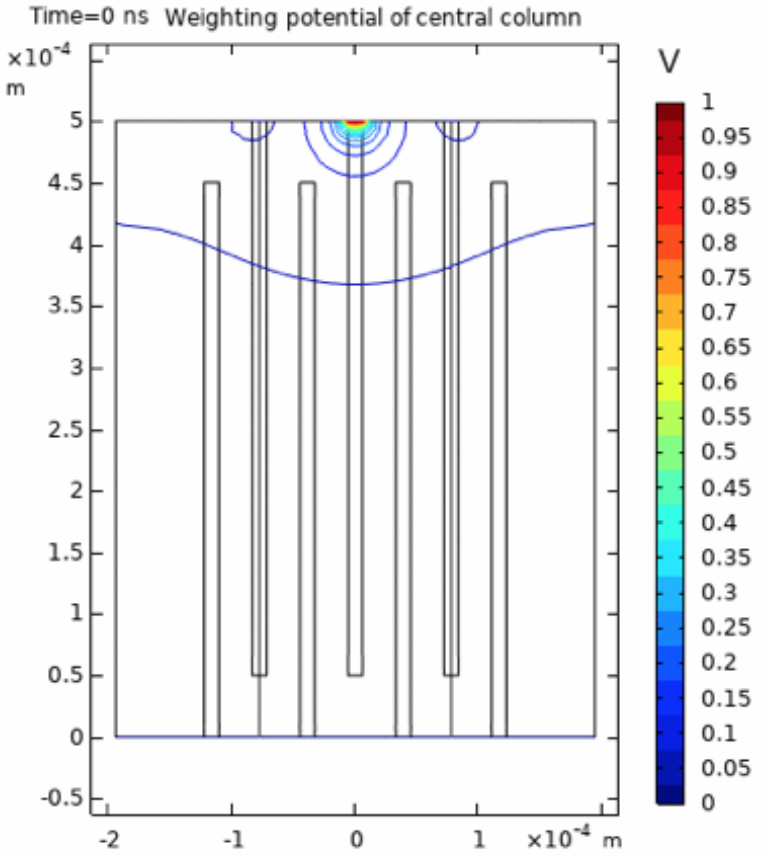

Thanks to the fruitful discussions with the TIMESPOT collaboration.

3D Diamond sensor

In contrast to its silicon counterpart, the 3D electrode structure is achieved by inducing a local phase transition in the diamond, resulting in graphitic pillar electrodes that have a finite conductivity.

Simulated drift lines of e/h-pairs

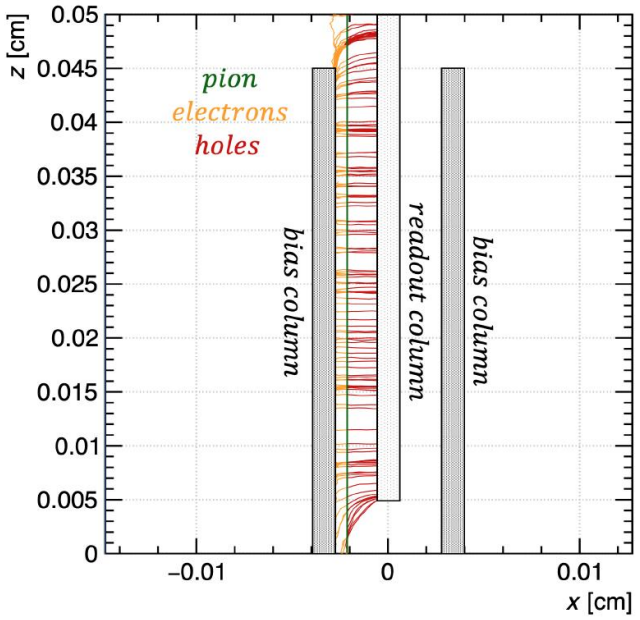

Induced signal on readout column

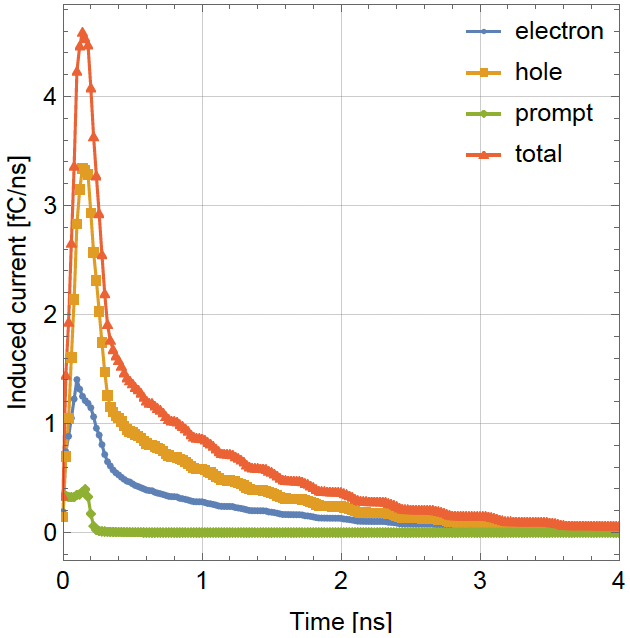

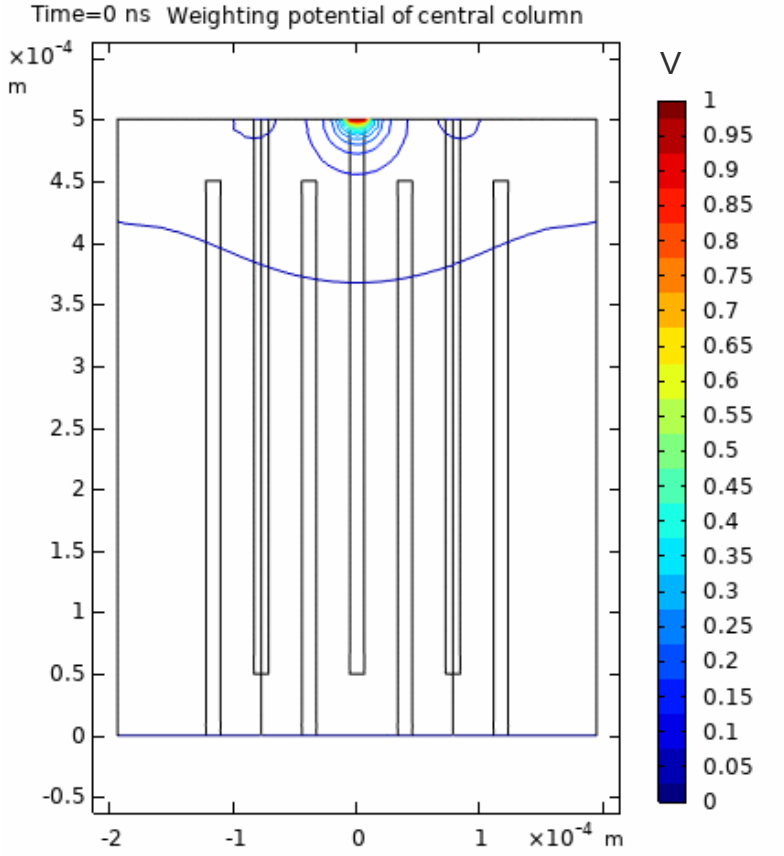

Djunes Janssens

Thanks to the fruitful discussions with the TIMESPOT collaboration.

3D Diamond sensor

Simulations are conducted by the TIMESPOT organization, and the analysis results can be compared with those from a beam test carried out in 2021 at CERN's SPS, using 180 GeV/c hadrons.

Simulated signal amplitude

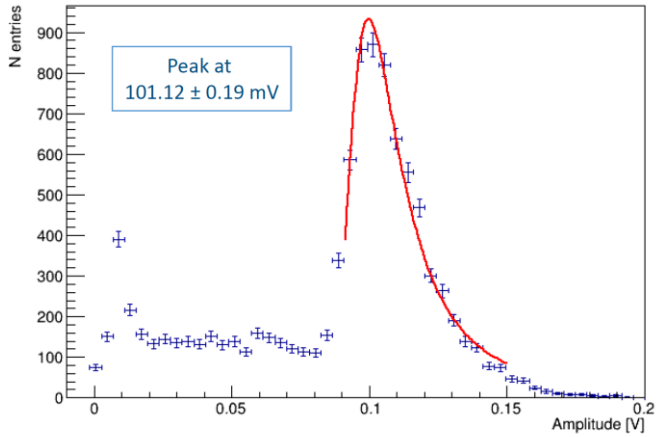

Measured signal amplitude

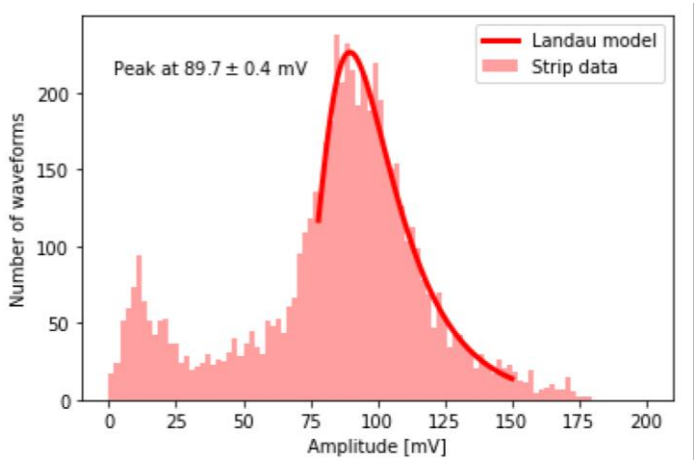

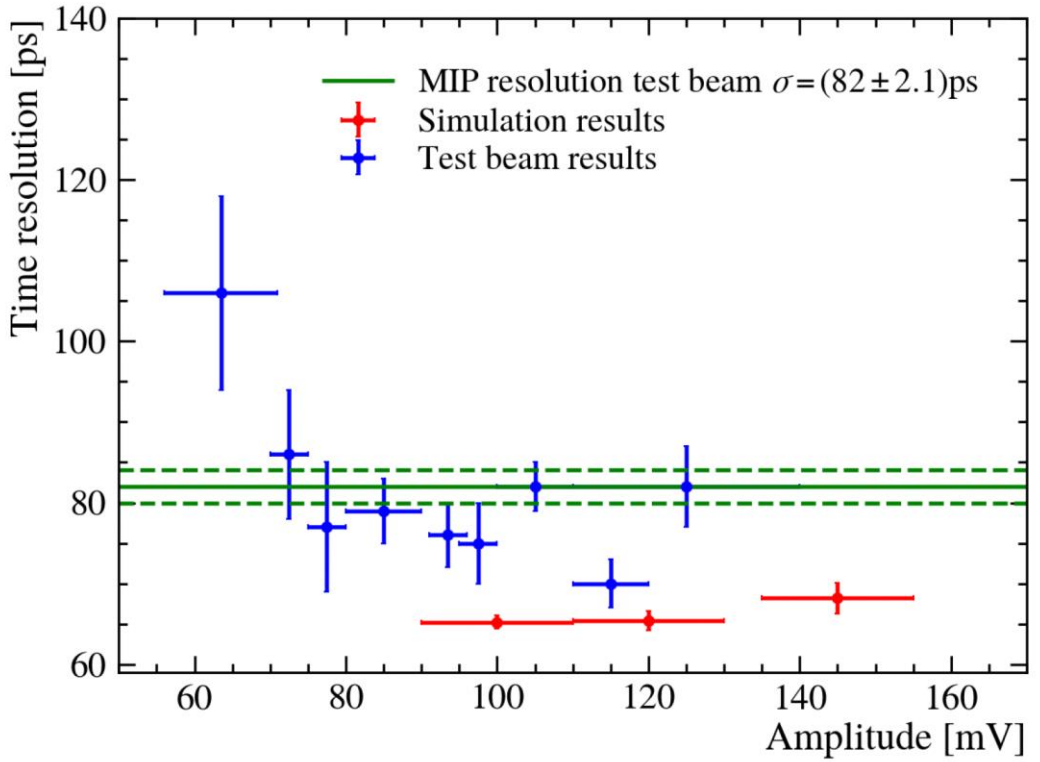

Djunes Janssens

Work from C. Buti's thesis, and, by extension, the TIMESPOT organization.

Further extensions of the theorem

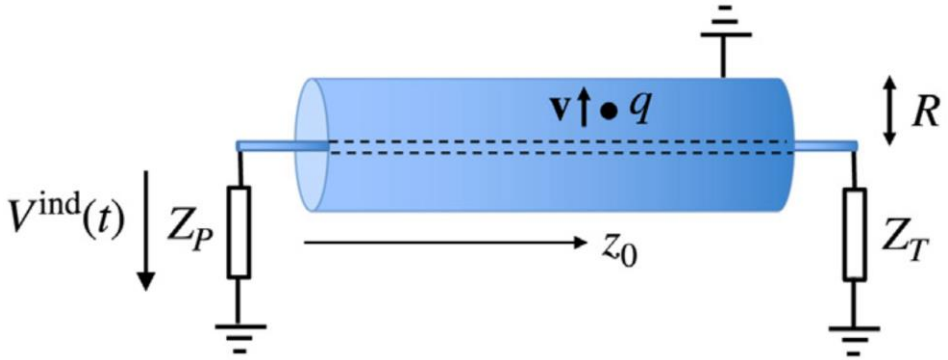

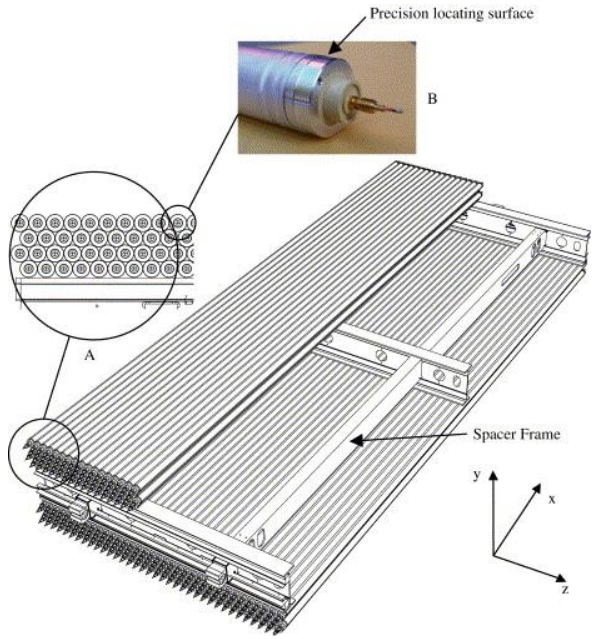

When calculating the induced signals in ‘long’ detectors e.g. wire chambers like the ATLAS muon drift tubes, we intuitively proceed the following way:

- → We calculate the induced signal in the geometry assuming the Ramo Shockley theorem.
- → We place this signal as a current source at one specific point inside the equivalent circuit of the detector, which is in this case a transmission line.
- → We find the propagated signal at the end of the transmission line.

Clearly this seems like an approximation.

- → The Ramo Shockley theorem assumes the instantaneous creation of the signal on the entire electrode.
- → The extension of the theorem for weak conductivity is clearly not applicable. The propagation of the signal in a transmission line needs the full set Maxwell equations

Can one further extend the Weighting field concept ?

Further extensions of the weighting field concept

https://en.wikipedia.org/wiki/Reciprocity_(electromagnetism)

Electrostatic Reciprocity

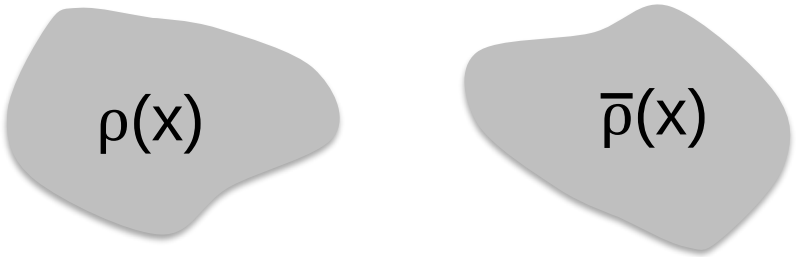

$$\int \overline{\rho}(\mathbf{x})\varphi(\mathbf{x})d^3x = \int \rho(\mathbf{x})\overline{\varphi}(\mathbf{x})d^3x$$

Lorentz reciprocity [edit]

Specifically, suppose that one has a current density $\mathbf{J}_1$ that produces an electric field $\mathbf{E}_1$ and a magnetic field $\mathbf{H}_1$, where all three are periodic functions of time with angular frequency ω, and in particular they have time-dependence $\exp(-i\omega t)$. Suppose that we similarly have a second current $\mathbf{J}_2$ at the same frequency ω which (by itself) produces fields $\mathbf{E}_2$ and $\mathbf{H}_2$. The Lorentz reciprocity theorem then states, under certain simple conditions on the materials of the medium described below, that for an arbitrary surface S enclosing a volume V:

$$\int_V [\mathbf{J}_1 \cdot \mathbf{E}_2 - \mathbf{E}_1 \cdot \mathbf{J}_2]\, \mathrm{d}V = \oint_S [\mathbf{E}_1 \times \mathbf{H}_2 - \mathbf{E}_2 \times \mathbf{H}_1] \cdot \mathrm{d}\mathbf{S}\ .$$

Equivalently, in differential form (by the divergence theorem):

$$\mathbf{J}_1 \cdot \mathbf{E}_2 - \mathbf{E}_1 \cdot \mathbf{J}_2 = \nabla \cdot [\mathbf{E}_1 \times \mathbf{H}_2 - \mathbf{E}_2 \times \mathbf{H}_1]\ .$$

This general form is commonly simplified for a number of special cases. In particular, one usually assumes that $\mathbf{J}_1$ and $\mathbf{J}_2$ are localized (i.e. have compact support), and that there are no incoming waves from infinitely far away. In this case, if one integrates throughout space then the surface-integral terms cancel (see below) and one obtains:

$$\int \mathbf{J}_1 \cdot \mathbf{E}_2\, \mathrm{d}V = \int \mathbf{E}_1 \cdot \mathbf{J}_2\, \mathrm{d}V\ .$$

This result (along with the following simplifications) is sometimes called the **Rayleigh-Carson reciprocity theorem**, after Lord Rayleigh's work on sound waves and an extension by Carson (1924; 1930) to applications for radio frequency antennas. Often, one further simplifies this relation by considering point-like dipole sources, in which case the integrals disappear and one simply has the product of the electric field with the corresponding dipole moments of the currents. Or, for wires of negligible thickness, one obtains the applied current in one wire multiplied by the resulting voltage across another and vice versa; see also below.

Further extensions of the weighting field concept

Nuclear Inst. and Methods in Physics Research, A 980 (2020) 164471

Contents lists available at ScienceDirect

Nuclear Inst. and Methods in Physics Research, A

journal homepage: www.elsevier.com/locate/nima

Philipp Windischhofer

Signals induced on electrodes by moving charges, a general theorem for Maxwell's equations based on Lorentz-reciprocity

W. Riegler [a,*], P. Windischhofer [b]

[a] CERN, Switzerland
[b] University of Oxford, United Kingdom of Great Britain and Northern Ireland

ARTICLE INFO

Keywords:
Ramo–Shockley theorem
Signals
Weighting fields

ABSTRACT

We discuss a signal theorem for charged particle detectors where the finite propagation time of the electromagnetic waves produced by a moving charge cannot be neglected. While the original Ramo–Shockley theorem and related extensions are all based on electrostatic or quasi-electrostatic approximations, the theorem presented in this report is based on the full extent of Maxwell's equations and does account for all electrodynamic effects. It is therefore applicable to all devices that detect fields and radiation from charged particles.

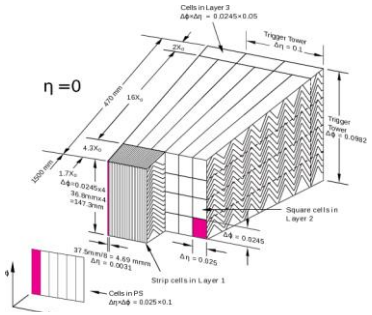

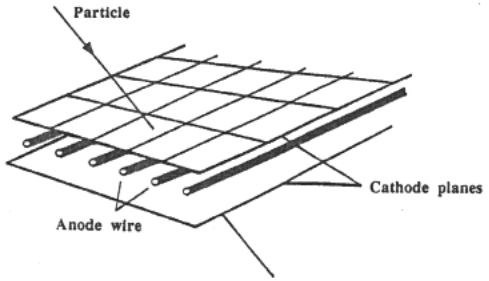

q

=

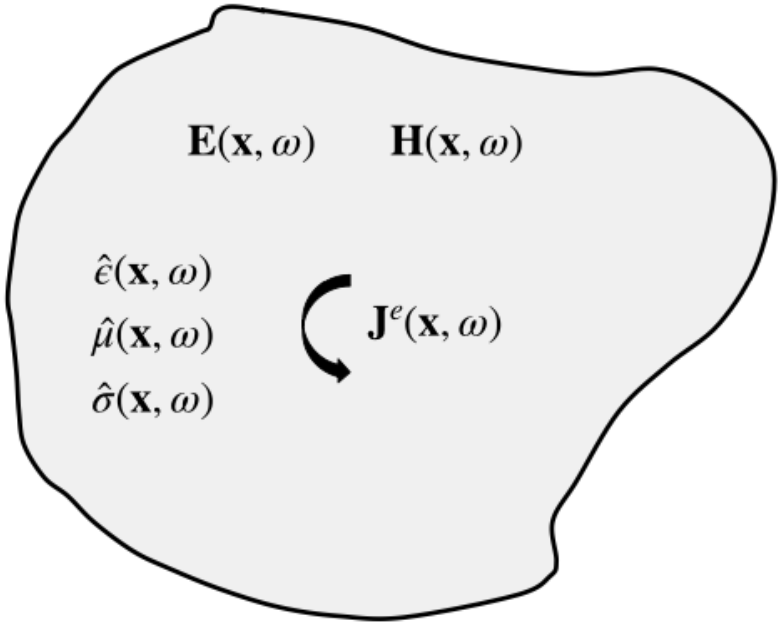

Any ‘object’ can, in classical electro-dynamic terms, be described by a position and frequency dependent

permittivity ε
permeability μ
conductivity σ

A charge moving around these objects represents a current, which produces fields.

Further extensions of the weighting field concept

Maxwell's Equations in the frequency domain

$$\mathbf{D} = \hat{\varepsilon}\mathbf{E} \qquad \mathbf{B} = \hat{\mu}\mathbf{H} \qquad \mathbf{J} = \hat{\sigma}\mathbf{E}$$

$$\nabla \cdot \hat{\varepsilon}\mathbf{E} = \rho \qquad \nabla \cdot \hat{\mu}\mathbf{H} = 0$$

$$\nabla \times \mathbf{E} = -i\omega\hat{\mu}\mathbf{H} \qquad \nabla \times \mathbf{H} = \mathbf{J}^e + \hat{\sigma}\mathbf{E} + i\omega\hat{\varepsilon}\mathbf{E}$$

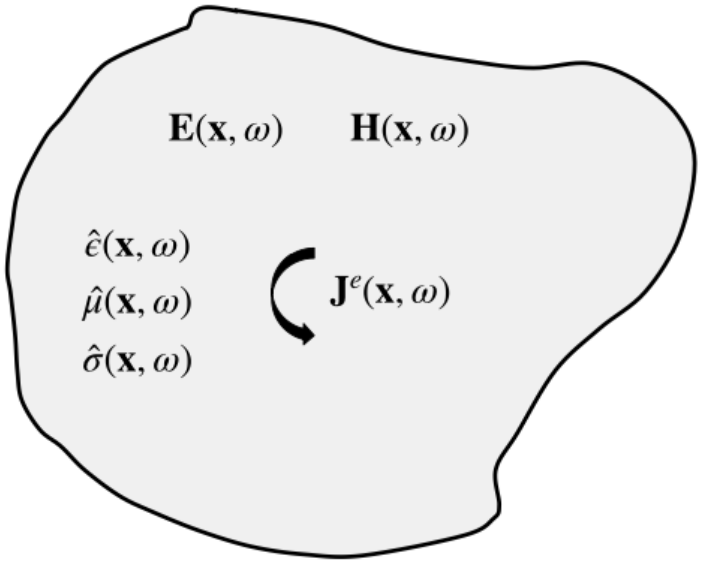

The solution of these equations will result in electric and magnetic fields that will define the signals in these detectors.

Further extensions of the weighting field concept

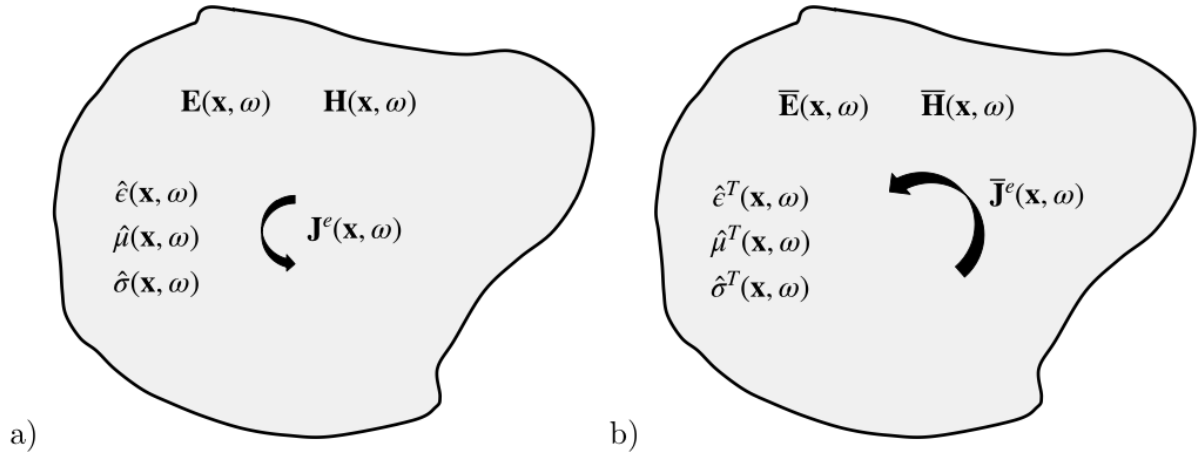

Fig. 1. Two different current densities in two material distributions that are related by a transposition of the response matrices.

We define another situation with a 'transposed' material distribution and a different current density $\bar{J}^e$.

Solving the Maxwell Equations with this current density will resilt in different electric and magnetic fields $\overline{E}$, $\overline{B}$.

$$\begin{aligned}\nabla\cdot(\mathbf{E}\times\overline{\mathbf{H}}) &= \overline{\mathbf{H}}(\nabla\times\mathbf{E}) - \mathbf{E}(\nabla\times\overline{\mathbf{H}})\\ &= -\mathbf{E}\overline{\mathbf{J}}^e - i\omega\overline{\mathbf{H}}\hat{\mu}\mathbf{H} - \mathbf{E}(\hat{\sigma}^T + i\omega\hat{\epsilon}^T)\overline{\mathbf{E}}\\ \nabla\cdot(\overline{\mathbf{E}}\times\mathbf{H}) &= \mathbf{H}(\nabla\times\overline{\mathbf{E}}) - \overline{\mathbf{E}}(\nabla\times\mathbf{H})\\ &= -\overline{\mathbf{E}}\mathbf{J}^e - i\omega\mathbf{H}\hat{\mu}^T\overline{\mathbf{H}} - \overline{\mathbf{E}}(\hat{\sigma} + i\omega\hat{\epsilon})\mathbf{E}\end{aligned}$$

subtract

$$\nabla(\mathbf{E}\times\overline{\mathbf{H}} - \overline{\mathbf{E}}\times\mathbf{H}) = \overline{\mathbf{E}}\mathbf{J}^e - \mathbf{E}\overline{\mathbf{J}}^e$$

$$\oint_A (\mathbf{E}\times\overline{\mathbf{H}} - \overline{\mathbf{E}}\times\mathbf{H})d\mathbf{A} = \int_V (\overline{\mathbf{E}}\mathbf{J}^e - \mathbf{E}\overline{\mathbf{J}}^e)dV$$

→

$$\int_V \overline{\mathbf{E}}(\mathbf{x},\omega)\mathbf{J}^e(\mathbf{x},\omega)dV = \int_V \mathbf{E}(\mathbf{x},\omega)\overline{\mathbf{J}}^e(\mathbf{x},\omega)dV$$

Lorentz Reciprocity Theorem

Two immediate consequences:
→ Network Reciprocity
→ Antenna Reciprocity

Network reciprocity

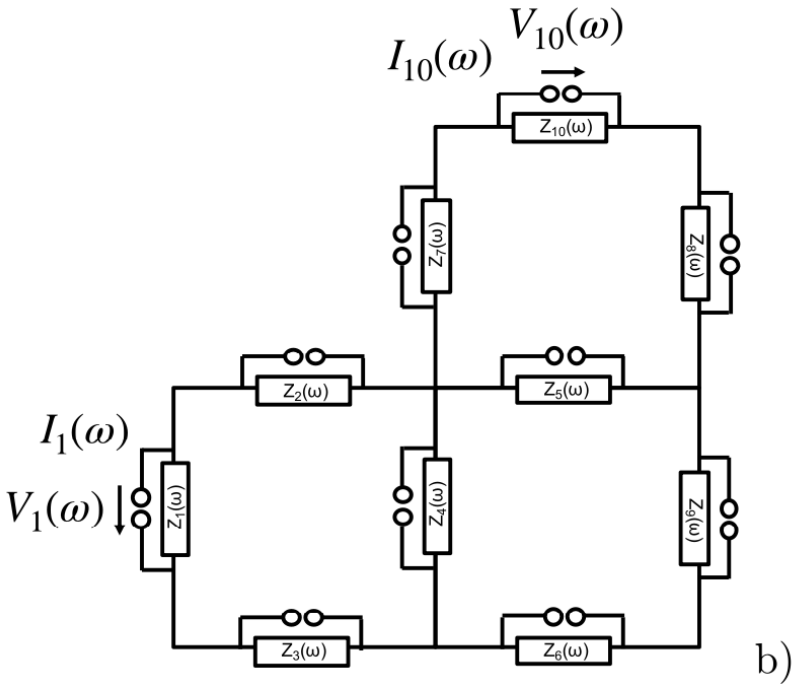

b)

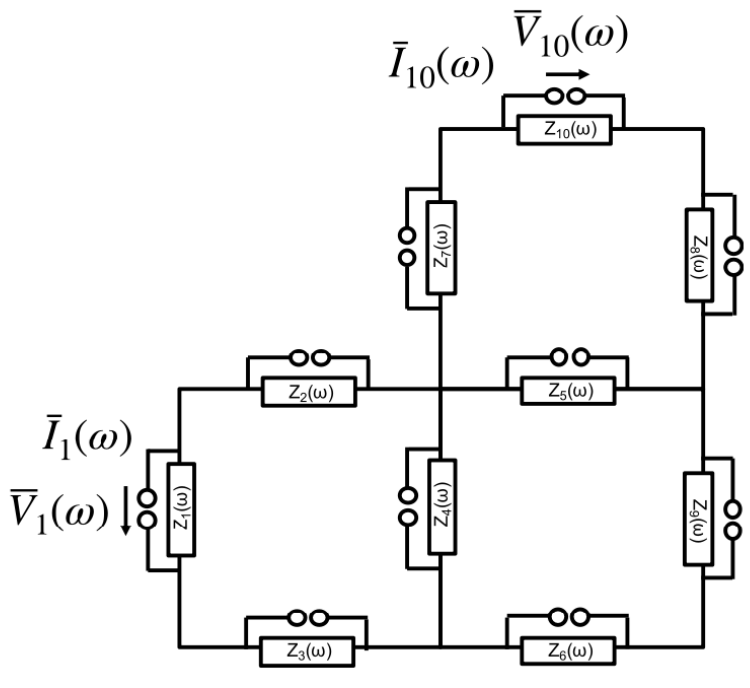

$$\sum_{n=1}^{N=10} I_n(\omega)\bar{V}_n(\omega) = \sum_{n=1}^{N=10} \bar{I}_n(\omega)V_n(\omega)$$

$$I_1(\omega)\bar{V}_1(\omega) = \bar{I}_{10}(\omega)V_{10}(\omega) \quad \rightarrow \quad \frac{I_1(\omega)}{V_{10}(\omega)} = \frac{\bar{I}_{10}(\omega)}{\bar{V}_1(\omega)} \qquad (13)$$

This is the network reciprocity theorem [28]:

The voltage across an impedance element $Z_m(\omega)$ due to a current $I(\omega)$ on a different element $Z_n(\omega)$ is equal to the voltage across $Z_n(\omega)$ for the same current $I(\omega)$ on $Z_m(\omega)$.

Antenna reciprocity

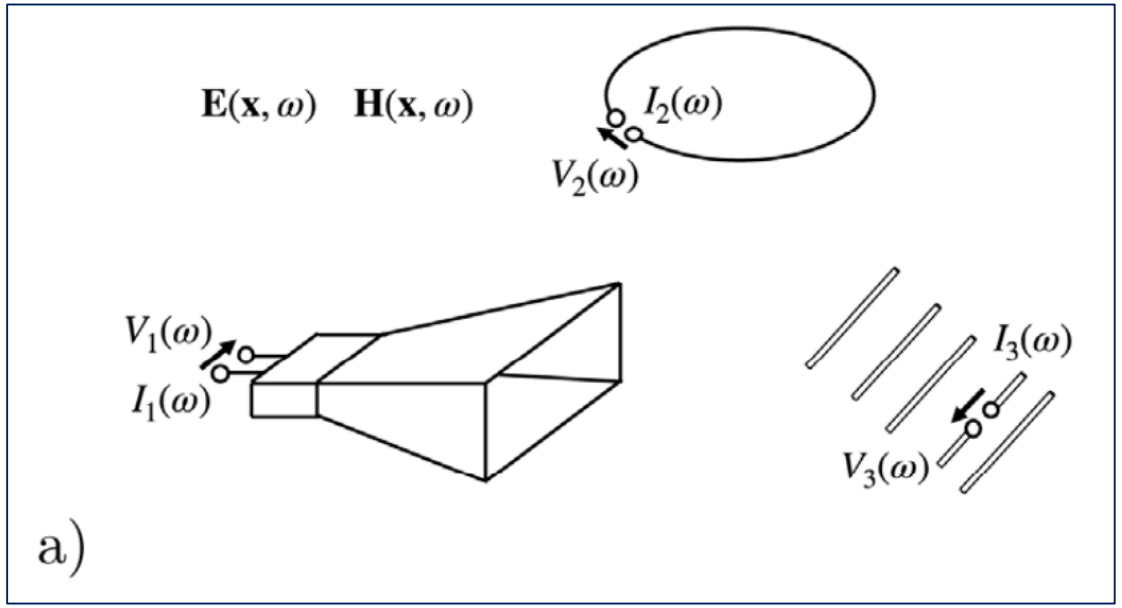

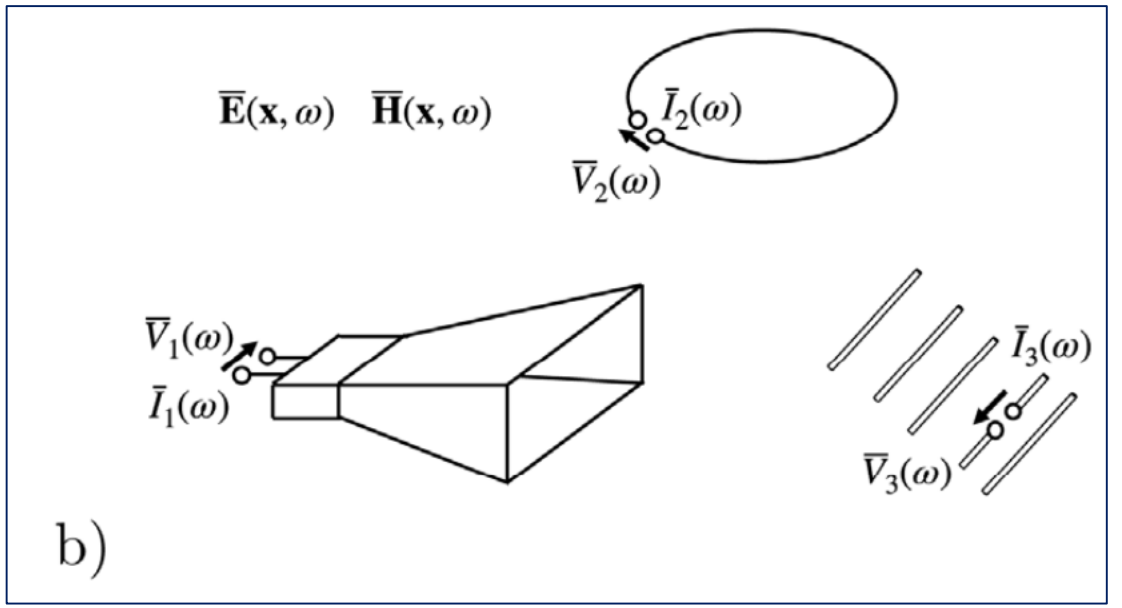

$$\sum_{n=1}^{N=3} I_n(\omega)\overline{V}_n(\omega) = \sum_{n=1}^{N=3} \overline{I}_n(\omega)V_n(\omega)$$

If we again assume just the first antenna to be driven by a current $I_1(\omega) = I(\omega)$, and in the second situation we assume the second antenna to be driven by the same current $\overline{I}_2(\omega) = I(\omega)$, we find that $V_2(\omega) = \overline{V}_1(\omega)$. Since this relationship holds for arbitrary antenna geometries and arbitrary relative orientations, we deduce the remarkable result that the reception and transmission characteristics of each antenna must be identical. This is called the antenna reciprocity theorem.

Weighting field

A charge moving in a general material along $x_q(t)$.
The signal defined as the integral of the field along a path S.

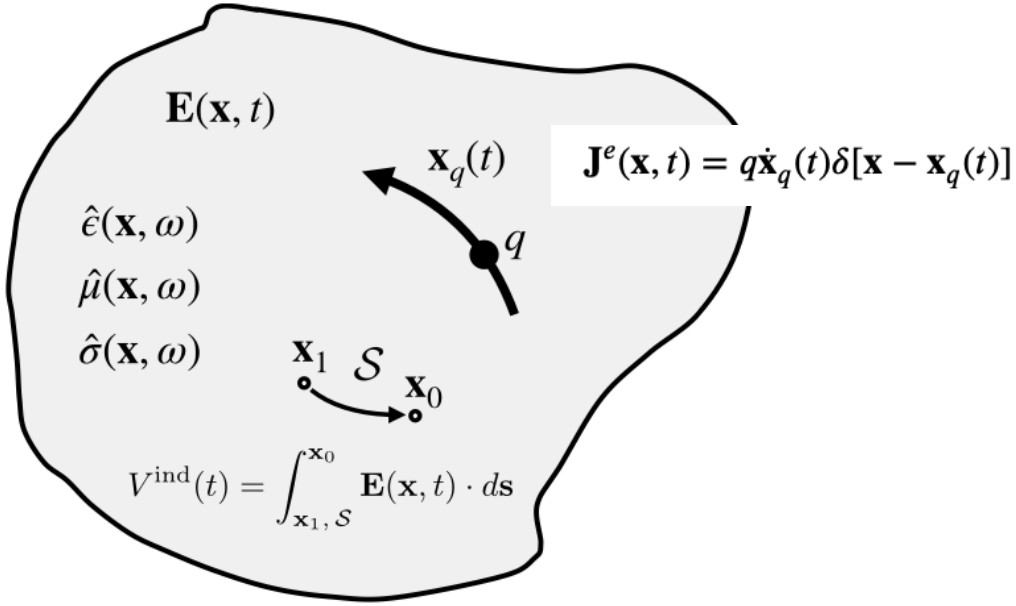

No charge. A delta current along the same path S.

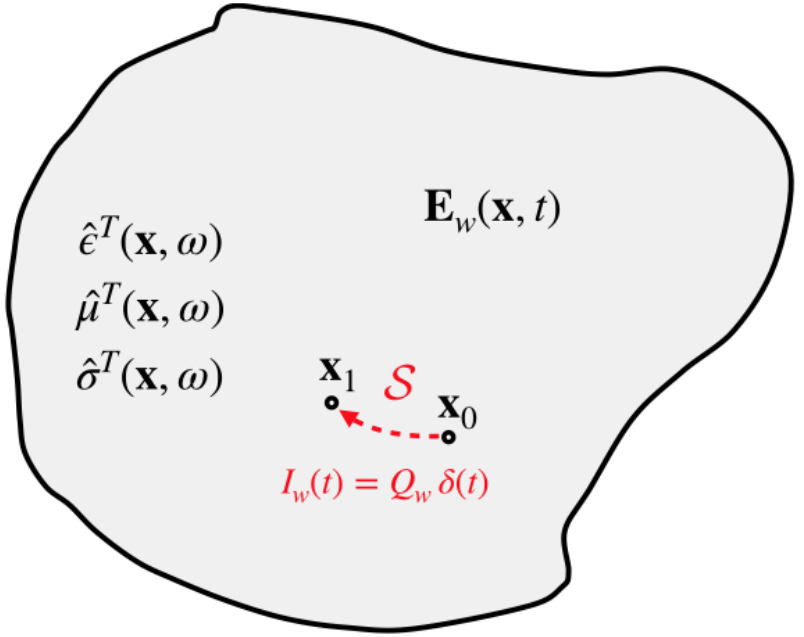

$$V^{\text{ind}}(\omega) = \int_{\mathbf{x}_1, \mathcal{S}}^{\mathbf{x}_0} \mathbf{E}(\mathbf{x}, \omega) d\mathbf{s} = -\frac{1}{I_w(\omega)} \int_V \mathbf{E}_w(\mathbf{x}, \omega)\mathbf{J}^e(\mathbf{x}, \omega) dV$$

$$V^{\text{ind}}(t) = -\frac{q}{Q_w} \int_{-\infty}^{\infty} \mathbf{E}_w(\mathbf{x}_q(t'), t - t')\dot{\mathbf{x}}_q(t') dt'$$

→ An extension for the weighting field method to the full extent of Maxwell's equations !

Transmission line

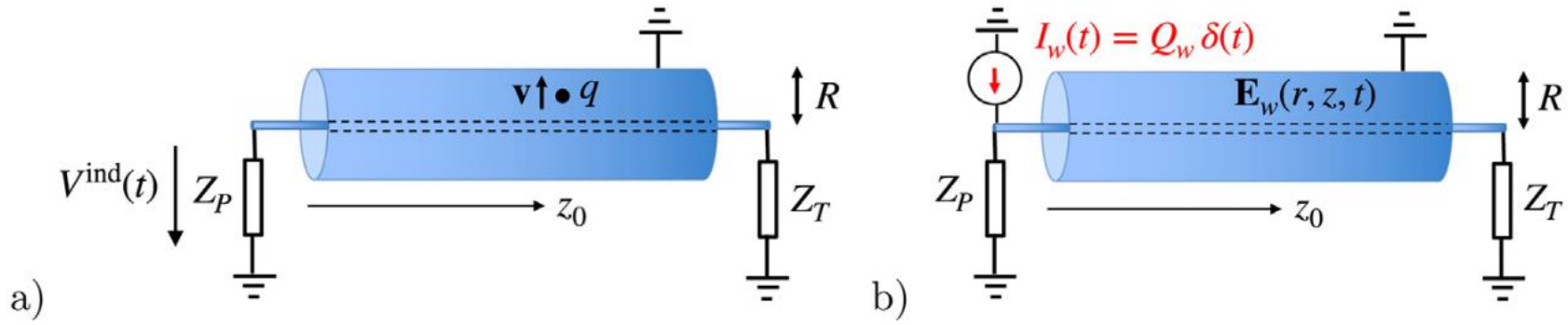

We want to know the signal V(t) at the end of a transmission line due to a charge moving radially inside the transmission line.

→ We remove the charge, place a delta current on the end of the line and calculate the electric field inside the transmission line.

We assume that only TEM field modes are travelling along the transmission line, which is true for frequencies lower than c/R. In this case there are no field components along the z direction. The potential Difference between the conductors can then be defined in a unique way and we have

$$\mathbf{E}_w(r,z,t) = V(z,t)\frac{\mathbf{E}_w^0(r)}{V_w} \qquad \mathbf{E}_w^0(r) = -\nabla\varphi(r)$$

$$\varphi(r)|_{r=a} = V_w \qquad \varphi(r)|_{r=R} = 0$$

The voltage V(z,t) is determined by the transmission line equations for the given stimulus and the potential corresponds to the two-dimensional static weighting potential of the central conductor.

$$V^{ind}(t) = -\frac{q}{Q_w}\int_{-\infty}^{\infty} V(z_0, t-t')\frac{1}{V_w}\mathbf{E}_w^0(r(t'))\dot{\mathbf{x}}(t')dt'$$

$$= \frac{1}{Q_w}\int_{-\infty}^{\infty} V(z_0, t-t')I_0(t')dt'$$

$$V^{ind}(\omega) = I_0(\omega)\frac{V(z_0,\omega)}{Q_w} = I_0(\omega)Z(\omega)$$

The voltage induced on a transmission line by a point charge moving radially at position z_0 can be calculated by first finding the induced current on a grounded electrode with the electrostatic two dimensional weighting fields and then placing this current as an ideal current source on the transmission line at position z_0.

Synchrotron radiation

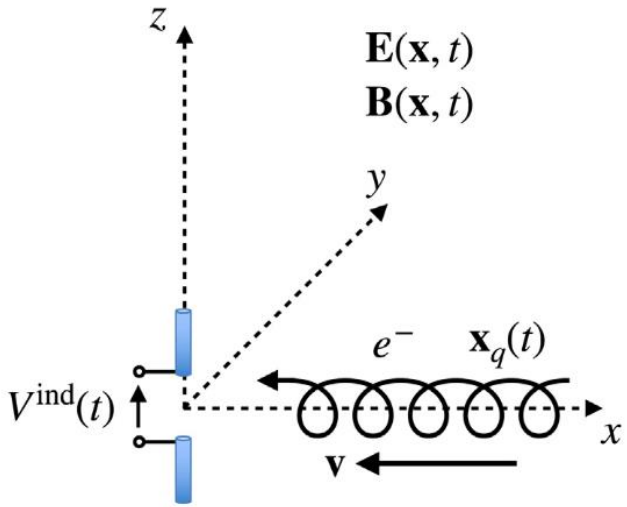

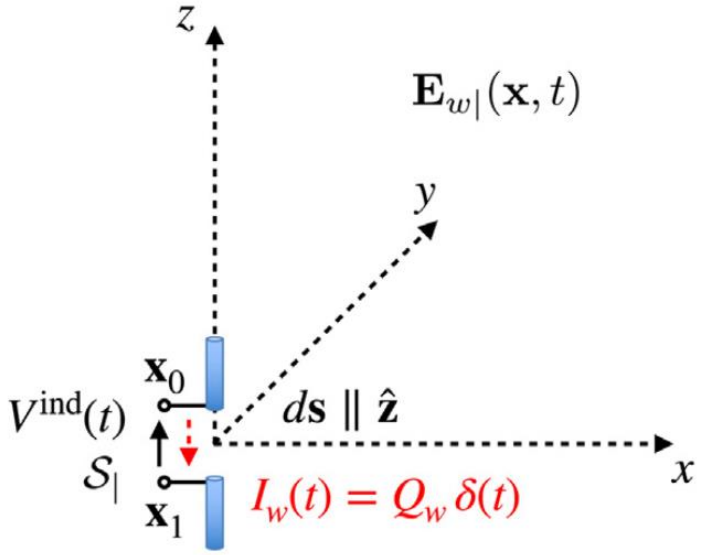

$$\mathbf{x}_q(t) = \begin{pmatrix} -vt \\ A\sin(\omega_0 t) \\ A\cos(\omega_0 t) \end{pmatrix} \qquad \dot{\mathbf{x}}_q(t) = \begin{pmatrix} -v \\ A\omega_0\cos(\omega_0 t) \\ -A\omega_0\sin(\omega_0 t) \end{pmatrix}$$

Dipole weighting field

$$E^{\theta}_{w|}(r,\theta) = -\frac{Q_w ds}{4\pi\varepsilon}\frac{\sin\theta}{r^3}\left[\Theta\left(t-\frac{rn}{c}\right)+\frac{rn}{c}\delta\left(t-\frac{rn}{c}\right)+\left(\frac{rn}{c}\right)^2\delta'\left(t-\frac{rn}{c}\right)\right],$$

$$E^{r}_{w|}(r,\theta) = -2\frac{Q_w ds}{4\pi\varepsilon}\frac{\cos\theta}{r^3}\left[\Theta\left(t-\frac{rn}{c}\right)+\frac{rn}{c}\delta\left(t-\frac{rn}{c}\right)\right],$$

$$E^{\phi}_{w|}(r,\theta) = 0,$$

Far Field approximation for large distances

$$E^{x}_{w|} = 0 \quad E^{y}_{w|} = 0 \qquad E^{z}_{w|}(r,t) \approx \frac{Q_w\, ds}{4\pi\varepsilon_0 c^2}\frac{1}{r}\delta'\left(t-\frac{r}{c}\right).$$

$$\begin{aligned} V(t) &= \frac{e_0}{Q_w}\int_{-\infty}^{\infty} E^{z}_{w|}(vt', t-t')A\omega_0\sin(\omega_0 t')dt' \\ &\approx -\frac{A\, e_0\, ds}{4\pi\varepsilon_0 c^2}\left[\frac{1}{c}\frac{\omega_0}{\beta t^2}\sin(\omega t) - \frac{1}{c}\frac{\omega_0^2\cos(\omega t)}{\beta t(1-\beta)}\right] \\ &\approx \frac{A\, e_0\, ds}{4\pi\varepsilon_0}\frac{1}{r(t)}\frac{\omega_0^2}{c^2}\frac{\cos(\omega t)}{(1-\beta)} \qquad \text{for} \qquad \beta \approx 1 \end{aligned}$$

with $\omega = \omega_0/(1-\beta)$.

with $\omega = \omega_0/(1-\beta)$. For galactic magnetic fields on the order of 1 nT, the frequency ω_0 is only 176 Hz. For electrons with a kinetic energy E the observed frequency is larger by a factor $1/(1-\beta) \approx 2(E/m_e c^2)^2$. For an electron with a kinetic energy of 5 GeV, the frequency is increased by a factor 2×10^6 so we measure radio waves of around 352 MHz.

The same expression describes the synchrotron radiation emitted by an electron beam that is passed through an undulator with a wavelength λ_0 and where the emitted radiation has a wavelength of $\lambda = \lambda_0(1-\beta)$.

Askaryan effect

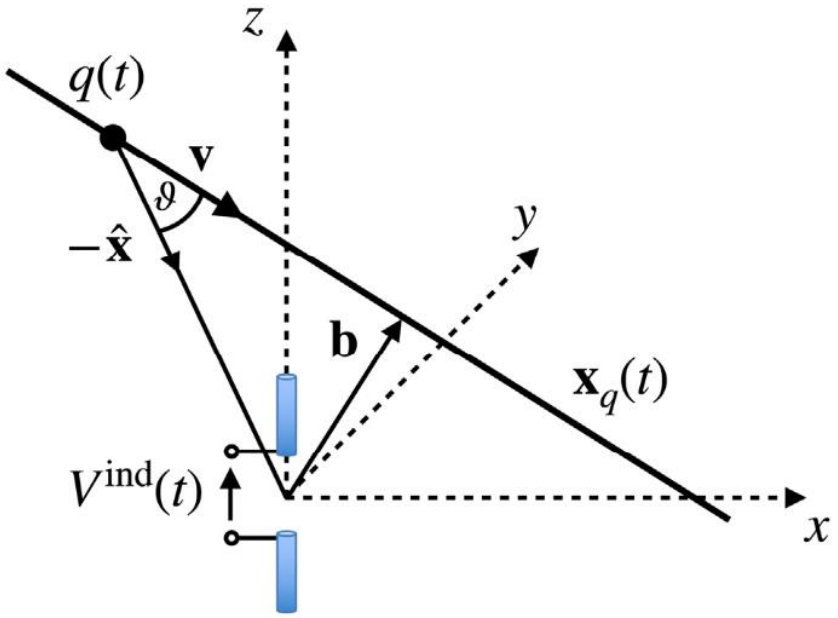

$$V^{\text{ind}}(t) = -\frac{ds}{4\pi\varepsilon}\int dt' q(t')\Theta\left(t-t'-\frac{rn}{c}\right)\frac{d}{dt'}\frac{z}{r^3} - \frac{ds}{4\pi\varepsilon}\int dt' q(t')\delta\left(t-t'-\frac{rn}{c}\right)\frac{rn}{c}\frac{d}{dt'}\frac{z}{r^3} + \frac{ds}{4\pi\varepsilon}\int dt' q(t')\delta'\left(t-t'-\frac{rn}{c}\right)\frac{n^2}{c^2r^3}\left(z\mathbf{x}\cdot\dot{\mathbf{x}}-r^2\dot{z}\right).$$

A particle shower will provide an produce an exponentially increasing number of charges particles, which produces a radio signal.

$$\mathbf{E}(t) = -\frac{ds}{4\pi\varepsilon}\left[\frac{q(t)}{|1-n\beta\cos\vartheta|^3}\frac{1}{r^2}\left(1-n^2\beta^2\right)(\hat{\mathbf{x}}+n\boldsymbol{\beta})\right]_{t_{\text{ret}}} + \frac{ds}{4\pi\varepsilon}\int_{-\infty}^{t_{\text{ret}}} dt'\dot{q}(t')\frac{\mathbf{x}}{r^3} - \frac{ds}{4\pi\varepsilon}\left[\frac{\dot{q}(t)}{|1-n\beta\cos\vartheta|(1-n\beta\cos\vartheta)}\frac{n}{rc}\left(n\boldsymbol{\beta}-(n\boldsymbol{\beta}\cdot\hat{\mathbf{x}})\hat{\mathbf{x}}\right)\right]_{t_{\text{ret}}},$$

Askaryan Radiation

$\mathbf{J}^e(\mathbf{x},t) = q(t)\mathbf{v}\delta(\mathbf{x}-\mathbf{x}_q(t))$. We take $q(t) = q\exp\left(\frac{\beta ct}{z_0}\right)$

Bandwidth limit

Another advantage of the weighting field concept is the implementation of the bandwidth limit:

Let us assume that the antenna signal will be processed by an electronics chain with delta response f(t).

In the traditional calculation one calculates the radiation produced by the particles, propagated the radiation through the medium, folds it with the antenna characteristics and the folds the signal with the linear processing chain.

In the weighting field concept, due to the linearity of the system, one can immediately apply the bandwidth limit of the electronics system to the weighting field, i.e. instead of applying a delta function to the system one can directly apply the electronics delta response f(t) to the antenna for the calculation of the weighting field.

This way one uses the minimum amount of bandwidth in the entire simulation.

$$E^{\theta}_{w|}(r,\theta) = -\frac{Q_w ds}{4\pi\varepsilon}\frac{\sin\theta}{r^3}\left[\Theta\left(t-\frac{rn}{c}\right)+\frac{rn}{c}\delta\left(t-\frac{rn}{c}\right)+\left(\frac{rn}{c}\right)^2\delta'\left(t-\frac{rn}{c}\right)\right],$$

$$E^{r}_{w|}(r,\theta) = -2\frac{Q_w ds}{4\pi\varepsilon}\frac{\cos\theta}{r^3}\left[\Theta\left(t-\frac{rn}{c}\right)+\frac{rn}{c}\delta\left(t-\frac{rn}{c}\right)\right],$$

$$E^{\phi}_{w|}(r,\theta) = 0,$$

$$K^{\theta}_{w|}(r,\theta) = -\frac{Q_w\, ds}{4\pi\varepsilon}\frac{\sin\theta}{r^3}\left[f_0\left(t-\frac{nr}{c}\right)+\frac{nr}{c}f\left(t-\frac{nr}{c}\right)+\left(\frac{nr}{c}\right)^2 f'\left(t-\frac{nr}{c}\right)\right]$$

$$K^{r}_{w|}(r,\theta) = -2\frac{Q_w\, ds}{4\pi\varepsilon}\frac{\cos\theta}{r^3}\left[f_0\left(t-\frac{nr}{c}\right)+\frac{nr}{c}f\left(t-\frac{nr}{c}\right)\right]$$

$$K^{\phi}_{w\circ}(r,\phi) = \frac{Q_w\, dA\,\mu}{4\pi}\frac{\sin\theta}{r^2}\left[f'\left(t-\frac{nr}{c}\right)+\frac{nr}{c}f''\left(t-\frac{nr}{c}\right)\right]$$

The high-energy landscape of our universe

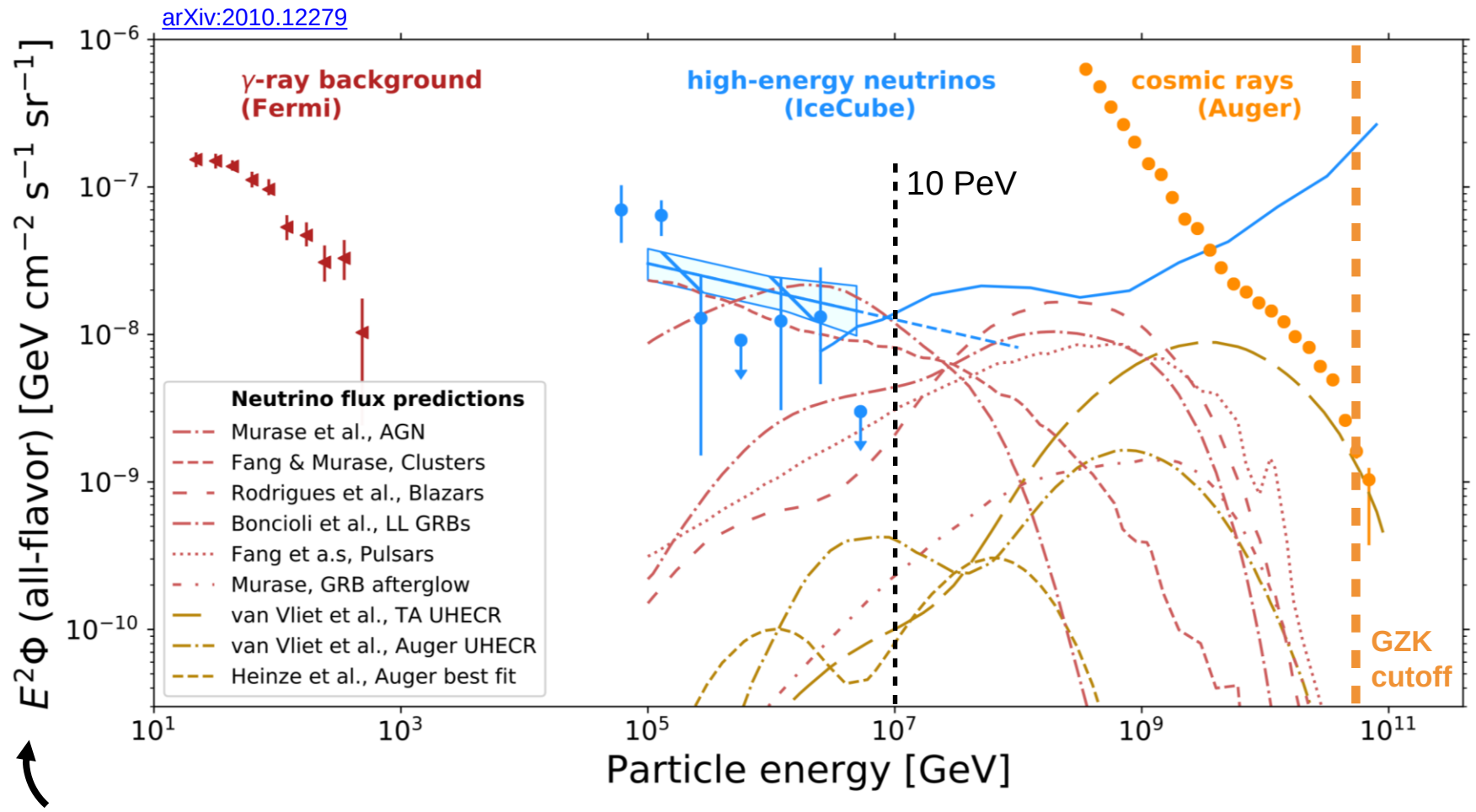

"Energy flux"

Th universe

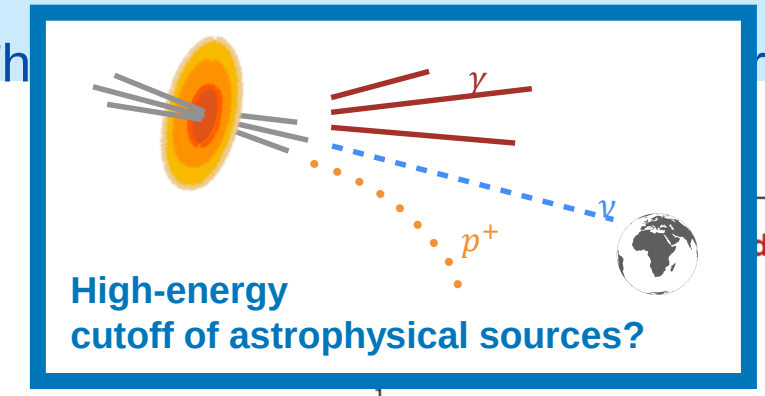

High-energy cutoff of astrophysical sources?

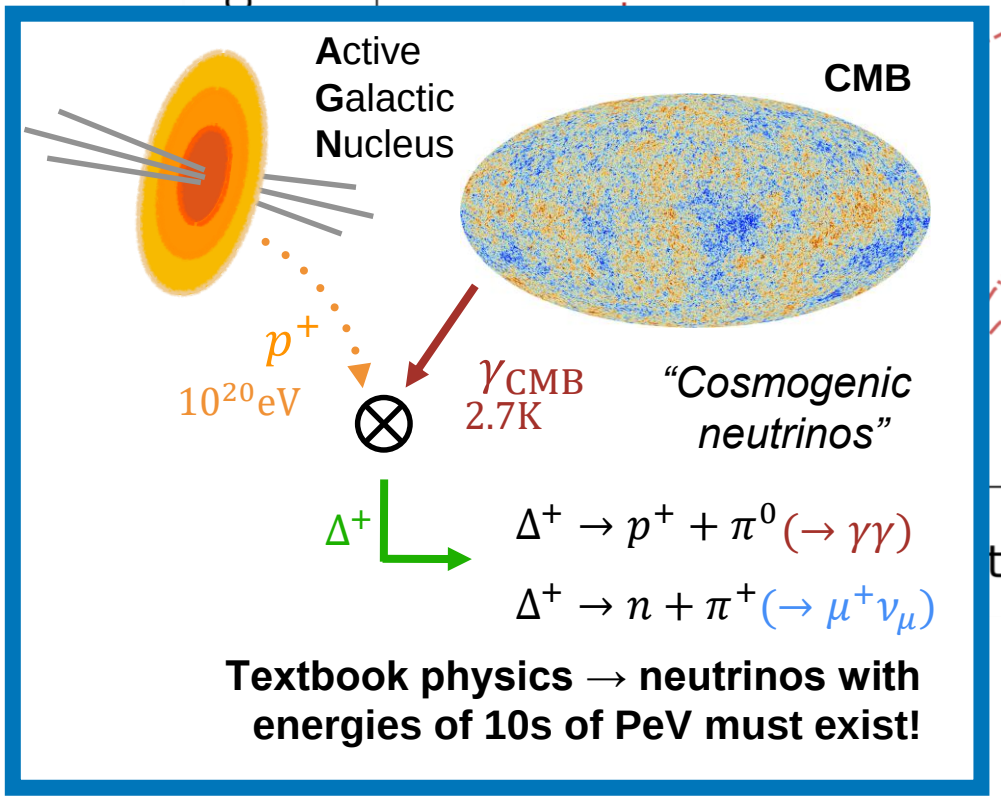

Textbook physics → neutrinos with energies of 10s of PeV must exist!

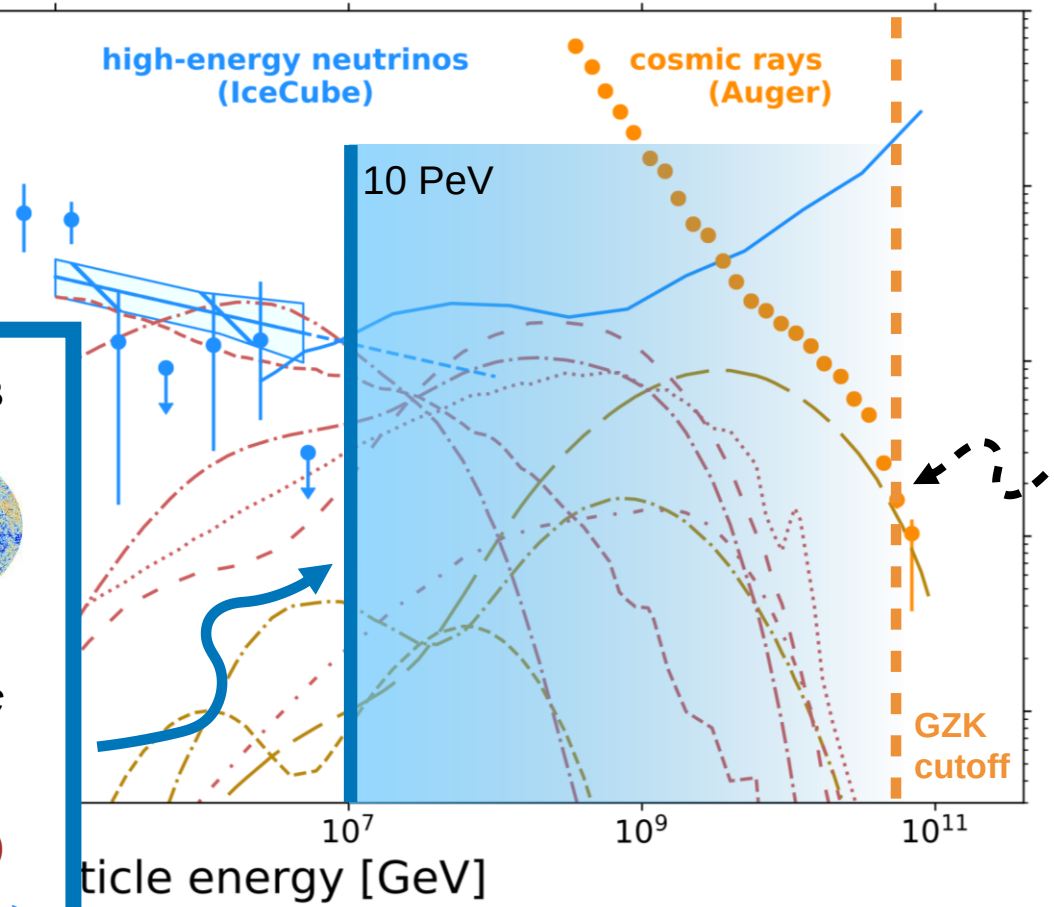

Expect

0.01

interactions / km^3 / year

of GZK-scale neutrinos

Requires instrumented volume of O(100) km³!

Radio Neutrino Observatory in Greenland (RNO-G)

First science-scale radio array *targeting* ***≥ 10 PeV neutrinos*** *in the* ***northern hemisphere***

Use Greenlandic ice as detector medium

Ice is dense!

Good target material for weakly-interacting particles

Net electric charge of shower front
→ **electric current**

Transverse size of shower front smaller than wavelength

→ **Coherent Askaryan emission**

Ice is clean and cold!

Very transparent to electromagnetic radiation in the MHz - GHz band

→ **Attenuation length O(1 km)**

$f \sim 500\text{MHz} \leftrightarrow \lambda \sim 0.4\text{m}$

Expect **strong signals** at high energies,
detectable over long distances

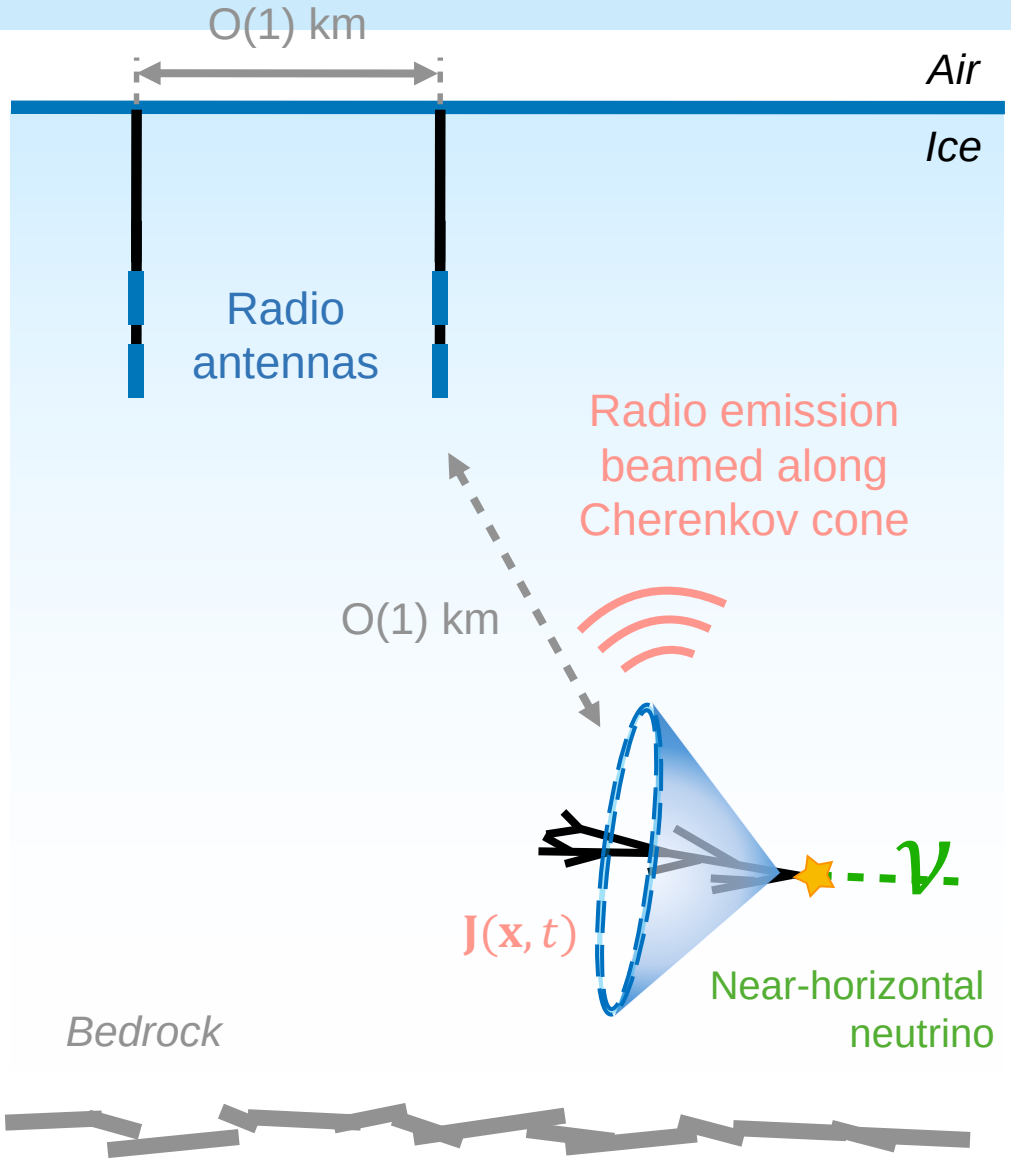

Neutrino crossection vs. energy

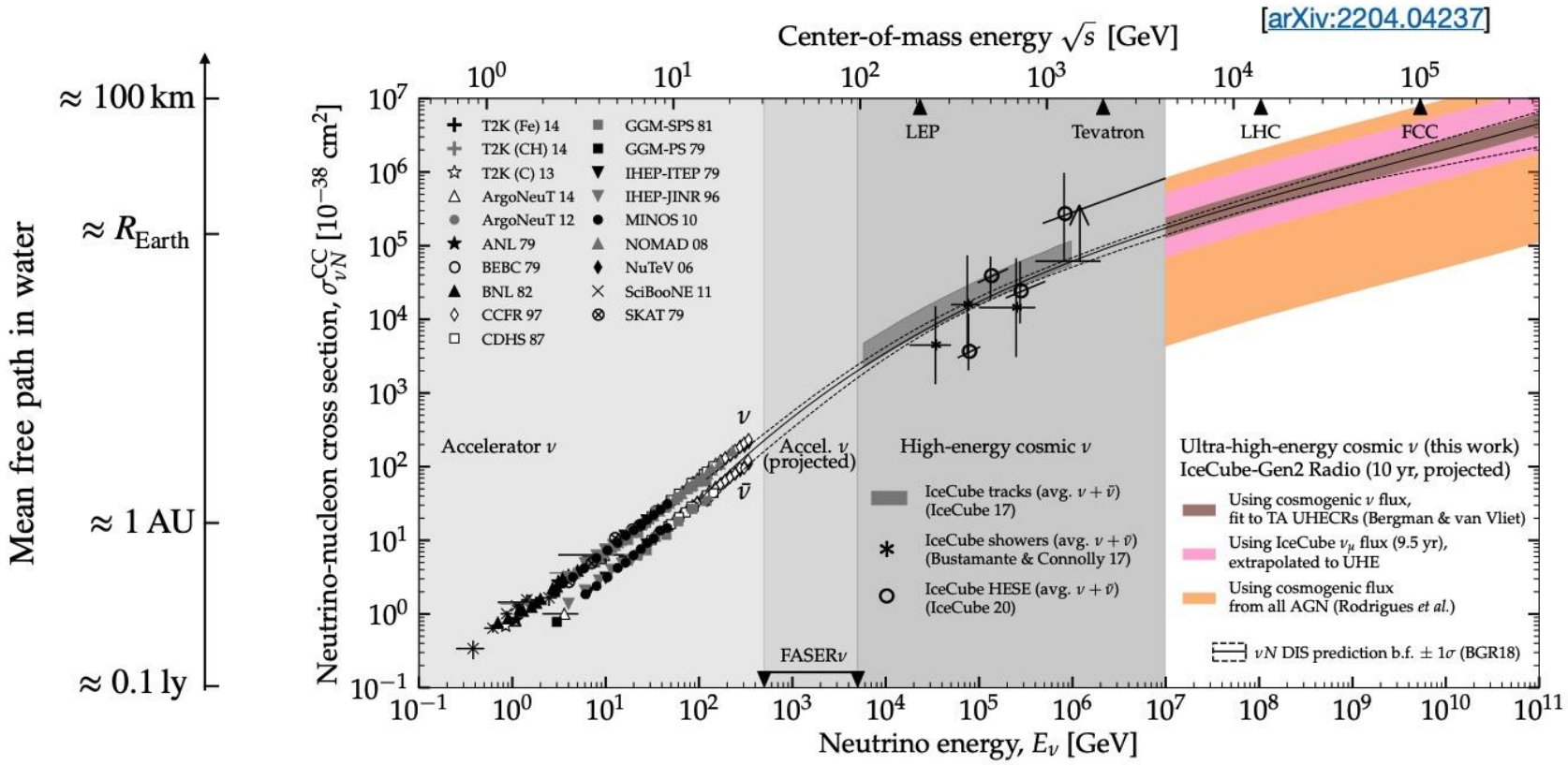

RNO-G: array design

RNO-G
Radio Neutrino Observatory - Greenland

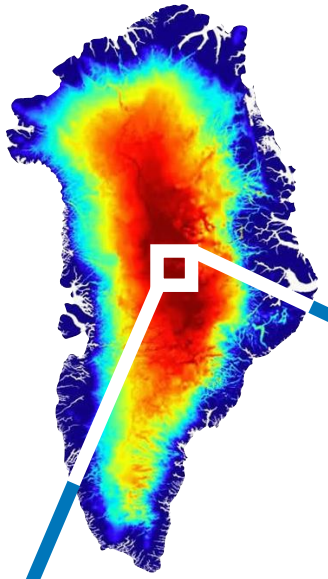

Ice thickness
3000 m
0 m

7 stations already deployed and taking data;

35-station array fully funded!

Summit station, Greenland *(NSF-operated)*

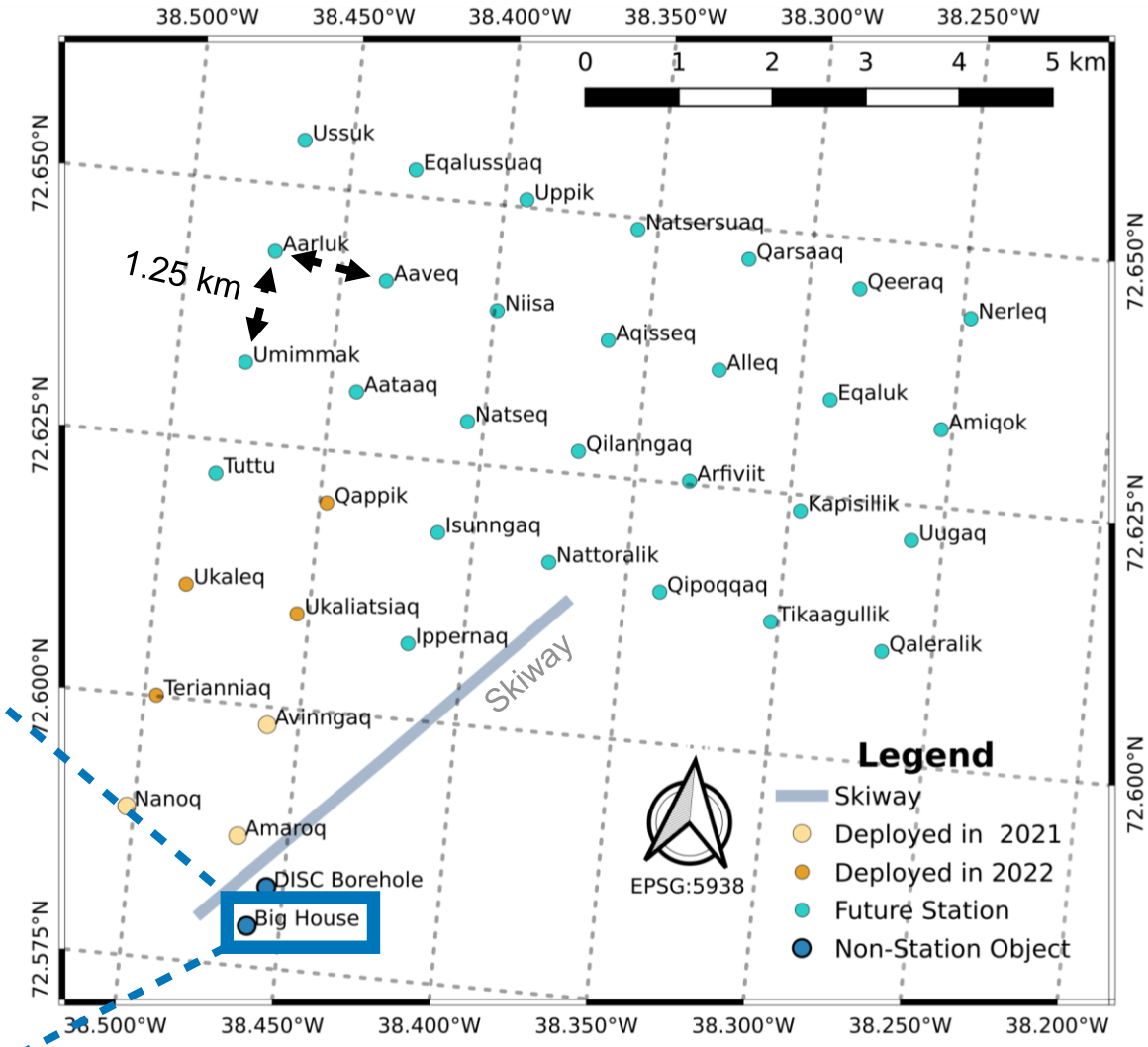

Triangular station layout with downhole and surface antennas

Downhole: Horizontally- *(Hpol)* and vertically-polarized *(Vpol)* dipole antennas

Hole ***≈ 100m deep*** *in* ***more-homogeneous*** *and* ***radio-quiet ice***

Polarization-sensitivity improves direction-finding

Surface: Upward- and downward-looking *(directional!)* log-periodic dipole antennas *(LPDAs)*

Sensitivity to (down-going) ***cosmic rays*** → ***veto***

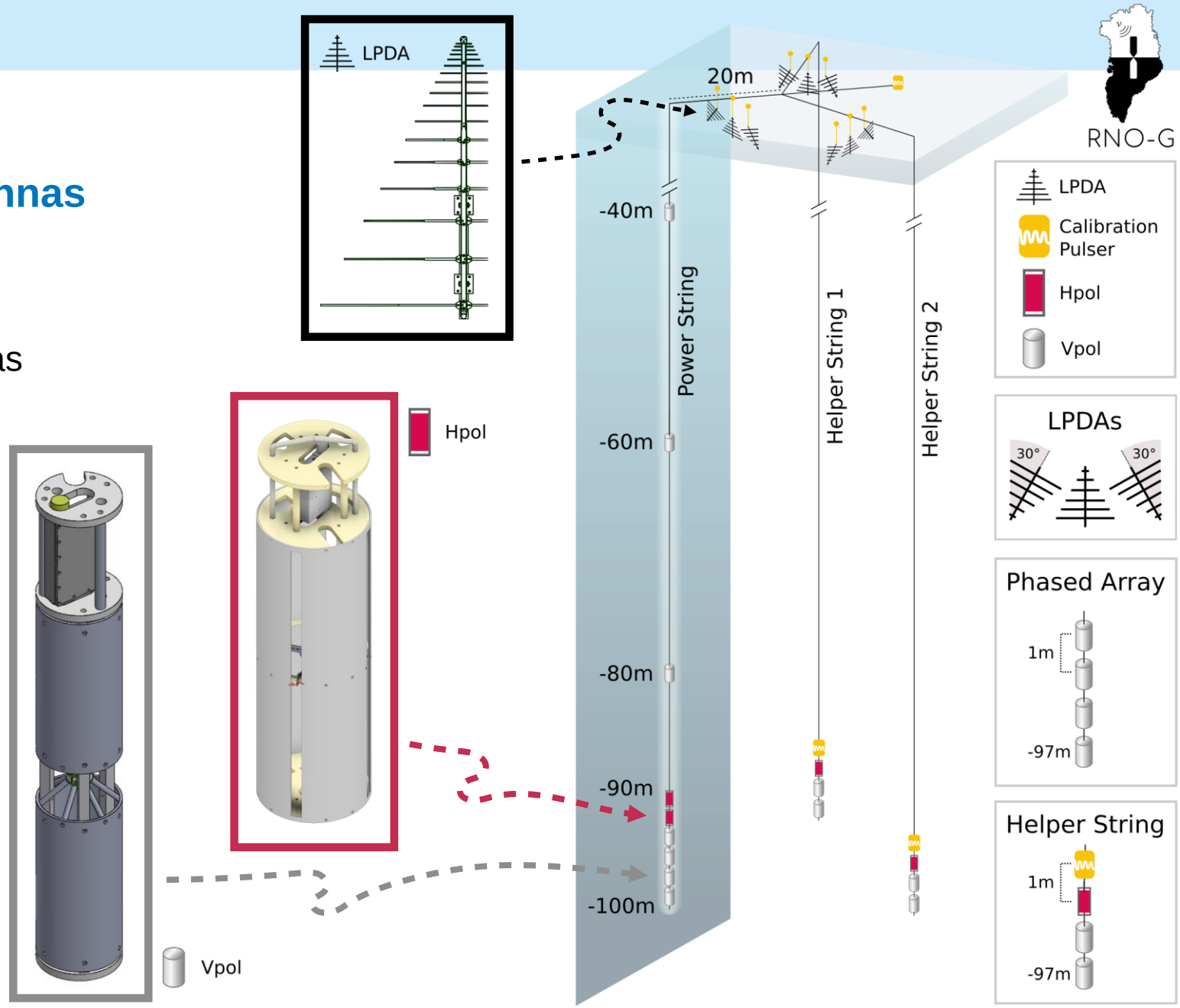

Antenna weighting field for uniform ice

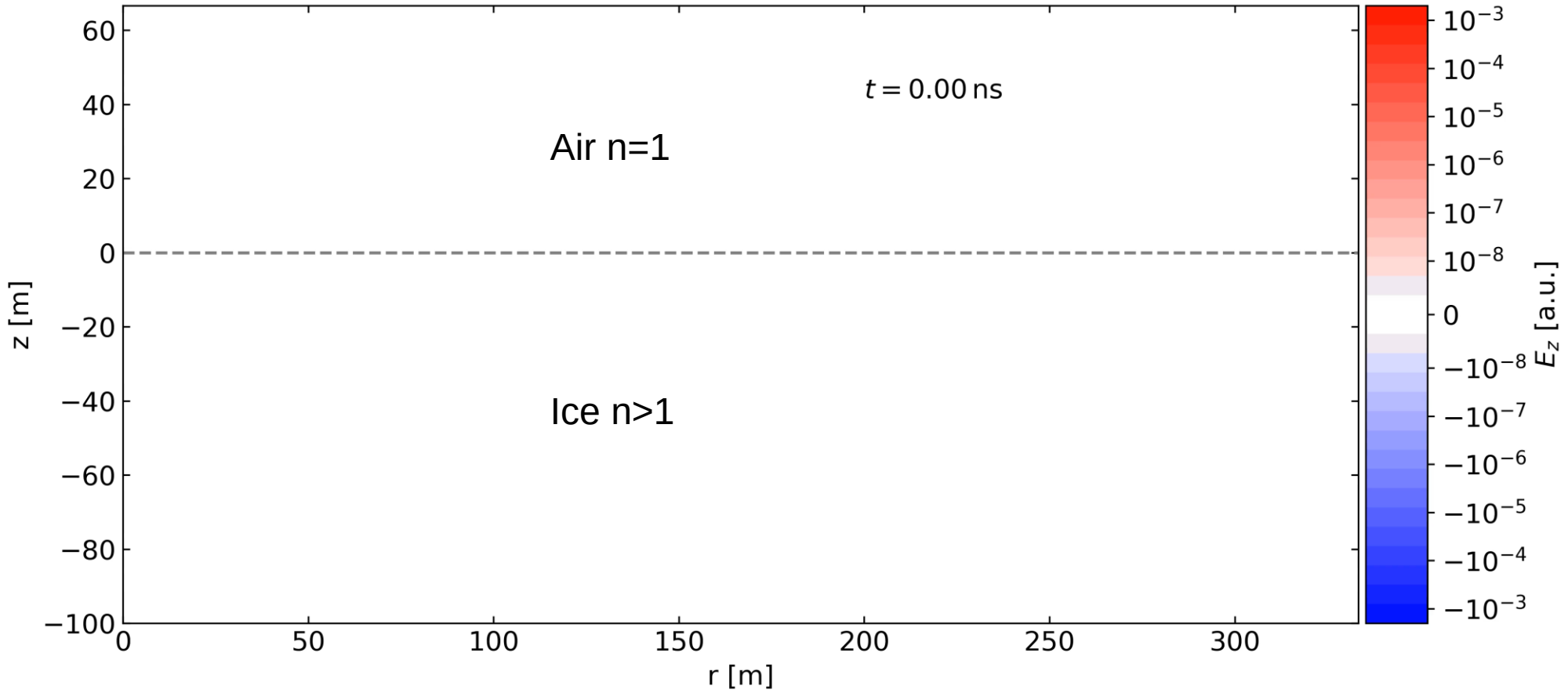

The need for accurate signal simulations

Non-neutrino backgrounds and radiation propagation effects must be understood

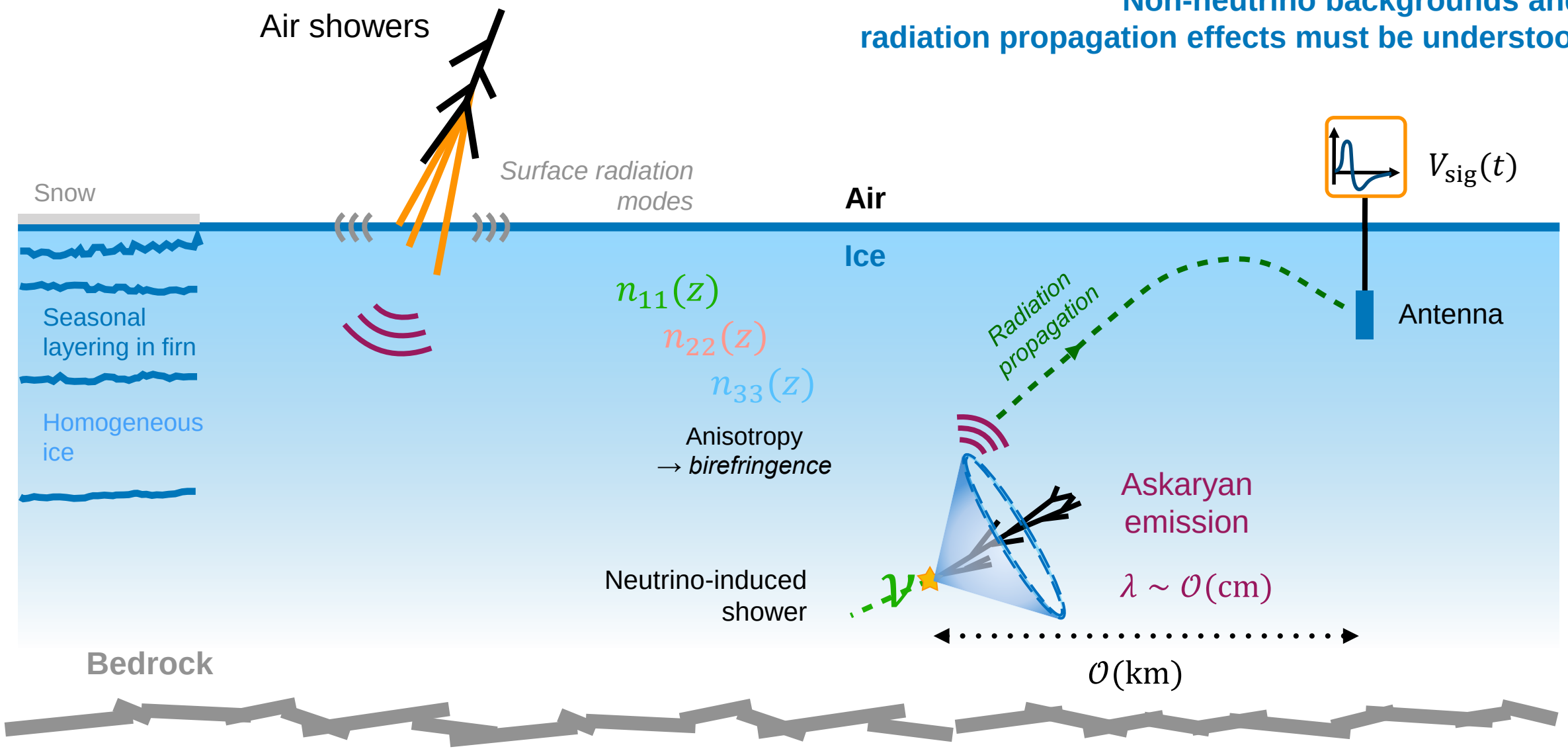

Refractive index of the ice

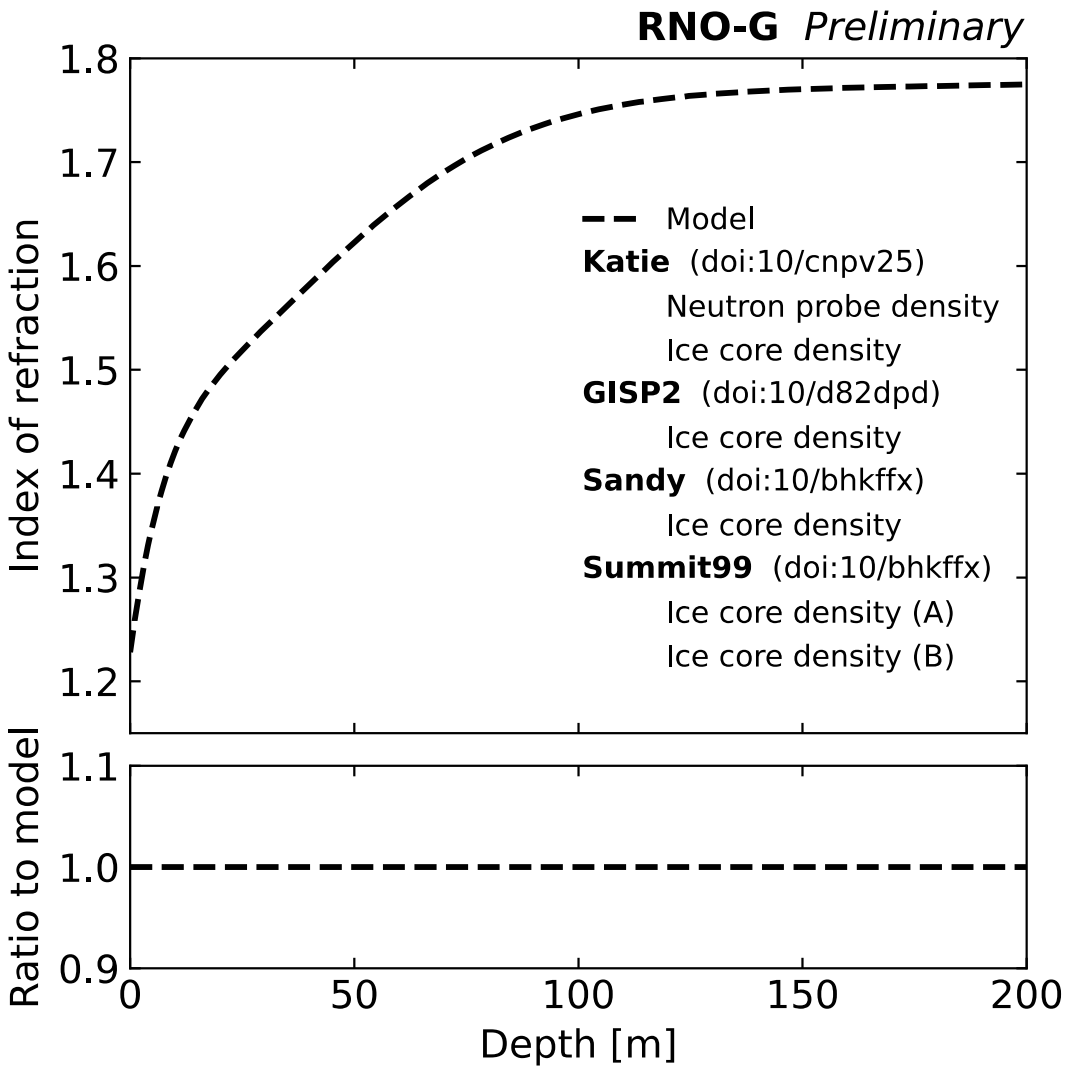

Refractive index depends on depth (pressure) and is not ‘smooth’ i.e. there are seasonal snow layers.

Antenna weighting field for realistic ice

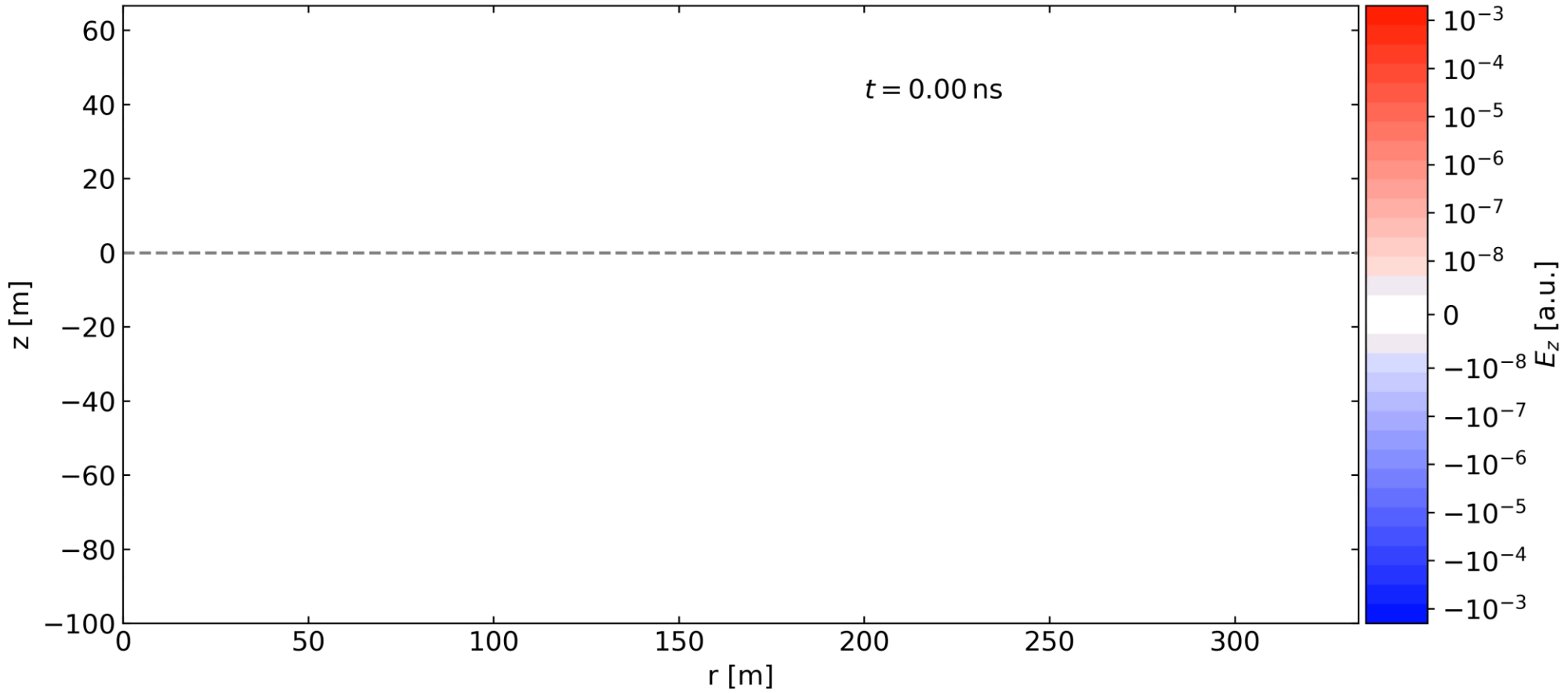

Weighting field for realistic ice geometry

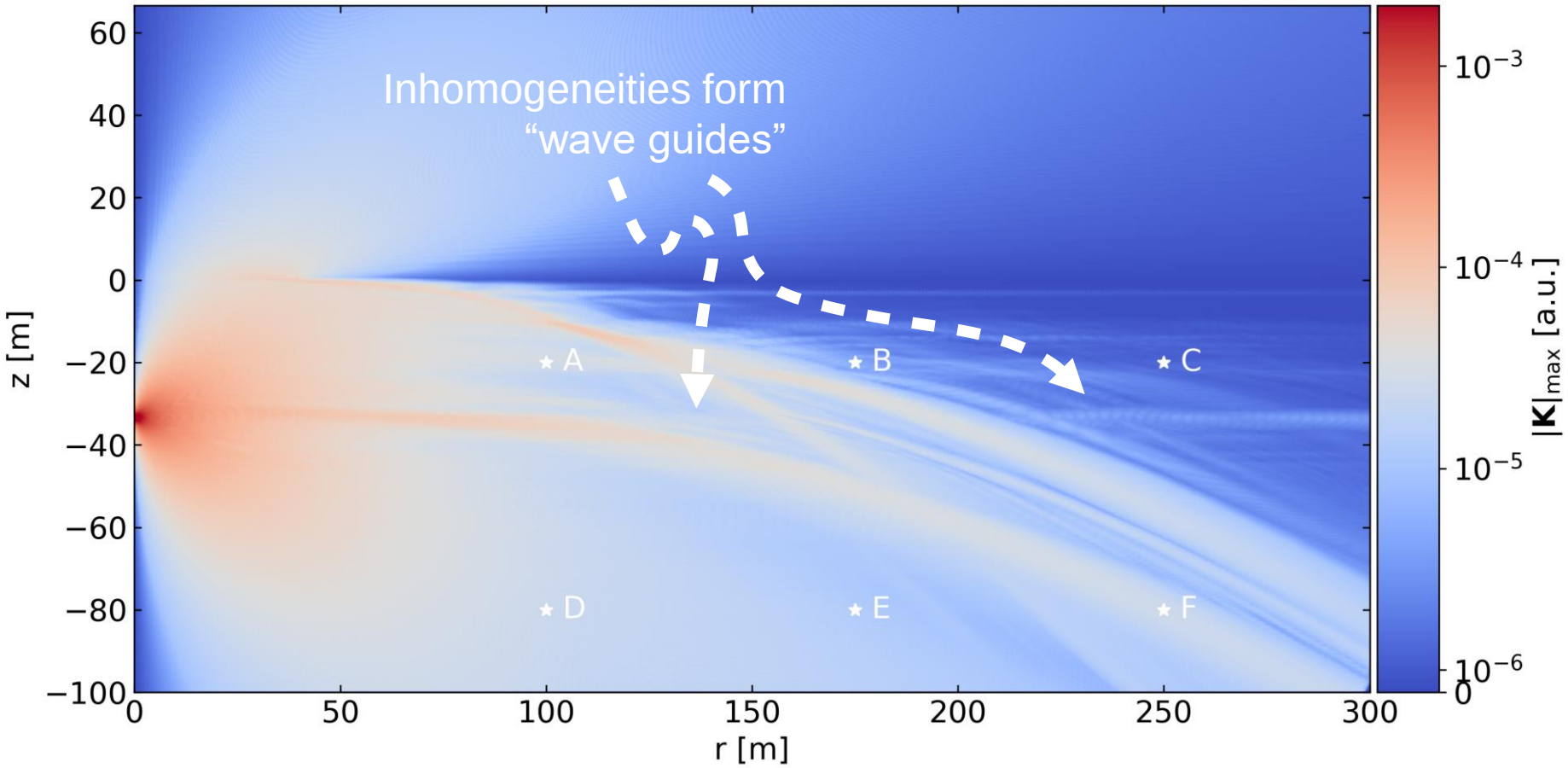

Signals from neutrino-induced showers

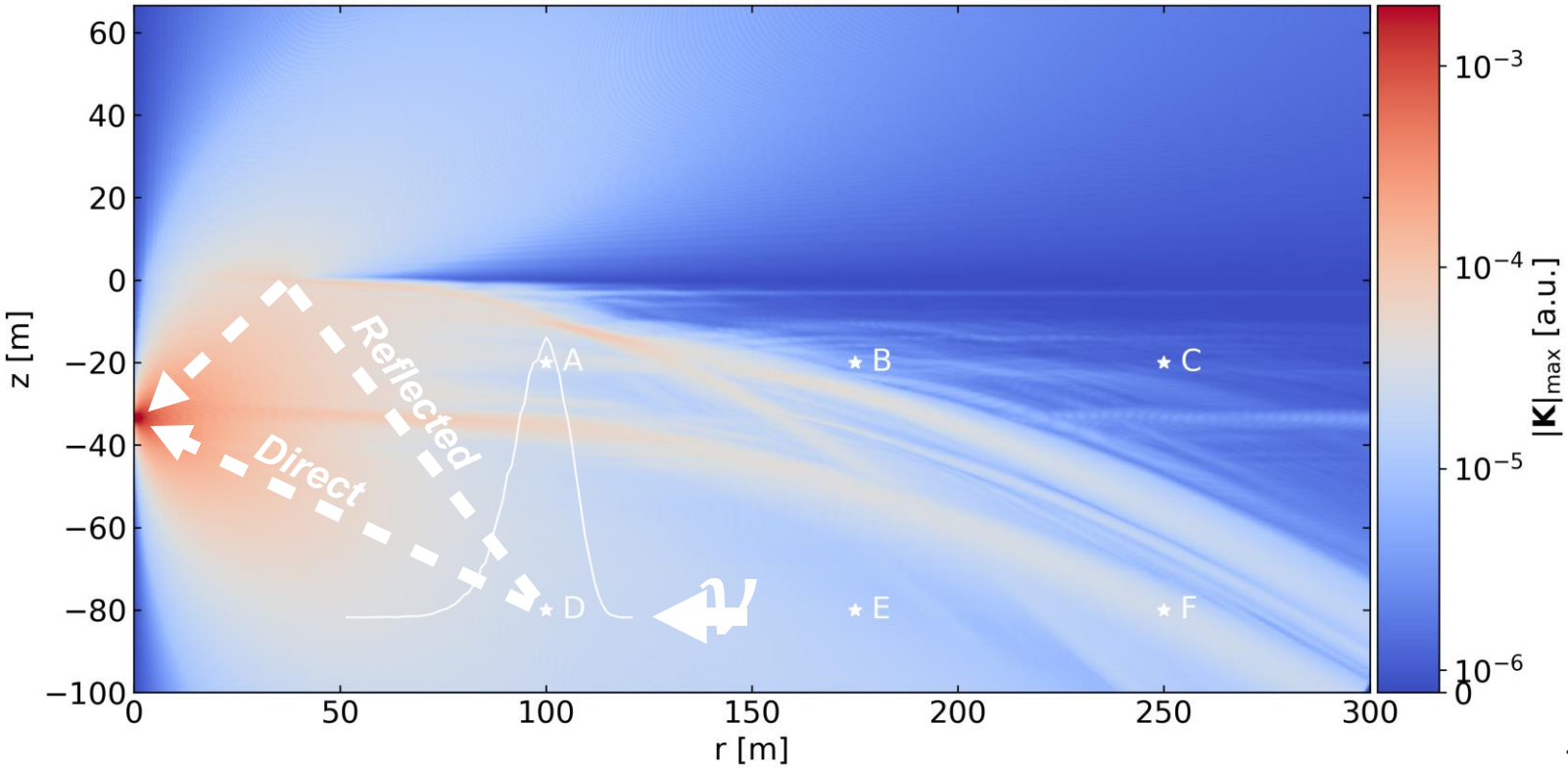

Simulated signal from
10^{18} eV hadronic shower

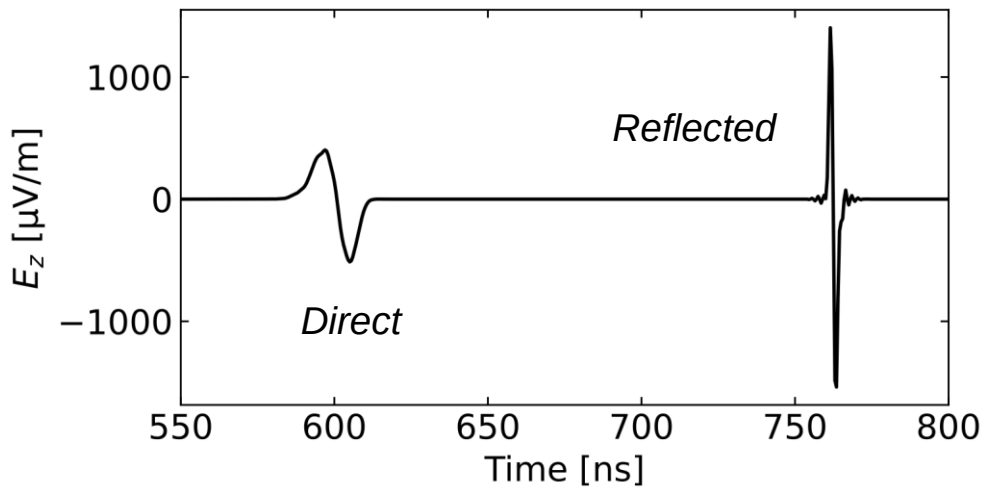

Signals from neutrino-induced showers

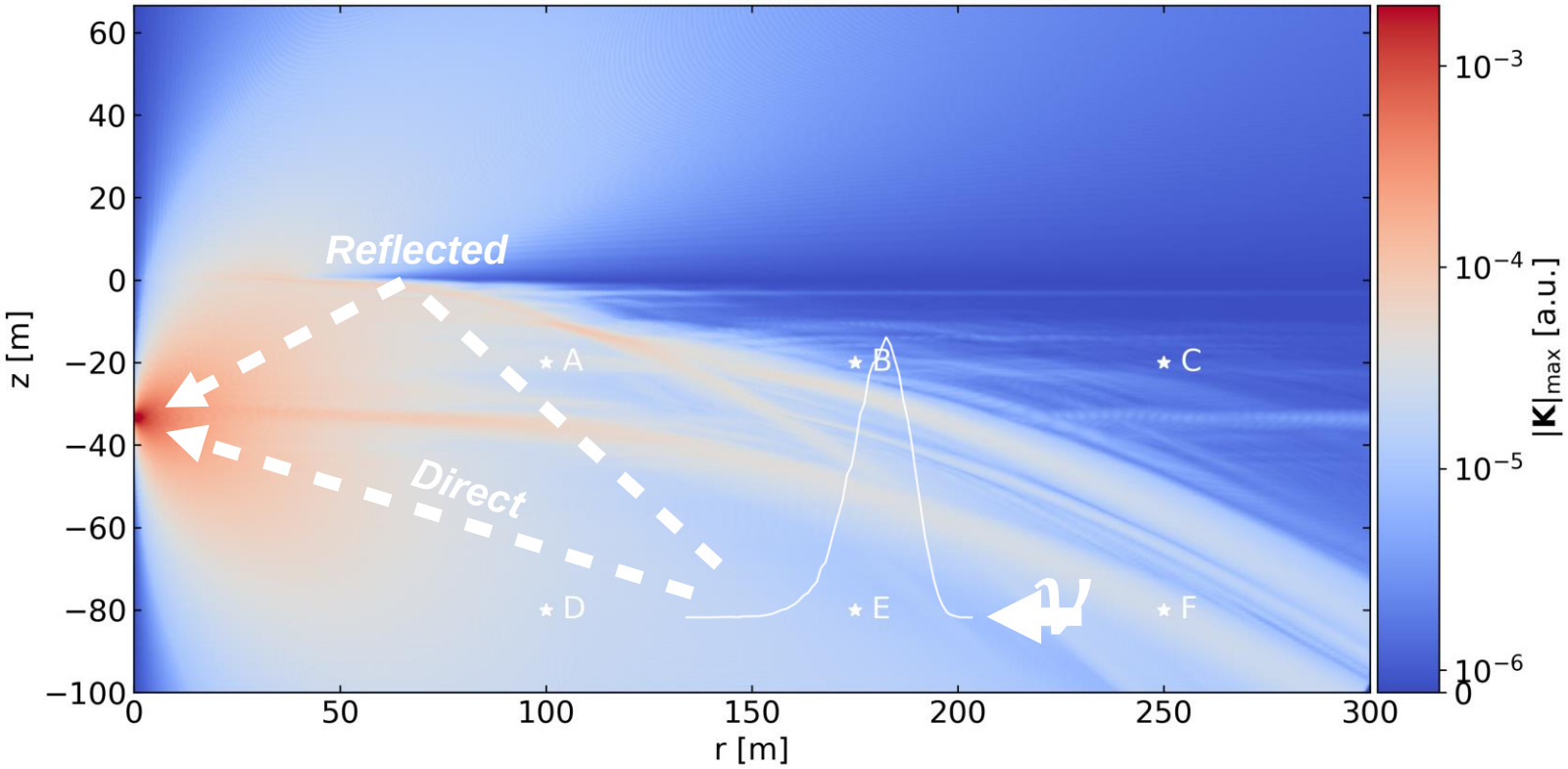

Simulated signal from
10^{18} eV hadronic shower

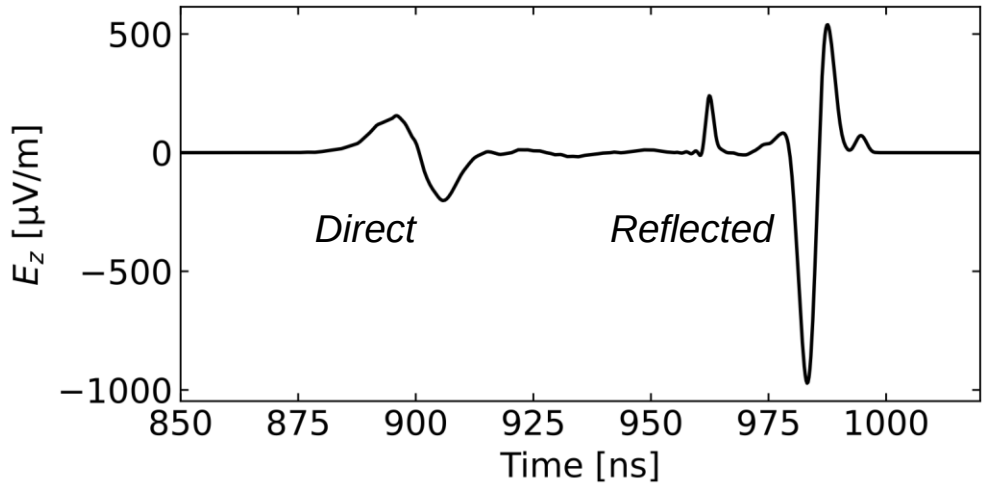

Signals from neutrino-induced showers

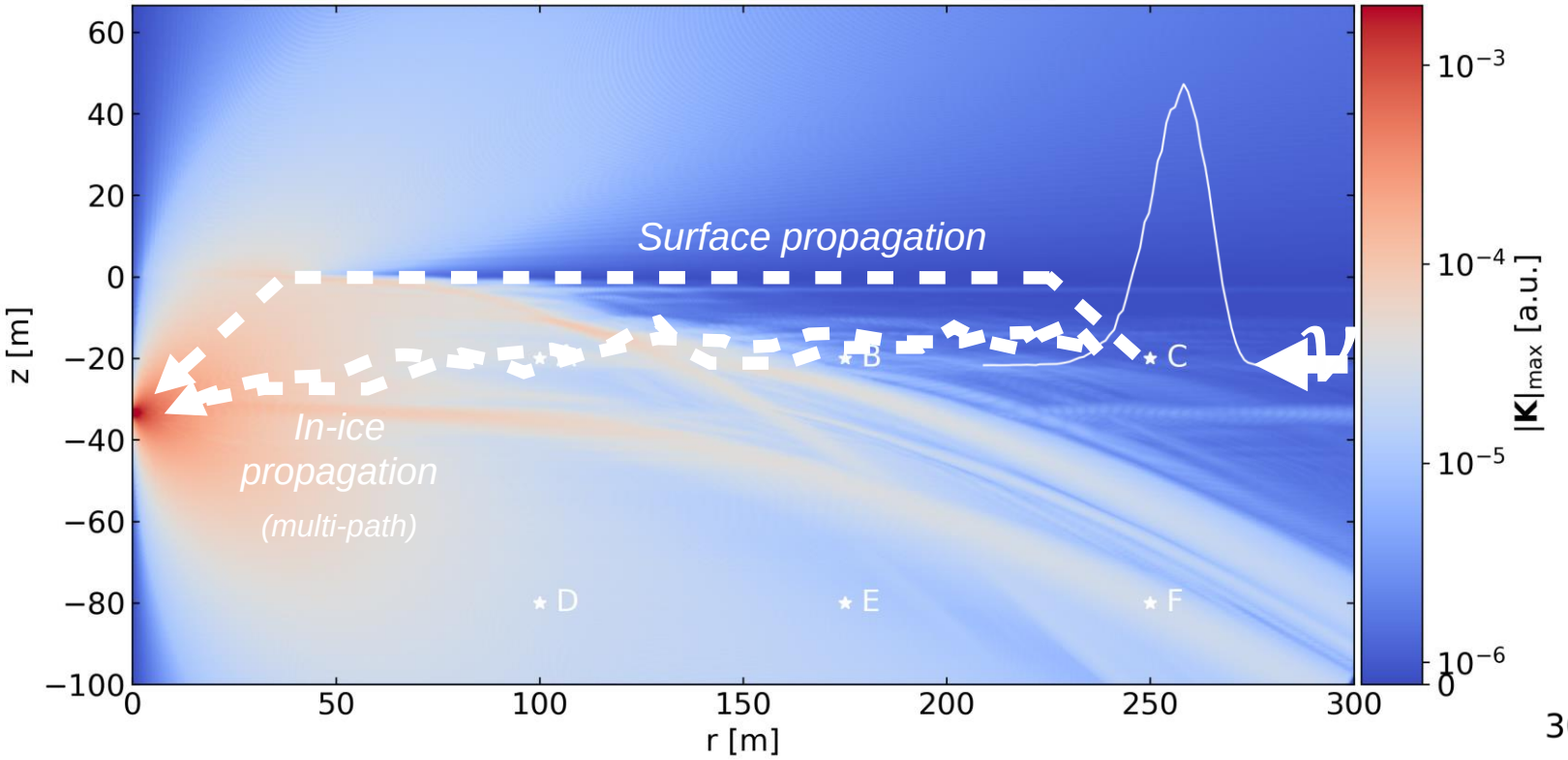

Simulated signal from
10^{18} eV hadronic shower

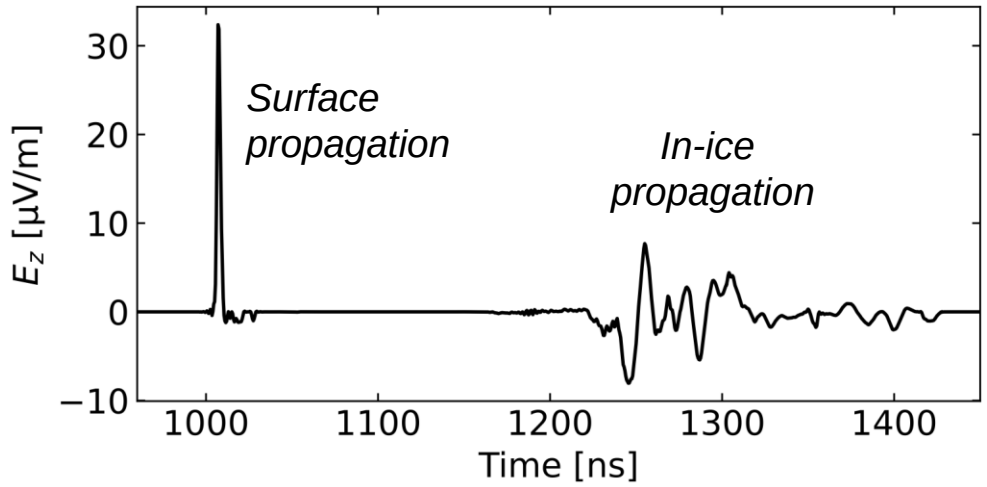

Conclusions

The weighting field concept can be extended to the full extent of Maxwell's equations and it allows an accurate calculation of signals in the most general type of detector.

For detectors where the quasi-static approximation applies, a full chain of simulation using COMSOL/TCAD and Garfield++ has been established.

The weighting field concept is now also used for detection of radio signals from particle showers.

Conclusions

The weighting field concept can be extended to the full extent of Maxwell's equations and it allows an accurate calculation of signals in the most general type of detector.

For detectors where the quasi-static approximation applies, a full chain of simulation using COMSOL/TCAD and Garfield++ has been established.

The weighting field concept is now also used for detection of radio signals from particle showers.

Theorem, induced voltage

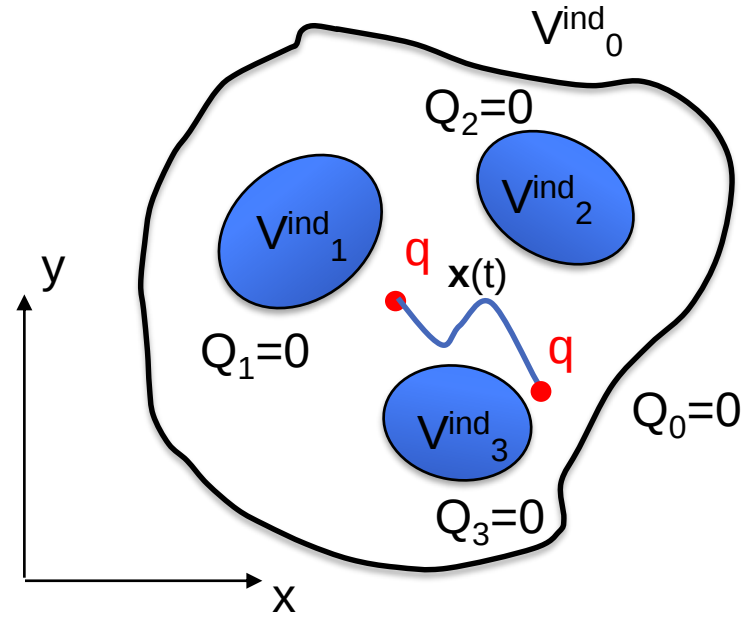

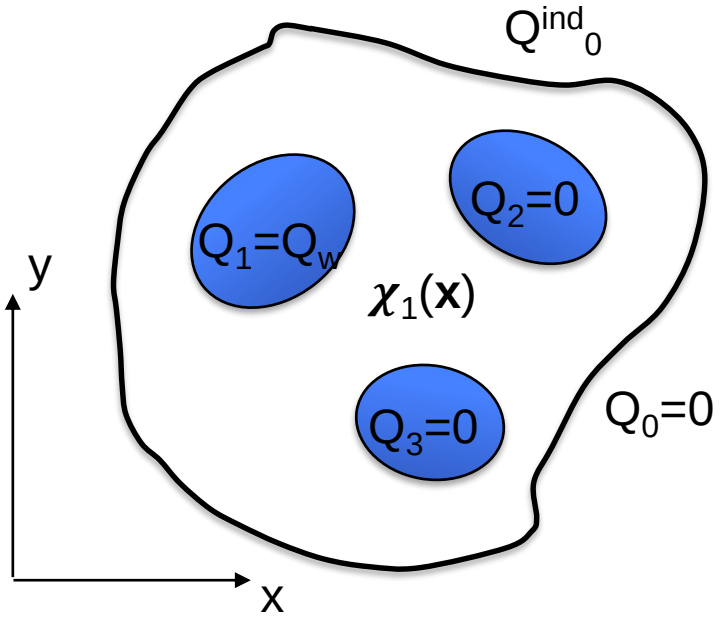

The voltage induced on an uncharged and insulated conducting electrode by a point charge q at position **x** can be calculated the following way:

Remove the point charge, put a charge Q_w on the electrode in question while keeping all other electrodes insulated and uncharged.

This defines the potential $\chi_n(\mathbf{x})$ and the induced voltage is

$$V_n^{ind}(t) = \frac{q}{Q_0}\chi_n(\mathbf{x}(t))$$

Relation between induced current and induced voltage

$$V_n^{ind}(t) = \frac{q}{Q_w}\chi_n(\mathbf{x}(t))$$

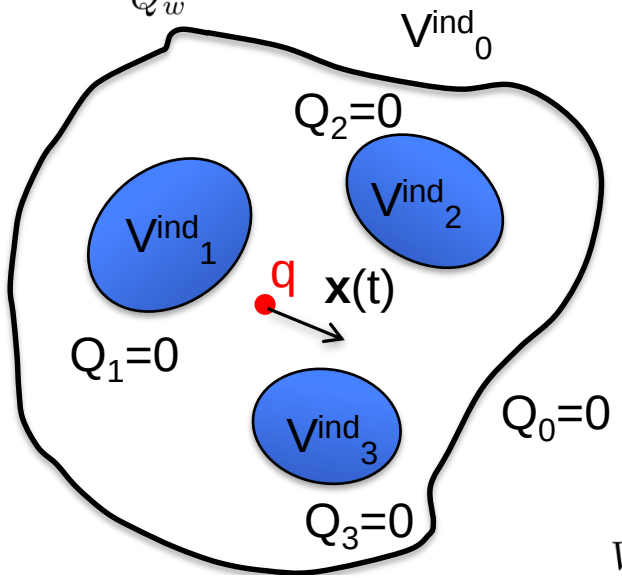

$$\chi_n(\mathbf{x}) = \frac{Q_w}{V_w}\sum_{m=0}^{N} c_{mn}^{-1}\psi_m(\mathbf{x})$$

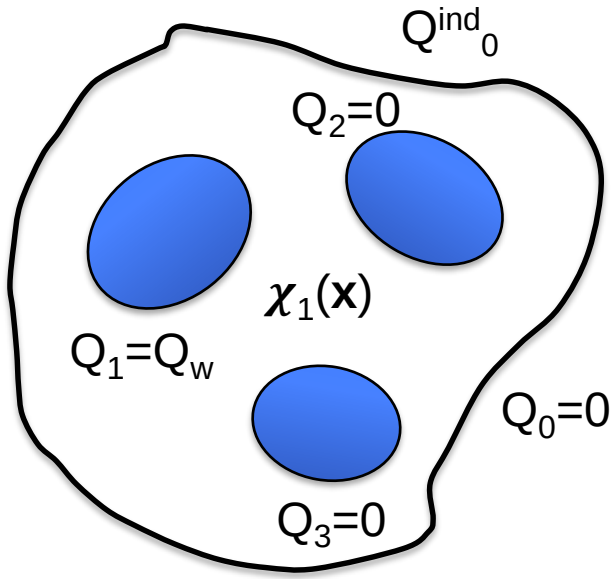

$$V_n^{ind}(t) = -\sum_{m=0}^{N} c_{nm}^{-1} Q_m^{ind}(t) \qquad Q_n^{ind}(t) = -\sum_{m=0}^{N} c_{nm} V_m^{ind}(t)$$

$$Q_n^{ind}(t) = -\frac{q}{V_w}\psi_n(\mathbf{x}(t))$$

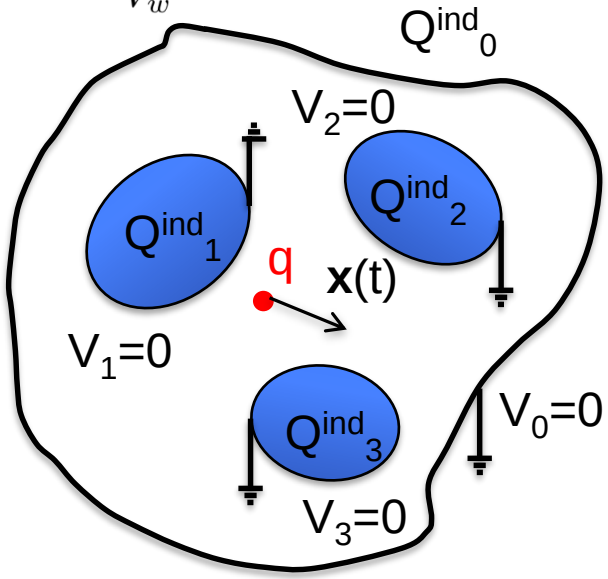

$$I_n^{ind}(t) = \sum_{m=0}^{N} c_{nm}\frac{V_m^{ind}(t)}{dt}$$

The voltages induced on insulated electrodes and the charges induced on grounded electrodes are related by the capacitance matrix.

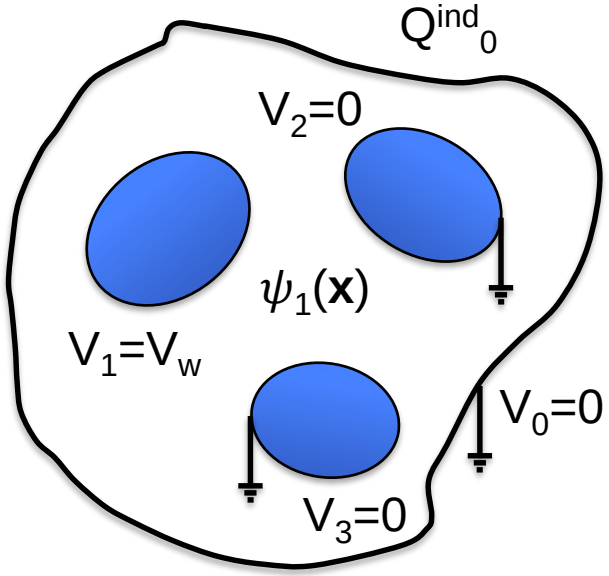

Electrostatic in dielectric media

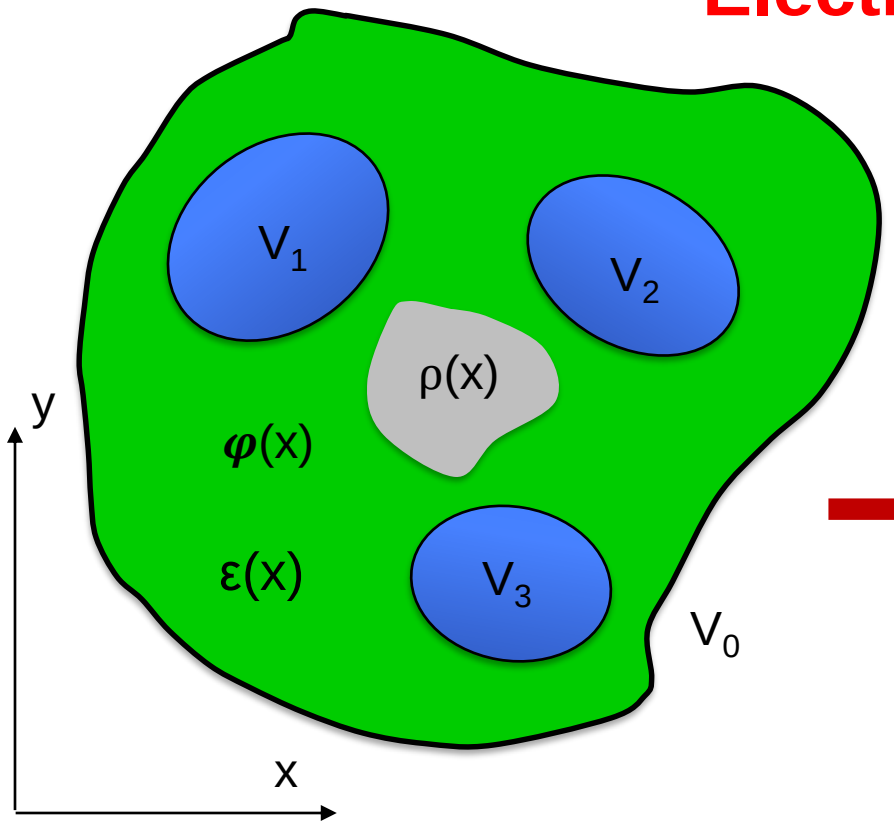

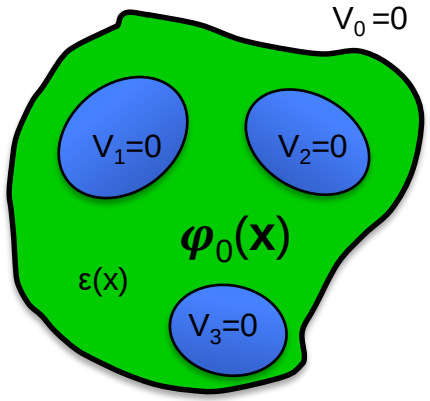

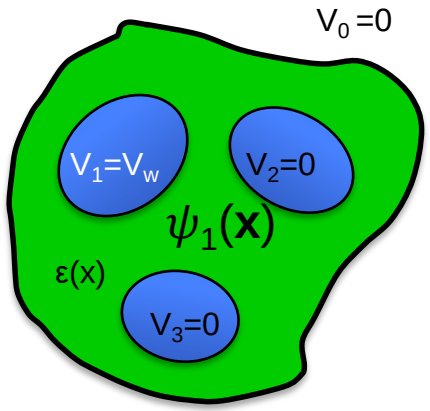

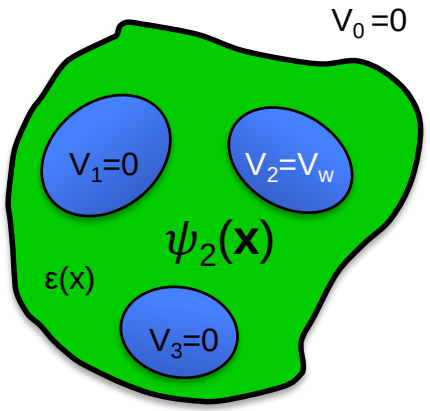

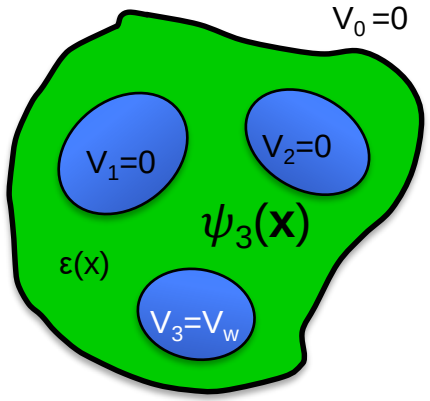

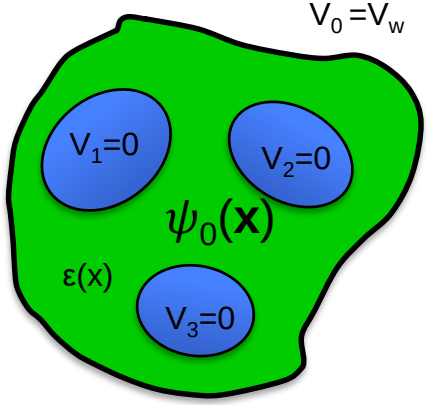

$$\nabla\left[\varepsilon(\mathbf{x})\nabla\varphi(\mathbf{x})\right] = -\rho(\mathbf{x}) \qquad \varphi(\mathbf{x})|_{\mathbf{x}=\mathbf{A}_n} = V_n$$

A solution that satisfies the boundary conditions (and is therefore unique):

$$\nabla\left[\varepsilon(\mathbf{x})\nabla\varphi_0(\mathbf{x})\right] = -\rho_0(\mathbf{x}) \qquad \varphi(\mathbf{x})|_{\mathbf{x}=\mathbf{A}_n} = 0$$

$$\nabla\left[\varepsilon(\mathbf{x})\nabla\psi_n(\mathbf{x})\right] = 0 \qquad \psi_n(\mathbf{x})|_{\mathbf{x}=\mathbf{A}_n} = V_w\delta_{mn}$$

$$\varphi(\mathbf{x}) = \varphi_0(\mathbf{x}) + \sum_{n=0}^{N}\frac{V_n}{V_w}\psi_n(\mathbf{x})$$

$$Q_n = \oint_{\mathbf{A}_n}\varepsilon(\mathbf{x})\mathbf{E}(\mathbf{x})d\mathbf{A}$$

$$c_{mn} = \frac{1}{V_w}\oint_{\mathbf{A}_n}\varepsilon(\mathbf{x})\nabla\psi_m(\mathbf{x})d\mathbf{A}$$

Ramo-Shockley theorem holds for detectors with perfect conductors embedded inside insulating media !